# Petrology , Geochemistry and Petrogenesis of gabbroic rocks(Central sector) of Mawat Ophiolite Complex, NE Iraq.

**A Thesis**
**Submitted to the College of Science**
**University of Baghdad**
**In Partial Fulfillment of the Requirements for the Degree of Master of Science**
**In**
**Geology**

**By**
**Imad Kadhim Abdulzahra alsaffi**
**B.Sc. in Geology (1996)**

***2008***

# دراسة بترولوجية وجيوكيميائية ونشوئية الصخور الكابروية(الجزء المركزي) لمعقد ماوات الاوفيولايتي/ شمال شرق العراق

**رسالة مقدمة الى**
**كلية العلوم – جامعة بغداد**
**وهي جزء من متطلبات نيل درجة الماجستير**
**في**
**علوم الارض**


**تقدم بها**
**عماد كاظم عبد الزهره الصافي**
**بكلوريوس 1996**


**2008**

**Supervisor Certification:**

We certify that this thesis has been prepared under my supervision in the Department of Geology at the University of Baghdad in partially fulfillment of requirement for the degree of master in geology.

| | |
|---|---|
| Signature: | Signature: |
| Name : Ayten H.A.Ridah | Name: Ahmed M. Aqrawi |
| Title : Assistant Professor | Title : Assistant Professor |
| Data : | Data : |

**The Certification of the president of the committee of higher studies**.

According to recommendation submitted by supervisors, I nominate this thesis for discussion.

Signature

Name

Title

Data

## ***ACKNOWLEDGMENTS***

*First and foremost, I sincerely appreciate and thank my supervisors Dr. Ayten Hadi for her supervision and support during this study. Special thanks to co-advisor Dr. Ahmad Aqrawi for his critical and constructive comments and help.*

*I also appreciate the assistance of the Department of geology, College of science, University of Baghdad.*

*I am grateful to the support of the State Company of Geological Survey and Mmining for giving me this chance to get master degree with Special thanks to the D.G. Dr. Khaldoun S. Al-Bassam.*

*I would like to thank Dr. Muhemmed. E. Al-Hassan for his criticism and aid during this research.*

*Thanks to M rs. Sallama Challoob for her assistance in making chemical analysis.*

*Thanks to Mr. Varoujan K. Sissakian, Dr. Saffa F. A. Fouad, Dr. Rafaa Zair, Mr. Khaldon A. Maala, Mr. Shakir Qanbar, Alaa Shakir and all my friends in the department of survey for their support during my study.*

*I am very grateful to Dr. Khalid J. Aswad at Mosul University for his assistance.*

*Also I am thankful to Dr. Kamal Hajje and Mr. Eirfan Musa at Sulaimanya University for their support and help.*

*At the end, thanks to my family for their encouragement, support and patience.*

# المستخلص:


تقع وحدة صخور الكابرو لمعقد ماوات الاوفيولايتي ضمن نطاق زاكروز التصادمي على الحدود بين الصفيحة العربية والصفيحة الايرانية، وهي مرتبطة باحداث ما بعد التصادم وتموضعها ضمن القشرة القارية بعد التصادم خلال عصر المايوسين.

تتالف صخور الكابرو من الكابرو المتطبق الذي يمتاز بكونة الاكثر انتشارا والكابرو الطرفي الذي يكون اكثر تاثرا بالتشوه ،وتجمعات من قواطع الكابرو البغمتايتي .

اثبتت الدراسة الصخارية لمائه (100) شريحة بان الصخور المدروسة تتكون من معادن اساسية : بلاجيوكليس ( لابرادورايت- بايتونايت) وكلاينوبايروكسين (اوجايت) وفي حالالت نادرة اورثوبايروكسين اما المعادن الثانوية فتشمل الامفيبول (تريمولايت- اكتينولايت) ،كلورايت،ابيدوت، سيريسايت ومغنتايت ثانوي بالاضافة الى ذلك فان الاخير يتواجد ايضا كطوراولي مساعد. تعاني صخور الكابرو لمعقد ماوات من التحلل والتحول وبدرجات متفاوتة مع احلال معادن الامفيبول الثانوي والكلورايت محل معادن البايروكسين الاولي. معدن البلاجيوكليس يبقى نسبيا بصورة نقية في هذه الصخور.

لوحظت العديد من الانسجة الصهيرية حيث تعكس الصخور المدروسة النسيج الحبيبي الناقص الاوجة والنسيج البيني والنسيج البويكليتي و النسيج الاوفيتي وشبه الاوفيتي. اما الانسجه التشوهية فتكون مرتبطة بتواجد وزيادة عملية التحبب ،التوئمة الثانوية وانتشار الانسجة النضيدية.

تعاني صخور الدراسة ثلاثة انواع من التشوة : التشوة المرن والتشوة شبة المرن والتشوة الهش اما انماط التحلل فتشمل التحلل الشكلي الكاذب، والتحلل الشكلي غير الكاذب.و تعتبر صخور الكابرو الطرفي من اكثر انواع الصخور تاثيرا بالتشوه والتحلل.

اثبتت التحاليل الجيوكيميائية بان صخور كابرو ماوات تتميز بقلة تراكيز التيتانيوم و البوتاسيوم و الصوديوم و العناصر ذات جهد الجذب العالي والعناصر الارضية النادرة وتمتاز بتراكيز عالية نسبيا للالمنيوم والكالسيوم والمغنيسيوم وتمتاز الصخور الاكثر تشوها والمتمثلة بالكابرو الطرفي بمحتوى عالي من البوتاسيوم والصوديوم والحديد ($Fe_2O_3$)ومحتوى واطي من المغنيسيوم والكالسيوم والالمنيوم مقارنة مع الكابرو الطباقي والبغمتايتي.

تمتاز صخور الدراسة الحالية بدرجة واطئه نسبيا من التفاضل الصهيري بالاعتماد على نسبة ($FeO^t/MgO$) والتي تكون اقل من 2،حيث تعكس هذه الصخور الطبيعة الثوليتية مع دليل تبلور (Mg#) يتراوح بين 49.9-64.6 وبمعدل 51.28 والذي يعتبر اقل مما موجود في الصهير البدائي .

مقارنة هذه الصخور مع مختلف الصهارة والصخوروالبيئات العالمية تعكس هذه الصخور التركيب البازلتي والاصل التراكمي ،وان البيئة المثالية لتكون هذه الصخور هي بيئة الجزر القوسية الثوليتية بالاعتماد على النسبة الواطئه للتيتانيوم الزركونيوم وانخفاض نسبة V/Ti والتي تكون اقل 10.

اثبتت دراسة نشوئية هذه الصخوربان هذه الصخورمشتقة من مصدر جبي مستنزف وان درجة الانصهار جزئي لا تزيد عن 30% .يعتبر معدني البلاجيوكليز والكلاينوبايروكسين هما الطورين المسيطرين على تبلور هذه الصخور بصورة اساسية.

## 1.1 Preface:

The Mawat Ophiolite Complex is a part of the Zagros-Thrust Belt, which extends of about 2000 kilometers from southeastern Turkey through northern Syria and Iraq to western and southern Iran (Alavi, 2004). Mawat Ophiolite Complex represents one of the Tethyan ophiolites, and it is considered to be part of the Le Crossant Ophiolitique peri-Arabe (Ricou, 1971) (Fig. 1.1).

From the base to the top, the typical rock types of Mawat ophiolite complex include ultrabasic rocks, mafic intrusives, sub volcanic, volcanic igneous rocks, and overlaid by oceanic sediments called (Gimo group).

## 1.2 Location:

The Mawat Ophiolite Complex is located in the Iraqi Kurdistan region of about 30 kilometers northeast of Sulaimaniya city and five kilometers north of Chwarta village (Fig.1.2). It lies between longitude (45° 28′ 30″- 45° 33′ 45″ E) and latitude (35° 47′ 30″- 35 ° 50′ 45″ N).

The study area has a complicated topography, consisting of rugged mountains. The elevation is about (2184) meters in the Root Peak within the study area with very steep valleys

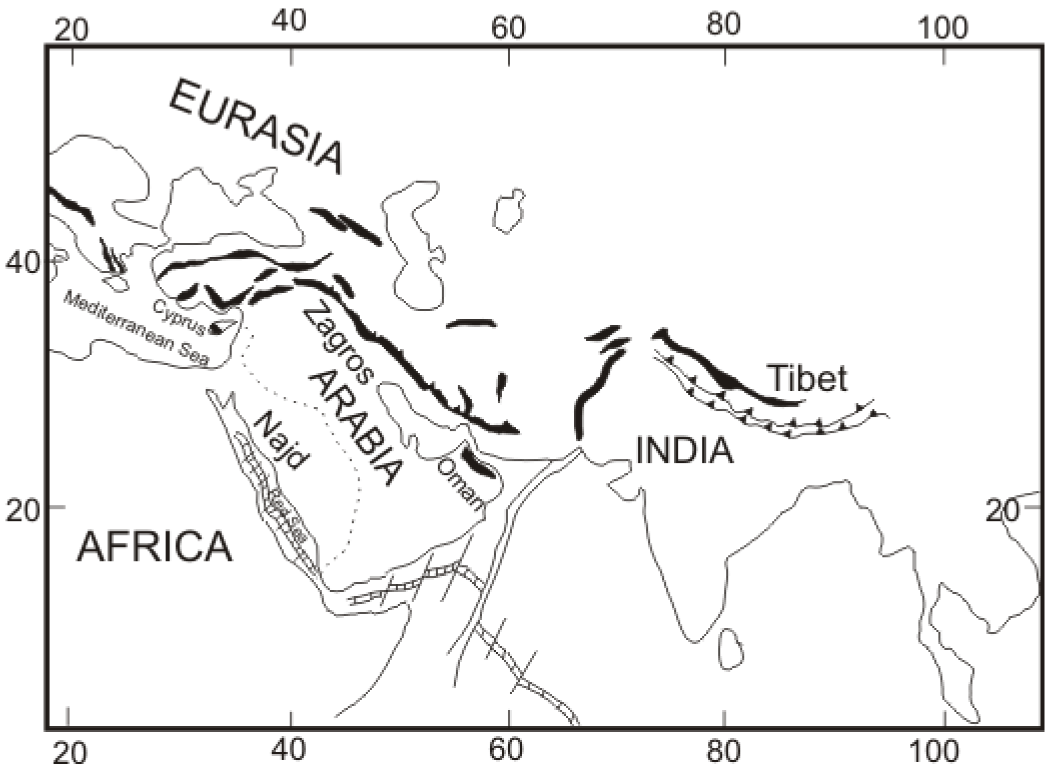


Figure (1.1)**:** Generalized tectonic map showing distribution of ophiolites along Tethys suture. Black areas include ophiolites and colored mélange zones. After Coleman (1981).

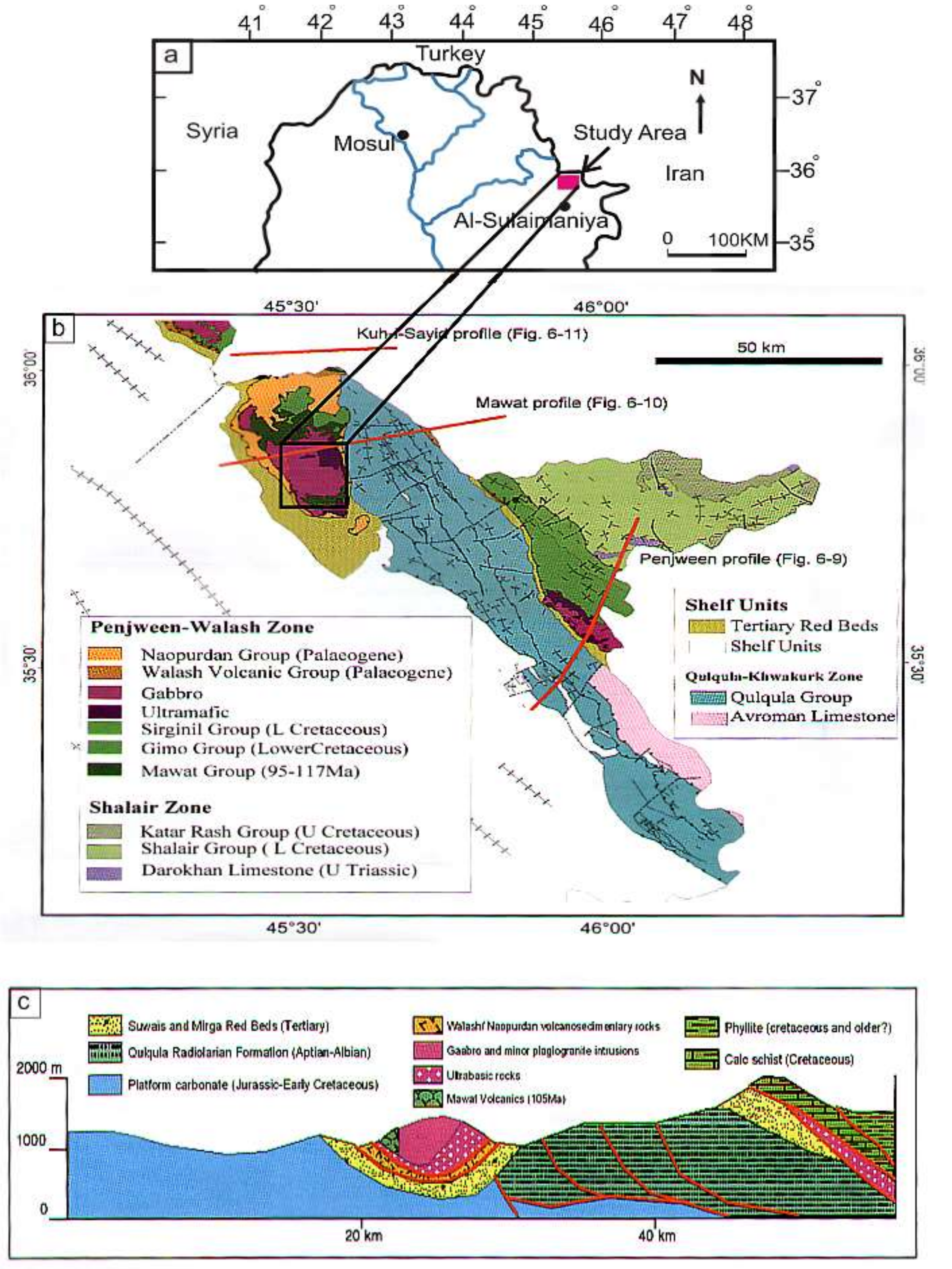


Figure (1.2): (a) Location map of northern Iraq showing the study area (b) Geological map of the SE part of the Zagros suture (After Jassim and Goff, 2006); (c) Cross section passing through Mawat area(After Jassim and Goff, 2006)

### 1.3 Tectonic Setting:

The Mawat Ophiolite Complex is located in Penjwin –Walash subzone in the central zone of geosynclinal unit according to Buday and Jassim (1987) (Fig.1.3 a).

Numan (1997) modified classifications of Bolton (1958) and Buday and Jassim (1987) (Fig.1.3 b) and according to this classification, the study area is located in the imbrications zone of the foreland basin. On the other hand, Jassim and Goff (2006) modified Buday and Jassim (1987) classification of Iraqi territories in to:

**I- Stable shelf**

A- Rotba-Jazira zone

1- Rotba zone

2- Jazira zone

B- Salman zone

C- Mesopotamian zone.

1- Zubair subzone

2- Tigirs subzone

3- Euphrates subzone

**II- Unstable shelf**

A- Foothill zone

1- Makhul-Hamrin subzone (Kirkuk Embayment)

2- Makhul-Hamrin subzone (Mosul high)

3- Makhul-Hamrin subzone (Sinjar basin)

4- Butmah-Chemchemal subzone (Mosul high)

5- Butmah-Chemchemal subzone (structurally lower blocks)

B- High folded zone

1- High folded zone

2- Imbricated zone

a- Balambo- Tanjero subzone

b- Northern (Ora) Thrust subzone

**III- Zagros Suture zone**

A- Qulqula-Khwakurk subzone

B- Penjwin –Walash subzone

C- Shalair subzone

According to this classification, the study area is located in Penjwin-Walash subzone within the Zagros Suture zone (Fig.1.4).

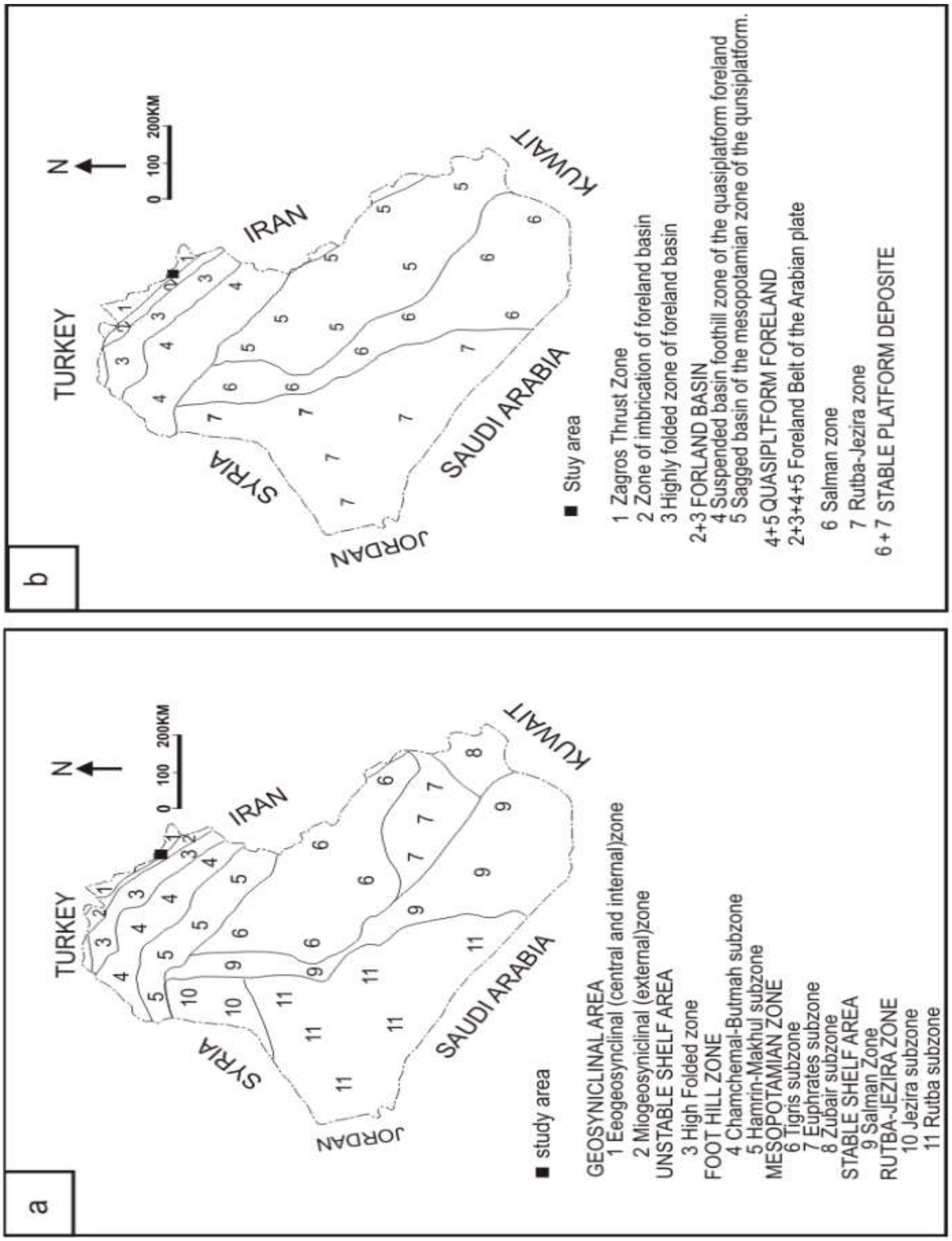


Figure 1-3 Major tectonic division in Iraq:(a),After Buday and Jassim(1987).,(b),After Numan (1997)

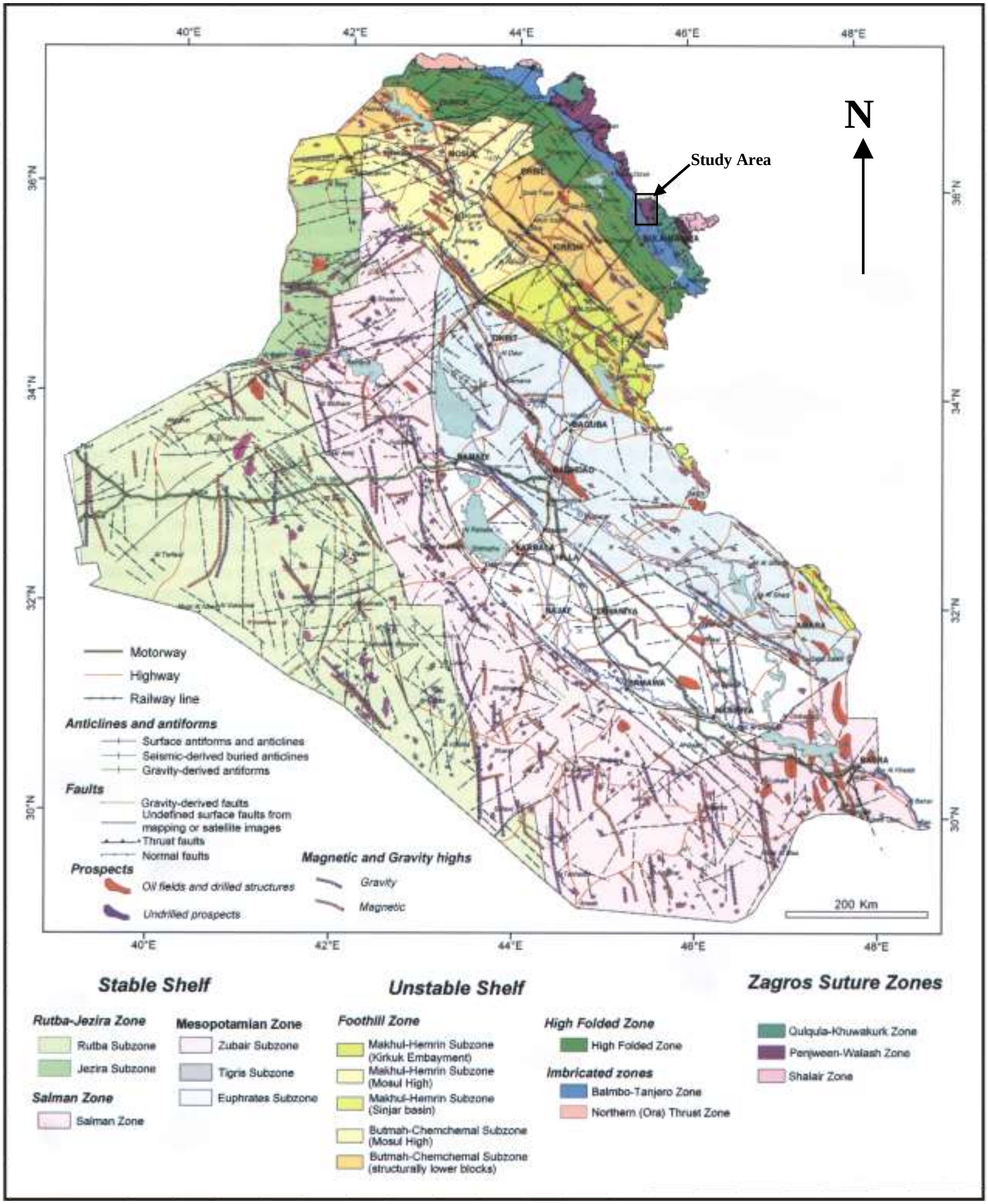


Figure (1.4): Tectonic map of Iraq after Jassim and Goff, (2006)

## 1.4 Geology of Chwarta –Mawat Area:

The general stratigraphy of Mawat –Chwarta area is summarized in the stratigraphic tectonic column produced by Al-Mehaidi (1974) (Fig. 1.5).

### 1- Qulqula Group:

This group is restricted in a narrow strip along the eastern part of Mawat range. This group consists of alternating and interfingering radiolarian mudstone, shale and chert, thin bedded foraminiferal limestone and pebbly conglomerate. The age of Qulqula Group ranges from Albian to Cenomanian (Al-Mehaidi, 1974).

Rocks of this group are allochthonous rock units and subdivied into four sequences (Jassim and Goff, 2006); shallow water carbonates sequence, carbonate-chert sequence, radiolarian chert, Qulqula conglomerate formation

### 2- Upper Cretaceous Rock Units:

This unit represents part of the external zone of the geosynclinal area (Buday and Jassim, 1987), while Al-Mehaidi (1974) regarded it to be a part of the folded zone. This rock unit consists of Shiranish, Tanjero and Aqra Formations:

#### A- Shiranish Formation:

Shiranish Formation is exposed along the western border of the Mawat area (Al-Mehaidi, 1974, Jassim and Goff, 2006). This formation consists of marl and marly limestone, with planktonic foraminifera (Al-Mehaidi, 1974) .The age of Shiranish formation is (Santonian-Maastrichtian) (Bolton, 1957).

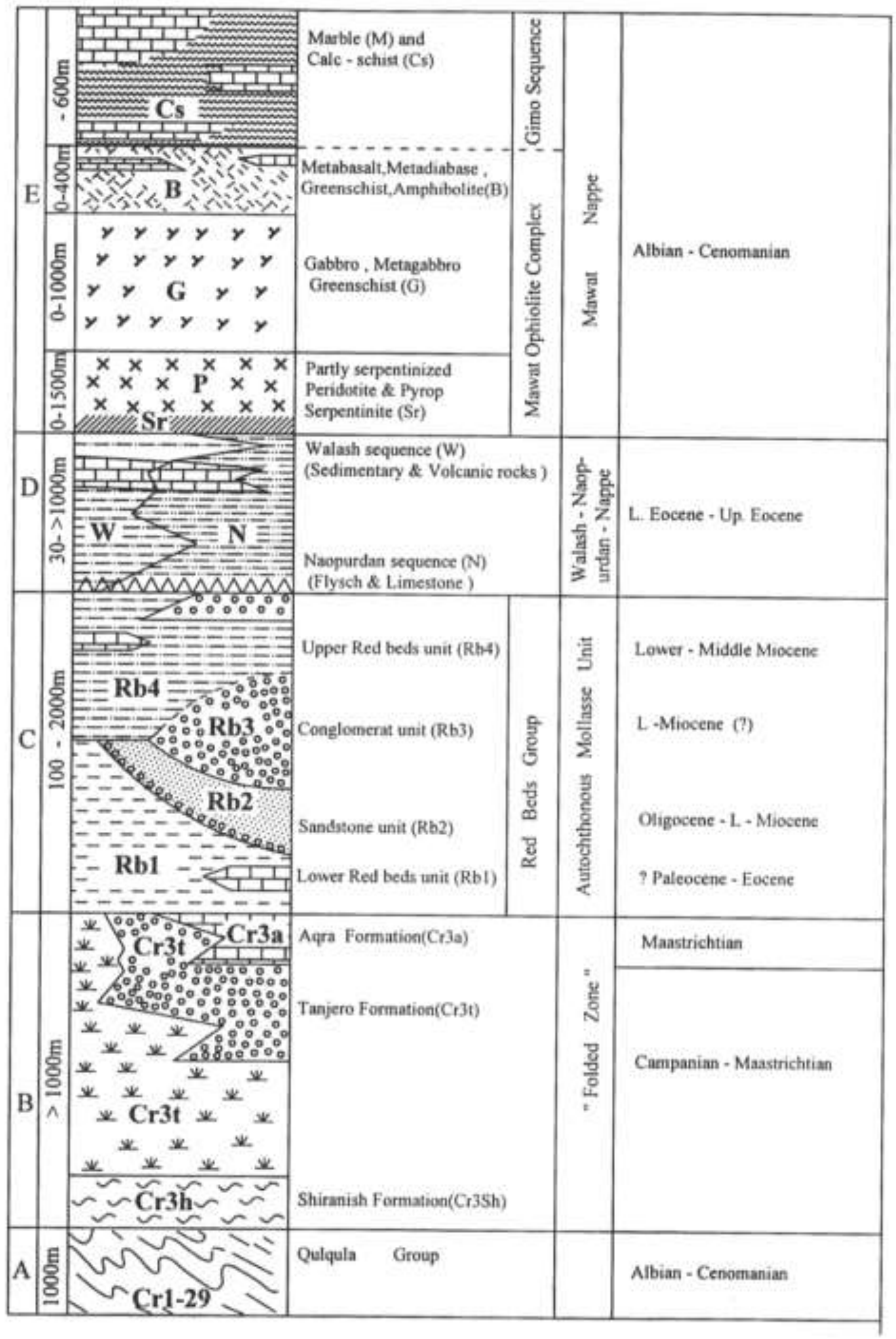


Figure (1.5): Stratigraphic columnar section of Chwarta-Mawat area after Al-Mehaidi, (1974).

**B- Tanjero Formation:**

Tanjero formation consists of shallow marine clastics of flysch character (Al-Mehaidi, 1974). The age of Tanjero formation ranges from Upper Campanian to Maastrichtian according to Bolton (1957) and Bellen et al. (1959).

**C- Aqra Formation:**

Aqra Formation overlies Tanjero formation with a sharp contact. It consists of clastic limestone and calcareous sandstone (Al-Mehaidi, 1974). The age of Aqra formation is Maastrichtian according to Al-Mehaidi (1974).

**3- Red beds Group (Autochthonous Unit):**

This group has a major unconformity with Cretaceous units. Al-Mehaidi., (1974) subdivided this group into four units (from bottom to top):

**A- Lower Red bed Unit :**

This unit consists of interbedded calcareous silty shale and claystone, radiolarian chert, detrital limestone, and pebbly conglomerate. The thickness of this group reaches up to 400 meter

**B- Sandstone Unit :**

The thickness of this group is up to 500 meter. This unit consists of shallow marine sediments. The contact with lower Red beds unit is marked by thin beds of conglomerate which might indicat unconformity between the two units (Al-Mehaidi, 1974).

**C- Conglomerate Unit:**

This unit consists of fragments ranging from pebble to boulder size and mostly consists of limestone, igneous, and metamorphic rock fragments. The age of conglomerate unit ranges from Oligocene to Miocene (Al-Mehaidi, 1974).

**D- Upper Red beds Unit:**

This unit consists of silty shale, marl, conglomerate and thin beds of coral limestone.

**4- Walash-Naopurdan Sequences:**

The Walash-Naopurdan sequences are exposed as a narrow strip around Mawat area (Al-Mehaidi, 1974). The age of these sequences ranges from Paleocene to Oligocene.

**A- Walash Sequence:**

The Walash sequence consists of volcanic rocks (basalt, andesite, tuffs and agglomerates), shale, greywacke, limestone and radiolarian chert, dikes and sills of diabase are frequently out the sequence.

**B- Naopurdan Sequence:**

This sequence is subdivided into two units: flysch unit consisting of silty shale, greywacke, sandy limestone, pebbly conglomerate and breccia and of Walash type volcanic rocks; the nummulitic limestone unit represents the lateral equivalent of the Walash limestone (Al-Mehaidi, 1974).

**5- Mawat Nappe:**

Mawat nappe comprises about 250 sq. km. and more than 2000 meters of metamorphosed igneous rocks (Mawat Ophiolite Complex) and metasedimentary rocks (Gimo Sequence).

**A- Mawat Ophiolite Complex:**

The Mawat Ophiolite Complex covers about 200 sq.km. and reaches up to more than 1000 meters in thickness. Al-Mehaidi, (1974) subdivided the Mawat ophiolite complex into three members (from bottom to top):

**1- Ultramafic Member:**

This member's thickness reaches few meters to about 1500 meters in Ser Shiw area. It consists of peridotite (Iherzolite), dunite and pyroxenite.

**2- Gabbro Member:**

The gabbro member lies in the central part of the ophiolite reaching about 1000 meters in thickness. Gabbro member is the main component of the complex (Jassim, 1972., 1973). It consists of medium to coarse grained and partly banded amphibolized gabbro, pyroxene gabbro, metagabbro, greenschist, epidosite and albite amphibolite.

**3- Metavolcanites Members:**

They are exposed in the northern and southern parts of the ophiolite complex and consist of spilitic basalt, metabasalt, metadiabase, greenschist, amphibolite and metapyroclastics

**B- Gimo Sequence:**

Gimo Sequence consists of alternating and interfingering marble and calc-schist with thin sheets of metabasalts in some places. The age of Gimo sequence ranges from upper Cretaceous to Paleocene according to Smirnov and Nelidov (1962).

**1.5 Previous works**:

The early work of Heron and Less (1943) suggested that the northeastern part of Iraq represents a nappe zone. They subdivided the area into three parts: the nappe of igneous rocks, the metamorphic nappe, and nape of radiolarian cherts and shale.

Heron and Less division in 1943 had been later modified by (Lehnor, 1954) who subdivided the area into the Jurassic radiolarian host block, the igneous and metamorphic nappe and the folded zone.

Bolton, 1957, introduced the division of the area from east to west:

1-Thrust zone which consists of (from bottom to top): Naopurdan series, Walash series, and Qandil series.

2- Intermediate zone which consists of Cretaceous Qulqula series and Tertiary Red beds

3- Fold Zone.

Smirnov and Nelidov (1962) concluded that the Mawat complex consists of peridotites, gabbros, granodiorites and granophyres, and they divided gabbroic rocks into normal gabbro and amphibolized gabbro.

Akif et al. (1972) studied the geology and mineralogy of ultramafic rocks in Sir-Shiw area. They divided these rocks into dunite, chromites dunite, pyroxene peridotite, and pyroxene hornblendite.

Etabi (1972) studied the petrography of Mawat igneous complex (basic and ultrabasic rocks) and indicated that the basic rocks are represented by gabbros and constitute the major part of the igneous complex.

Jassim (1972) investigated the geology of the central sector of the Mawat igneous complex .He indicated that this sector comprises the basic and ultrabasic igneous rocks and minor intrusions. He also recognized various types of banding in gabbro; they are: rhythmic, injection, and alteration banding.

Mashek and Etabi (1973) studied the petrography of igneous and metamorphic rocks of Mawat ophiolite complex. They indicated that the pyroxenite rocks are younger than mafic rocks.

Al-Mehaidi (1974) investigated the Mawat–Chwarta area .He produced a geological map of the area with detail description of all rock units. He also indicated that the Mawat nappe consists of Mawat ophiolite complex and Gimo sequence.

Al-Hashimi and Al-Mehaidi (1975): studied the dispersion of Cr, Ni, and Cu in Mawat ophiolite complex. They introduced maps to explain the distribution of these elements.

Al-Hassan (1975) made a comparative study between Mawat and Penjwin igneous complexes and found similarities in the mineralogy, texture and chemistry of the igneous complexes of both, and he also indicated that these complexes had suffered similar post magmatic history.

Jassim and Al-Hassan (1977) made a comparison between petrography and origin of the Mawat and Penjwin igneous complexes .They concluded that the post magmatic modification occurred during this emplacement and largely during thrusting in the climax of the Alpine orogeny.

Buda and Al-Hashimi (1977) studied the petrology of Mawat ophiolite complex and showed that the gabbro are mostly cumulate but often show foliation due to strong deformation .

Buday and Jassim (1987) concluded that Mawat ophiolite complex (Upper Cretaceous) lies within the Penjwin Walash subzone and they also concluded that banded gabbro is the main basic intrusion in the area.

Aqrawi (1990) studied the petrochemistry and petrogenesis of ultramafic and gabbroic rocks around Root Mountain, and he indicated that the petrographic evidence of gabbroic rocks is characterized by textural features due to tectonic deformation, recrystallization alteration and metamorphism.

Zekaria (1992) introduced the division of the gabbroic rocks on the basis of their mineral composition into: amphibolized gabbro and metagabbro.

Aswad (1999) introduced the division of the Chowarta-Mawat area into; Parautochthon, neo-autochthon, Tertiary sedimentary cover, allochthon Walash-Naopurdan Nappe, and allochthon Mawat Nappe.

Farjo (2006), studied geochemistry and petrogenesis of the volcanic rocks of Mawat ophiolite. He indicated that the Mawat ophiolite complex was derived from Fast-Spreading centers.

Musa, E.O (2007) studied the geochemistry and genesis of copper-iron mineralization and associated rocks in Waraz Area , and concluded that the studied gabbro has not reached the amount to be regarded as a mineralization.

Mirza, T. A. (2008) studied the pertogenesis of Mawat Ophiolite complex and the associated chromite. She classified the basic rocks as tholeiitic and related to island arc tholeiite

## 1.6 The Aims of the Study:

The aims of this study are:-

1- Detailed petrological study of Mawat gabbros to determine mineralogy, the primary and secondary textures and showing the effects of alteration and or metamorphism processes.

2- Utilizing, the chemical compositions, including major, and trace elements to interpret the magmatic origin and tectonic environmant of the Mawat gabbros.

## 1.7 Field description:

The gabbros in study area are light greenish grey to dark greenish grey in colour. Field observations show that most gabbros had experienced deformation. This is clearly shown by abundant evidence of jointing, fracturing, and crushing (Plate 1-1). These rocks are affected by shearing stress due to tectonic contact along the boundaries of the gabbros unit, and in the shear zones which are within the gabbroic rocks.

According to the field relations in the present study, the gabbroic rocks can be subdivided into three groups; layered gabbro, marginal gabbro, and the dyke swarms pegmatoid gabbro.

The layered gabbro is the most abundant type in the study area and covers the major parts in the rocks of the three locations, where it shows alternating layers of light and dark minerals. Two main types of igneous layering are recognized in the layered gabbros; the first is the grain size layering and second is the compositional layering, typically with variation from mafic to more felsic minerals. Both types of layering are commonly present together (Plate 1.2 and 1.3).

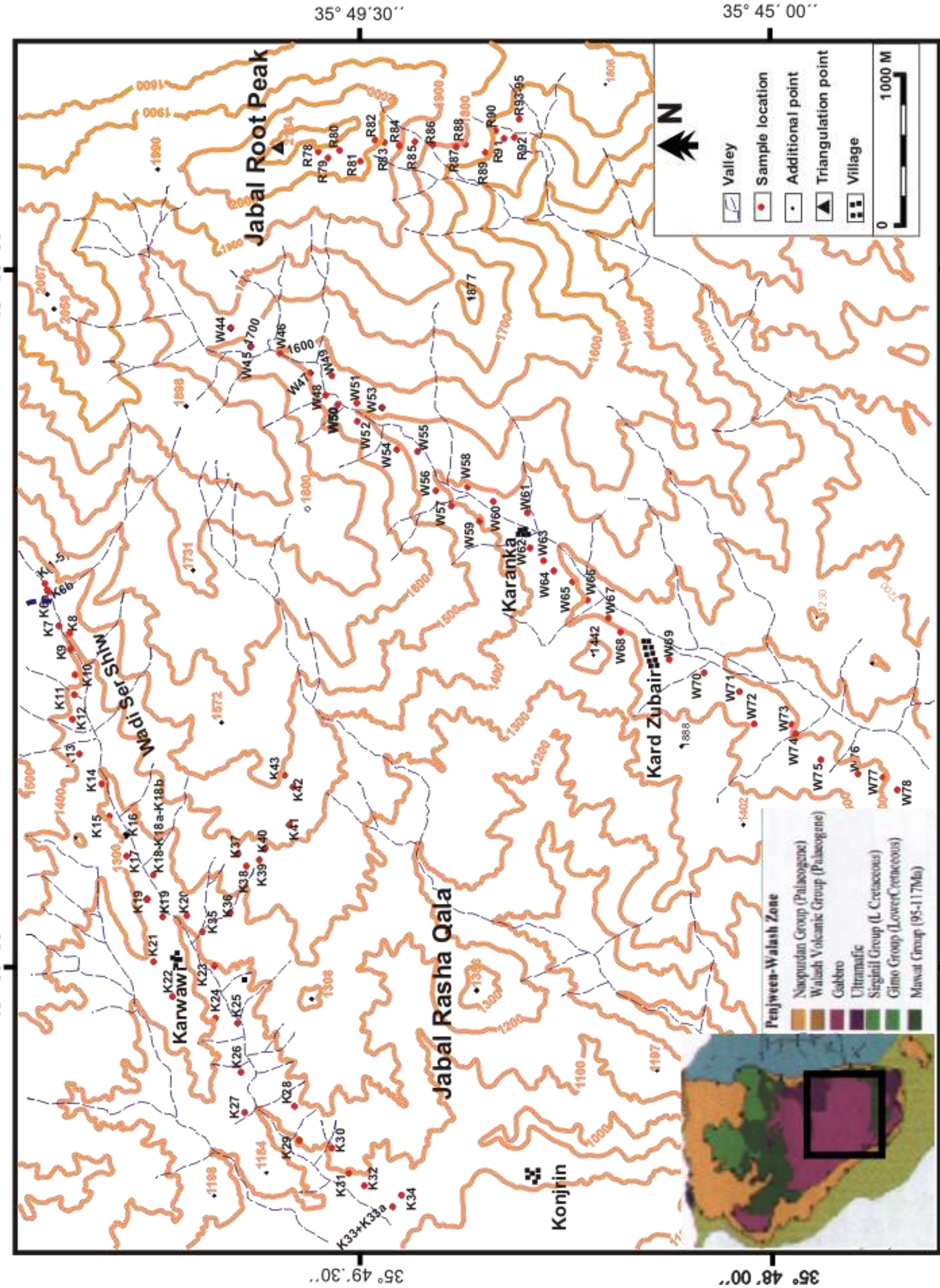


Figure (1.6): Topographic map of the study area.

The graded layers occur where the proportion of dark to light minerals decreases. This leads to the succession of melagabbro, gabbro, and leucogabbro.The layering is well developed and ranges in thickness from few centimeters to 60 centimeters.

Megascopic features in layered gabbros of this study such as ratio layering, size layering, graded bedding result in sedimentary appearance of the layered gabbros; these features suggested that this type of layering is due to crystal settling mechanism (Campbell, 1978., Irvine, 1980).

The layered gabbros also show narrow shear zones not exceeding few meters (Plate 1.4). In these zones, the rocks are highly deformed and are light greenish gray in colour.

In the northeastern part of the study area (upper part of all three locations), the layered gabbro has sharp contact with the ultra basic rocks in Ser Shiw area and it is a remarkable feature in this area where numerous pyroxenite dykes are found between these two rock bodies (Plate1.5). These dykes decrease in occurrences and in thickness toward the gabbros body with thickness ranging from (1.5-3 meters).

The marginal gabbro is restricted in the southern part of the study area. It is found in the lower part of W-location near Waraz village. These rocks are intensively deformed (Plate 1.6) with light green to dark green in colour and medium to low toughness. The transition from the layered gabbro to marginal gabbro rocks is gradual.

In the upper part of K-location, the ultrabasic body in Ser Shiw area shows dyke of pegmatoid gabbros which occur within the ultrabasic rocks and they are about 1.1 meter in thickness. These pegmtoid gabbros are coarse-grained (about 2.5 centimeter) and generally, show no trace of layering.

## 1.8 Sampling:

The topographic maps (1:20 000) of the study area covered by sheet no.75/700 and 75/710 in the Mawat region have been used.

Three locations were chosen for sampling (Fig.1.6); the first lies about one kilometer north of the Konjrin village (K-location) extending NE-SW and is about 4670 meters in length. The second is located west of the Waraz village in the Kard Zubair valley (W-location) extending NE-SW and is about 5300 meters in length. The third (R-location) extends N-S and it lies of about few kilometers north Kanaro near Root Peak with 1330 meters length. The sampling included 47 samples in K- location, 35 samples in W-location 18 samples in R- location.

**Plate (1.1): Jointing, fracturing, and crushing in layered gabbro**.

**Plate (1.2): Graded layers, the proportion of dark to light minerals decreases upward.**

**Plate (1.3): Coarse-grained gabbros with graded bedding in layered gabbro**

**Plate (1.4): Narrow shear zone within the layered gabbros, showing deformation.**

**Plate (1.5): Pyroxenite dykes within the layered gabbros**

**Plate (1.6): Intense deformation in the marginal gabbros.**

## 2.1 Introduction :

Thin sections of 100 representative samples from the three locations were examined using polarized microscope to find out the mineral composition and textures and to clarify the effects of deformation and alteration /and or low grade metamorphism on these rocks.

XRD analysis is also used for identification of minerals difficult to determine under polarized microscope.

Basic igneous rocks were classified globally by different authors, Streikeisen classification (1976) is an important one. It is based on abundance of primary minerals, when modal analysis can be reliably obtained. Rock names are assigned based on the primary phases present prior to alteration. All studied rocks in the present study show variable degrees of alteration, where alteration in these rocks is so extensive that the estimation of the primary mineral assemblages is not possible. In this case, it is difficult to use this global classification

In general, the studied rocks partially or completely are replaced by secondary minerals. The rock name used is based on the reconstructed primary minerals and is termed either (urilite or amphibolized) (i.e. urilite gabbros, and amphibolized gabbros).

The modal mineral abundances which are estimated by point counting are shown in Table (2.1) and they show microscopic visual estimates of the extent of alteration intensities according to ratio of secondary mineral assemblages. In addition, granulations were estimated by point counting shown in Table (2.2).

Table (1.2): Model and analyses of Mawat gabbros; (a), K-location; (b), R-location and ( c), W-location

| Rock types | Pegmatoid gabbro | | | | Layered gabro | | | | | | | | | | | | |
|---|---|---|---|---|---|---|---|---|---|---|---|---|---|---|---|---|---|
| Sample No. | K3 | K4 | K6a | K6b | K7 | K9 | K11 | K13 | K19 | K20 | K24 | K26 | K32 | K33 | K43 | K41 | K36 |
| Plagioclase | 42.3 | 53.1 | 45.3 | 49.3 | 62.3 | 52.9 | 52.9 | 44.3 | 39.3 | 53.4 | 50.1 | 42 | 56 | 26 | 58.6 | 46.1 | 40.3 |
| Amphibole | 31.6 | 31.9 | 30.8 | 29.3 | 33 | 37.8 | 37.8 | 39.9 | 52.2 | 39.1 | 46.4 | 53.1 | 38 | 46.2 | 36.6 | 51.2 | 55 |
| Chlorite | 11.9 | 8.8 | 9.2 | 10.2 | 1.6 | 4.3 | 4.3 | 5.6 | 4.5 | 7.3 | 1.0 | 1.1 | 3.1 | 6.5 | 1.9 | 2.4 | 1.2 |
| Clinopyroxene | 13.1 | 4.1 | 12.1 | 8.4 | 0 | 0 | 0 | 4.3 | 0 | 0 | 0 | 0 | 0 | 0 | 2.4 | 0 | 0 |
| Orthopyroxene | 0 | 0 | 0 | 0 | 0 | 0 | 0 | 2.3 | 0 | 0 | 0 | 0 | 0 | 0 | 0 | 0 | 0 |
| Opaque Minerals | 1.3 | 2.1 | 1.7 | 2.8 | 3.1 | 5 | 5 | 3.6 | 4 | 0.2 | 2.2 | 3.8 | 2.9 | 18.5 | 0.5 | 0.3 | 3.5 |
| Quartz | 0 | 0 | 0 | 0 | 0 | 0 | 0 | 0 | 0 | 0 | 0.3 | 0 | 0 | 2.8 | 0 | 0 | 0 |
| Sum. | 100 | 100 | 100 | 100 | 100 | 100 | 100 | 100 | 100 | 100 | 100 | 100 | 100 | 100 | 100 | 100 | 100 |

(a)

| Rock types | Layered gabbros | | | | | | | |
|---|---|---|---|---|---|---|---|---|
| Sample No. | R78 | R80 | R81 | R85 | R87 | R88 | R91 | R93 |
| Plagioclase | 18.6 | 49.9 | 50.2 | 45.4 | 32.1 | 51.1 | 40.3 | 65 |
| Amphibole | 74.5 | 40.6 | 43.5 | 44.4 | 55.8 | 42.6 | 51.3 | 28.2 |
| Chlorite | 6.2 | 8.9 | 5.9 | 4.2 | 11.3 | 6 | 7.5 | 6.1 |
| Opaque Minerals | 0.7 | 0.6 | 0.4 | 6 | 0.8 | 0.3 | 0.9 | 0.7 |
| Sum. | 100 | 100 | 100 | 100 | 100 | 100 | 100 | 100 |

(b)

| Rock types | Layered gabbros | | | | | | | | | | | | | Marginal gabbro | | | | | |
|---|---|---|---|---|---|---|---|---|---|---|---|---|---|---|---|---|---|---|---|
| Sample No. | W45a | W45b | W46 | W51 | W55 | W57 | W61 | W60 | W62 | W64 | W67 | W71 | W72 | W73 | W74 | W75 | W76 | W77 | W78 |
| Plagioclase | 51 | 49.4 | 58.1 | 34.9 | 50 | 32.4 | 45.9 | 45.7 | 44.2 | 64.1 | 50.2 | 35.6 | 52.2 | 39.6 | 50.5 | 33.3 | 38.3 | 45.1 | 38.6 |
| Amphibole | 42.2 | 43.9 | 39.6 | 58 | 41 | 56 | 41.1 | 43 | 38 | 31.9 | 46.2 | 52.7 | 30 | 40 | 41.7 | 46.1 | 43.2 | 46.0 | 46.6 |
| Chlorite | 5.3 | 5.8 | 2 | 6.6 | 7 | 11.3 | 12 | 2.1 | 11 | 3.7 | 2.8 | 2.2 | 7.4 | 1.7 | 2.3 | 2.1 | 1.6 | 1.8 | 2.8 |
| Clinopyroxene | 0 | 0 | 0 | 0 | 0 | 0 | 0 | 8.4 | 6 | 0 | 0 | 0 | 0 | 0 | 0 | 0 | 0 | 0 | 0 |
| Orthopyroxene | 0 | 0 | 0 | 0 | 0 | 0 | 0 | 0 | 0.3 | 0 | 0 | 0 | 0 | 0 | 0 | 0 | 0 | 0 | 0 |
| Opaque Minerals | 1.5 | 0.9 | 0.3 | 0.4 | 2 | 0.3 | 1 | 0.8 | 0.5 | 0.3 | 0.8 | 9.5 | 10.4 | 8.2 | 4.5 | 6.7 | 5.9 | 6.2 | 9.8 |
| Epidote | 0 | 0 | 0 | 0 | 0 | 0 | 0 | 0 | 0 | 0 | 0 | 0 | 0 | 0.5 | 1.0 | 1.8 | 1.3 | 0.9 | 2.2 |
| Sum. | 100 | 100 | 100 | 100 | 100 | 100 | 100 | 100 | 100 | 100 | 100 | 100 | 100 | 100 | 100 | 100 | 100 | 100 | 100 |

( c)

**Table (2.2a)** Granulations % of Mawat gabbros (K-location).

| **Rock types** | **Layered gabbros** | | | | **Pegmatoid gabbro** | |
|---|---|---|---|---|---|---|
| **Sample No.** | K20 | K13 | K11 | K7 | K3 | K6 |
| **Granulated** | 9 | 39.6 | 74.4 | 100 | 25.6 | 23.2 |
| **non-granulated** | 91 | 60.4 | 25.3 | 0 | 74.4 | 76.8 |
| **Sum.** | 100 | 100 | 100 | 100 | 100 | 100 |

**Table (2.2b)** Granulations % of Mawat gabbros (W-location).

| **Rock types** | **Layered gabbros** | | | | **Marginal gabbro** | |
|---|---|---|---|---|---|---|
| **Sample No.** | W60 | W46 | W45b | W7b | W76 | W78 |
| **Granulatied** | 8.2 | 18.7 | 51.5 | 100 | 70.3 | 75.9 |
| **non-granulated** | 91.8 | 81.3 | 48.5 | 0 | 29.7 | 24.1 |
| **Sum.** | 100 | 100 | 100 | 100 | 100 | 100 |

**Table (2.2c)** Granulations % of Mawat gabbros (R-location).

| **Rock types** | **Layered gabbros** | | | |
|---|---|---|---|---|
| **Sample No.** | R93 | R88 | R79 | R78 |
| **Granulated** | 5.5 | 15 | 36.8 | 100 |
| **non-granulated** | 94.5 | 85 | 63.2 | 0 |
| **Sum.** | 100 | 100 | 100 | 100 |

## 2.2 Petrography :

Basic rocks in the present study are composed of the primary minerals plagioclase and pyroxene (clinopyroxene and in rare cases orthopyroxene), secondary mineral assemblages include secondary amphiboles, chlorite, epidote, sericite, and opaque minerals.

Mineral and texture modifications in the studied rocks are the result of variable degrees of deformation and alteration. Many cumulus fabrics may be obscured by deformation and recrystallization during obduction (Best, 1982). Some of the studied rocks retained their original textures despite of alteration and deformation. Three types of deformation were recorded including crystal-plastic deformation, semibrittle deformation and brittle deformation.

Crystal-plastic deformation is marked by increasing abundance of mechanical twins, subgrains due to granulation in plagioclase ( Miller et al., 2003).Brittle deformation includes localized zones of highly deformed features, whereas semi-brittle deformation was assigned to features of both brittle and crystal-plastic structures (Blackman et al, 2006).

Two types of alteration can be distinguished; pseudomorphic and nonpseudomorphic. Both alteration types are pervasive, but the former indicates that the primary features are preserved, whereas in the latter destroyed.

Depending on field observations; three types of basic igneous rocks are recorded in the study area; layered gabbro, marginal gabbro, and dyke of pegmatoid gabbros. The description of these rocks is given as following:

### 2.2.1 Layered gabbro:

Layered gabbro is composed of alternating plagioclase rich and pyroxene rich layers. The pyroxene has been completely or partially altered to secondary amphibole (urilite) and chlorite .Under the microscope, most of the pyroxene minerals in these rocks are observed as relicts within the amphibole minerals.

Uralitization and sussuritization are typical alteration types in these rocks. Variable degrees of deformation are observed and hence the layered gabbro displays wide varieties of microstructure ranging from crystal-plastic to brittle features.

The layered gabbro samples show several narrow shear zones. In these zones and at the contact with the ultramafic body, the plagioclase and to lesser extent secondary amphiboles are granulated, and in many cases they also impregnated with opaque minerals. Most of these zones underwent extensive mineralogical and textural modifications.

Quartz occurs in a few samples. It is found in the western part of the studied area in the lower part of K-location.

Petrographical observation shows two types of textures; primary and deformation textures. Igneous textures that are completely free of any crystal-plastic pseudomorphic (overprint) are extremely rare, and are mainly found and preserved in the fine grained rocks. In the more common coarser grained rocks, the most pristine igneous texture consists of plagioclase with secondary twins, undulose extinction and/or subgrians which are described below.

Layered gabbros show a hypediomorphic granular texture (Plate 2.1.1). Most intrusive basaltic magmas crystallize by slow sequential growth of minerals producing hypediomrphic granular texture (Best, 1982). This texture has been found and described in many arc plutonic complexes; Vizcono Peninsula/California (Kimbrough and Moore., 2003), Oman ophiolite Suite (Shastry et al., 2001) and in Sazava intrusion, central Bohemian pluton (Janousek et al., 2004).

Poikilitic texture is also observed where secondary amphiboles oikycrysts enclose plagioclase chadacrysts (Plate 2.1.2) and shows plagioclase with reactional margins surrounding them. Sapountzis, (1979) suggested in his study on Thessalaniki gabbros that the plagioclase and clinopyroxene have been partially replaced by amphibole through reaction of the primary crystals with the liquid. The poikilitic texture is considered a common textural feature in Jormua ophiolite, Finland (Peltonen et al., 1998), and in gabbros from Aksaray and Kayseri regions, Turkey (Kocak et al., 2005).

Plate (2.3) shows intergranular texture, where the secondary amphiboles form grains interstitial with the plagioclase. Layered gabbro samples also have ophitic texture (Johannsen, 1931), Plate (2.1.4) illustrates subhedral and anhedral crystals of plagioclase which randomly arranged and completely enclosed in the secondary amphibole. Often, the plagioclase crystals penetrate into, but are not enclosed in the secondary amphibole. In this case, the sub-ophitic texture is developed (Plate 2.1.5). The ophitic and sub-ophitic textures have been described in many ophiolites of the world such as; Gabbroic pluton,Yildizeisivas Region, Turkey (Boztug et al., 1998), the Poanti-Karsanti ophiolite, Southern Turkey (Parlak, 2000), and Tuludimtu ophiolite suite, Western Ethiopia (Tadesse and Allen., 2005).

## Plate (2.1)

**Plate (2.1.1): Photomicrograph of sample K43 (X.N.), showing hypediomorphic granular texture in layered gabbro.**

**Plate (2.1.2): Photomicrograph of sample K36 (X.N.), poikilitic texture consisting of secondary amphiboles oikycrysts enclose plagioclase chadacrysts**

**Plate (2.1.3): Photomicrograph of sample K40 (X.N.), exhibiting intergranular texture including amphibole grains interstitial to the plagioclase.**

**Plate (2.1.4): Photomicrograph of sample K41 (X.N.), showing ophitic texture, plagioclase crystals which are completely enclosed in the amphibole.**

**Plate (2.1.5): Photomicrograph of sample W64 (X.N.), showing sub-ophitic texture, plagioclase crystals are partially enclosed in the amphibole.**

## Plate (2.1)

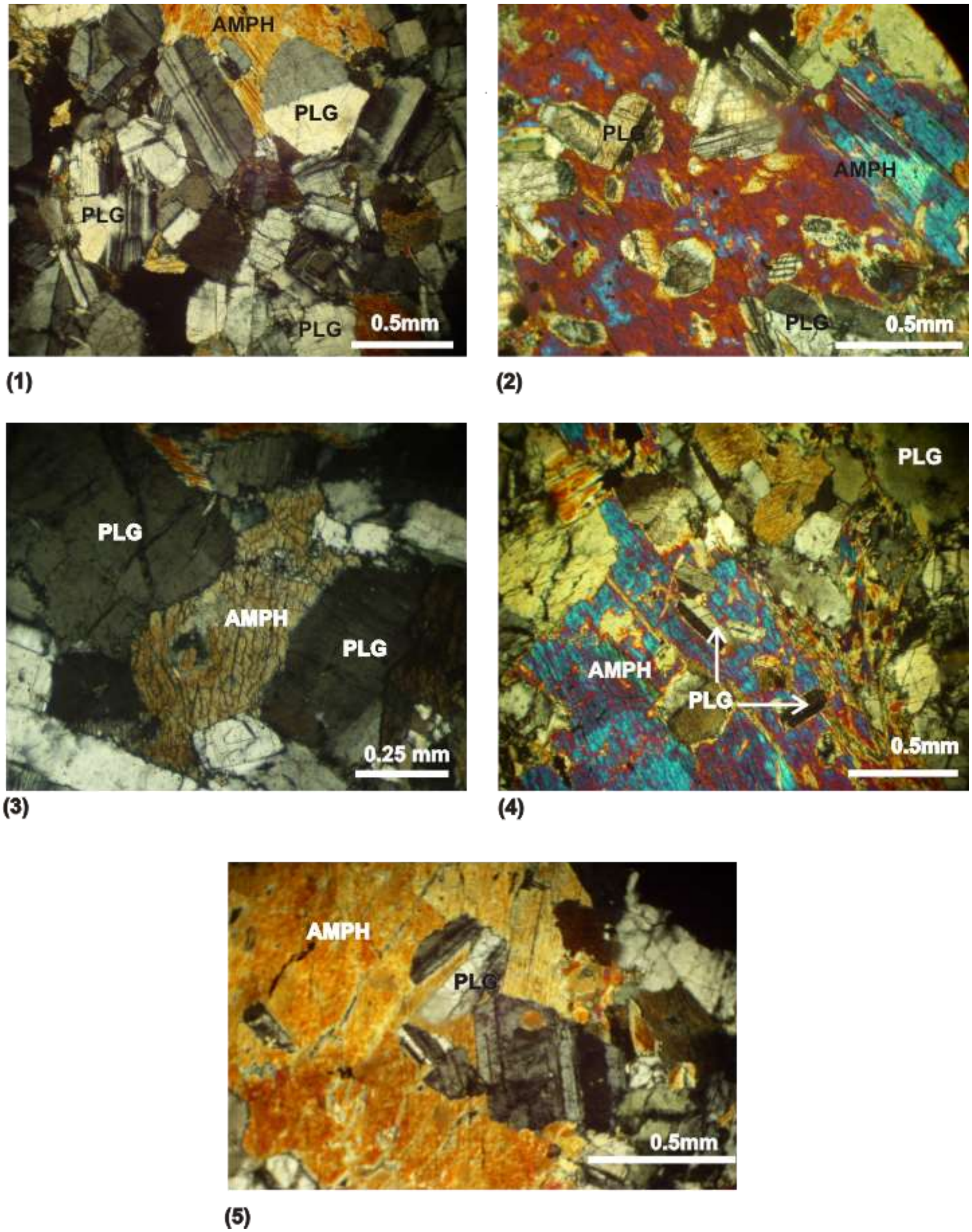
AMPH
PLG
PLG
PLG
0.5mm
(1)
PLG
AMPH
PLG
0.5mm
(2)
PLG
AMPH
PLG
0.25 mm
(3)
PLG
AMPH
PLG
0.5mm
(4)
AMPH
PLG
0.5mm
(5)

***Plagioclase*** is the most important constituent of the layered gabbro. Modal proportions of plagioclase vary between (18.6 -65) percent. The wide range of modal plagioclase is due to sampling related to layering nature. Plagioclase has mostly undergone granulation which affects grain size and shape, and its morphology ranges from subhedral unaffected by fracturing or granulation to anhedral. The grain size ranges from fine (mean size=0.3mm) to relatively coarse (4.0mm). Petrographic examination (using Michel-Levy estimates) showed that most of plagioclases are Bytownite in composition (An 85). Plate (2.2.1) shows relatively fresh plagioclase crystals, almost without trace of deformation.

Some of the thin sections from layered gabbros show crystal-plastic deformation where plagioclase displays undulose extinction, deformatiom twins, and subgrian formation where local patches of plagioclase subgrains on the margins of large grains were observed, particulary where the larger grains impinge on each other (Plate 2.2.2), where annealing recrystallizaion with sutured boundaries of smaller subgrains is obvious. Plate (2.2.3) clearly shows granulation of plagioclase into narrow zones along grain boundaries and internal cracks.

The semi-brittle deformation processes began at the end of crystal plastic deformation, in some cases; several of the most highly deformed samples contain plagioclase with tails of polygonal smaller subgrains (Plate 2.2.4).

# Plate (2.2)

**Plate (2.2.1): Photomicrograph of sample W61 (X.N.), showing relatively fresh plagioclase crystals.**

**Plate (2.2.2): Photomicrograph of sample K22 (X.N.), exhibiting granulation of plagioclase along grain boundaries.**

**Plate (2.2.3): Photomicrograph of sample K25 (X.N.), showing granulation in to narrow zone along internal cracks.**

**Plate (2.2.4): Photomicrograph of sample R86 (X.N.), showing plagioclase with tails of polygonal subgrains due to deformation.**

**Plate (2.2.5): Photomicrograph of sample R88 (X.N.), exhibiting schistose texture.**

**Plate (2.2.6): Photomicrograph of sampleR85 (X.N.), exhibiting mortar texture with completely granulated plagioclase crystals.**

# Plate (2.2)

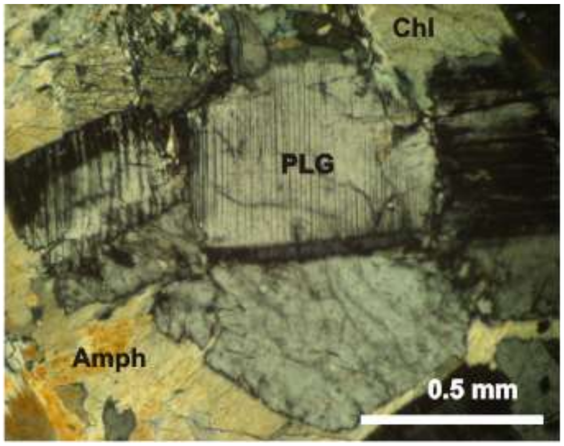


(1)

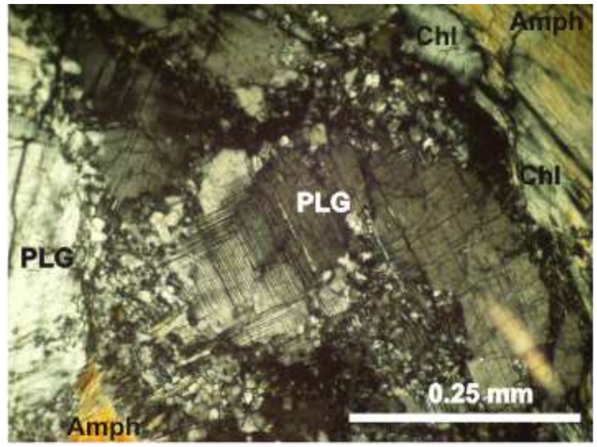


(2)

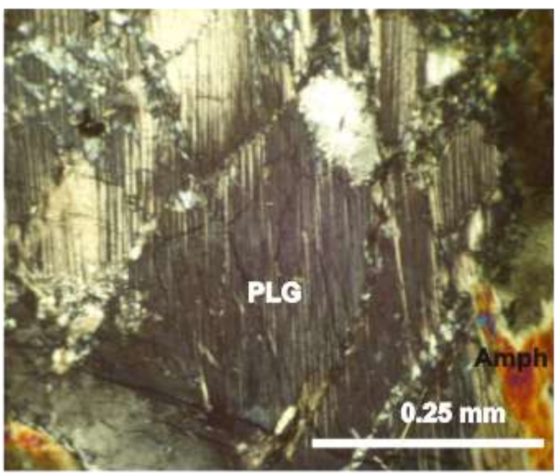


(3)

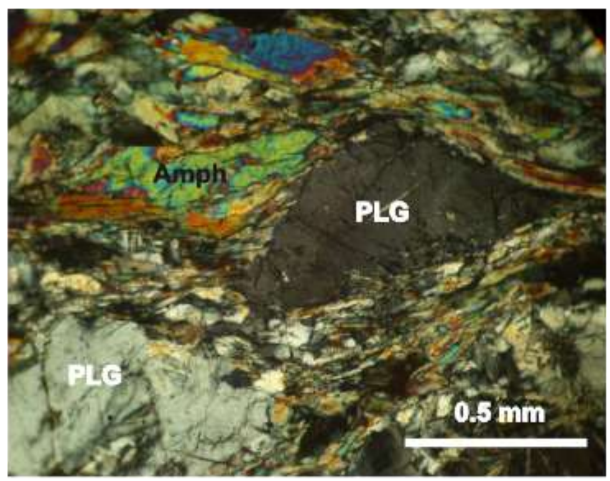


(4)

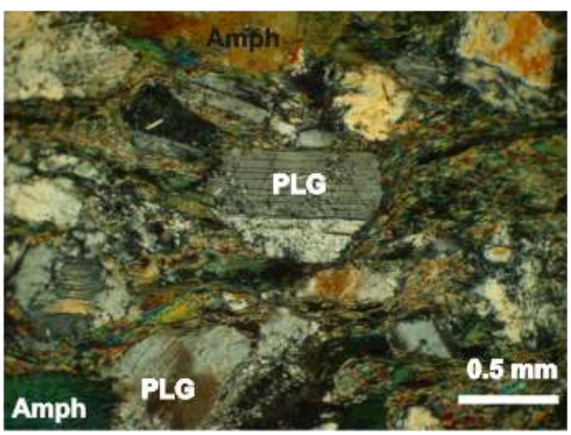


(5)

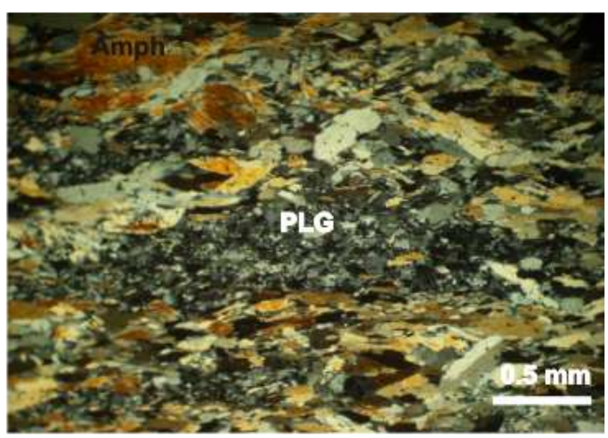


(6)

Samples near the contact between layered gabbro rocks and ultramafic body and near shear zones show more intense granulation by the influence of brittle deformation, which affected plagioclase by the formation of fine crystals. Also these rocks show a schistose texture (Plate 2.2.5).

Where the deformation intensity increase, the mortar texture is developed (Plate 2.2.6). It also shows completely granulated plagioclase crystals and more abundant acicular secondary amphiboles.

Deformation twining is also observed, Plate (2.3.1) illustrates curvature of the lamellae. The twin lamellae also show tapering away toward undeformed area, which is noted by cross twin lamellae (Plate 2.3.2).

Some plagioclase crystals can distinctly show displacement of twins lamellae along micro fracture which have developed within the crystal (Plate 2.3.3). Plate (2.3.4) illustrates uralitic amphibole which is invaded by plagioclase lath in shape.

Some plagioclase grains are clouded by abundant disseminated opaque minerals, acicular secondary amphibole and sericite (Plate 2.3.5).

In all specimens examined, plagioclase is the most stable phase, over large intervals of the layered gabbro; alteration of plagioclase is limited to narrow zones and enclose variable amounts of chlorite along cracks and grain boundaries (Plate 2.3.6). The most extensive alteration of plagioclase occurs in sheared rocks where the original grains are granulated, within these zones

the plagioclase crystals may also be replaced by minor epidote due to saussuritization process.

## Plate (2.3)

**Plate (2.3.1): Photomicrograph of sample K37 (X.N.), showing secondary twinning in plagioclase with tapering and curvature of the lamellae.**

**Plate (2.3.2): Photomicrograph of sample K43 (X.N.), showing cross lamellae in plagioclase due to deformation.**

**Plate (2.3.3): Photomicrograph of sample K13 (X.N.), showing displacement of twins lamellae along micro fractured in plagioclase.**

**Plate (2.3.4): Photomicrograph of sample W67 (X.N.), showing amphiboles which is invaded by plagioclase lath.**

**Plate (2.3.5): Photomicrograph of sample W55 (X.N.), showing plagioclase grains clouded by abundant disseminated opaque minerals, aciculare secondary amphibole and sericite**

**Plate (2.3.6): Photomicrograph of sample W64(X.N.), showing alteration of plagioclase is limited to narrow zones and enclose minor amounts of chlorite along cracks and grain boundaries**

# Plate (2.3)

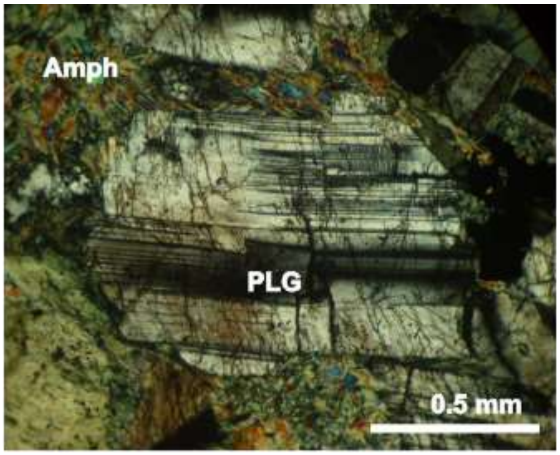

(1)

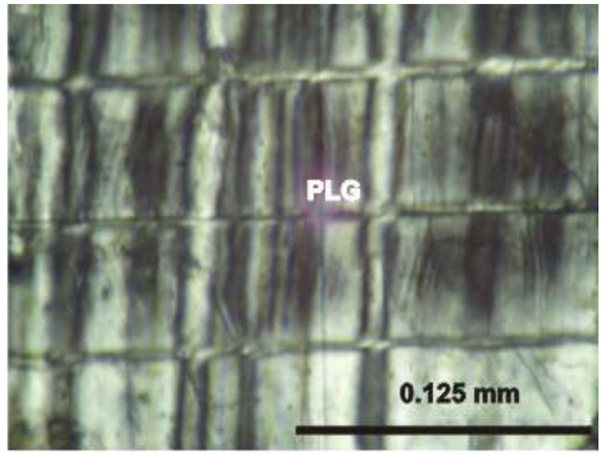

(2)

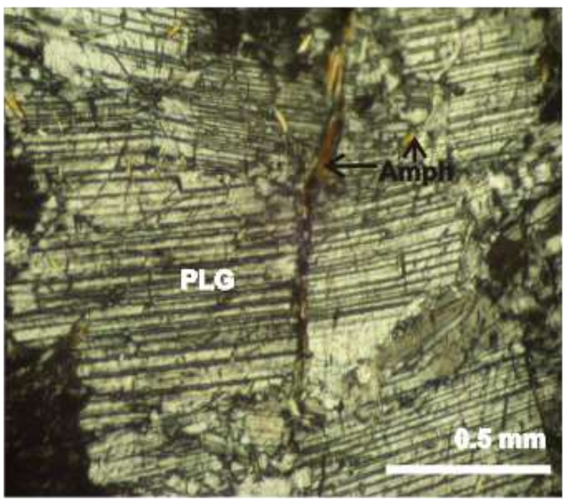

(3)

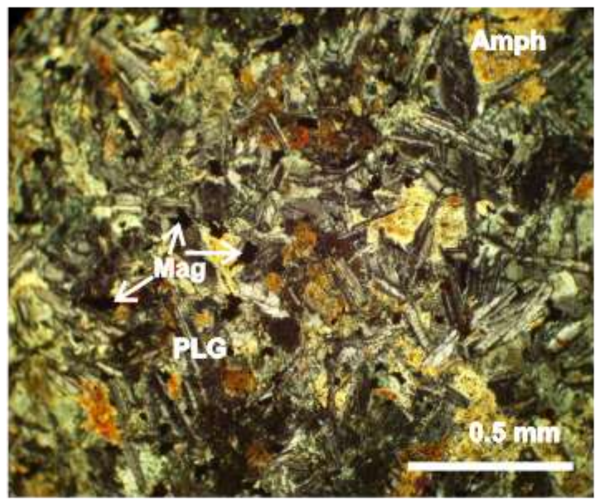

(4)

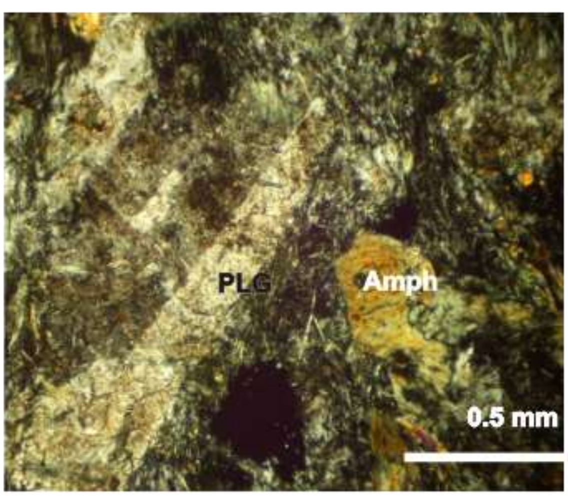

(5)

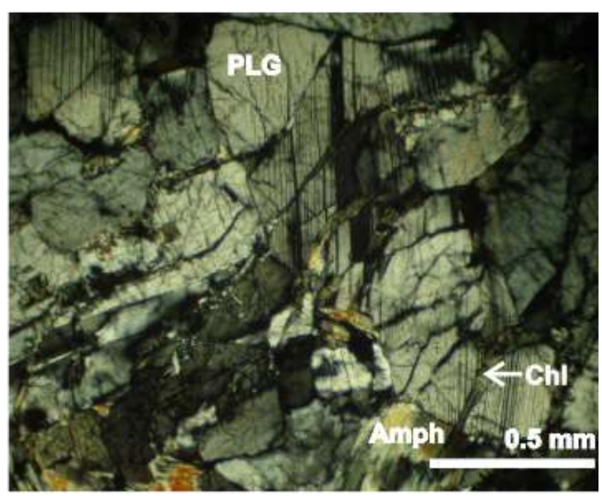

(6)

***Urilite*** is the major secondary mineral after pyroxene of the samples that had been studied in the layered gabbros. It is green in colour and strongly pleochroic in thin sections, from brownish green to deep green.

Two types of secondary amphibole are distinguished; less fibrous with anhedral to subhedral, and the distinctly fibrous amphibole. Both types are secondary in origin formed by uralitization product of pre-existing pyroxenes.

Throughout most of the rocks, the pyroxene is variably effected by alteration, more intense alteration is almost always adjacent to the contact between layered gabbro and dunite body and in the shear zone, hence, it is difficult to distinguish fresh pyroxene crystals, where relicts of pyroxene present within secondary amphiboles. Pyroxene is mainly augite, and occurs as colorless with weak peleochroism with extinction angle is equal 42.

The amphiboles form (25-74.5) percent of the total volume of the rocks, depending on the percentage of original pyroxenes.

The distinctly fibrous secondary amphiboles occur mainly in the shear zones and along contact with dunite body where the rocks have been deformed, but occur elsewhere as well, in contrast, the less fibrous secondary amphibole occurs in slightly deformed rocks. Shear zones are characterized by bands of granulated original plagioclase and elongated secondary amphibole. In many instances, the pyroxene grains are completely altered to fibrous secondary amphiboles (tremolite- actinolite). Plate (2.4.1) shows bending along cleavage planes in amphibole due to deformation.

The alteration occurs almost exclusively along the margins of the pyroxene grains and penetrates into the crystals along cleavage planes and / or along fractures, alteration also extends into adjacent plagioclase grains along fractures. The secondary amphibole may be accompanied by small amounts of pale green chlorite (Plate 2.4.2). This plate clearly shows kink bands.

The secondary amphibole is also present as pale green acicular (needle-like) crystals, this amphibole shows weak pleocroism and varies from pale green to very pale green. Acicular crystals of amphiboles also appear within coarse plagioclase crystals (Plate 2.4.3). In some samples, the secondary amphibole has frayed margins penetrating into the adjacent plagioclase crystals particularly where the grains impinge on each other due to deformation (Plate 2.4.4). These frayed margins resulted from slipping along cleavage planes.

Plate (2.4.5) shows fractures cutting plagioclase crystals which are filled with green amphiboles, occasionally, with minor amount of chlorite.

Secondary amphiboles generally show undulose extinction, displacement along microfractures, microfaults, slipping along cleavages and secondary twining (Plate 2.4.6). All these are deformational features.

# Plate (2.4)

**Plate (2.4.1): Photomicrograph of sample R45b (X.N.), showing bending along cleavage planes due to deformation in amphibole.**

**Plate (2.4.2): Photomicrograph of sample W45a (X.N.), showing the secondary amphibole which are accompanied by small amounts of pale green chlorite with kink bands.**

**Plate (2.4.3): Photomicrograph of sample K20 (X.N.), showing acicular crystals of secondary amphibole appear in coarse plagioclase crystals**

**Plate (2.4.4): Photomicrograph of sample K35 (X.N.), showing the secondary amphibole has frayed margins and penetrating into the adjacent plagioclase crystals.**

**Plate (2.4.5): Photomicrograph of sample K19 (X.N.), showing fractures cutting plagioclase crystals which are filled with green amphibole.**

**Plate (2.4.6): Photomicrograph of sample K37 (X.N.), showing secondary twining and microfault in amphibole.**

# Plate (2.4)

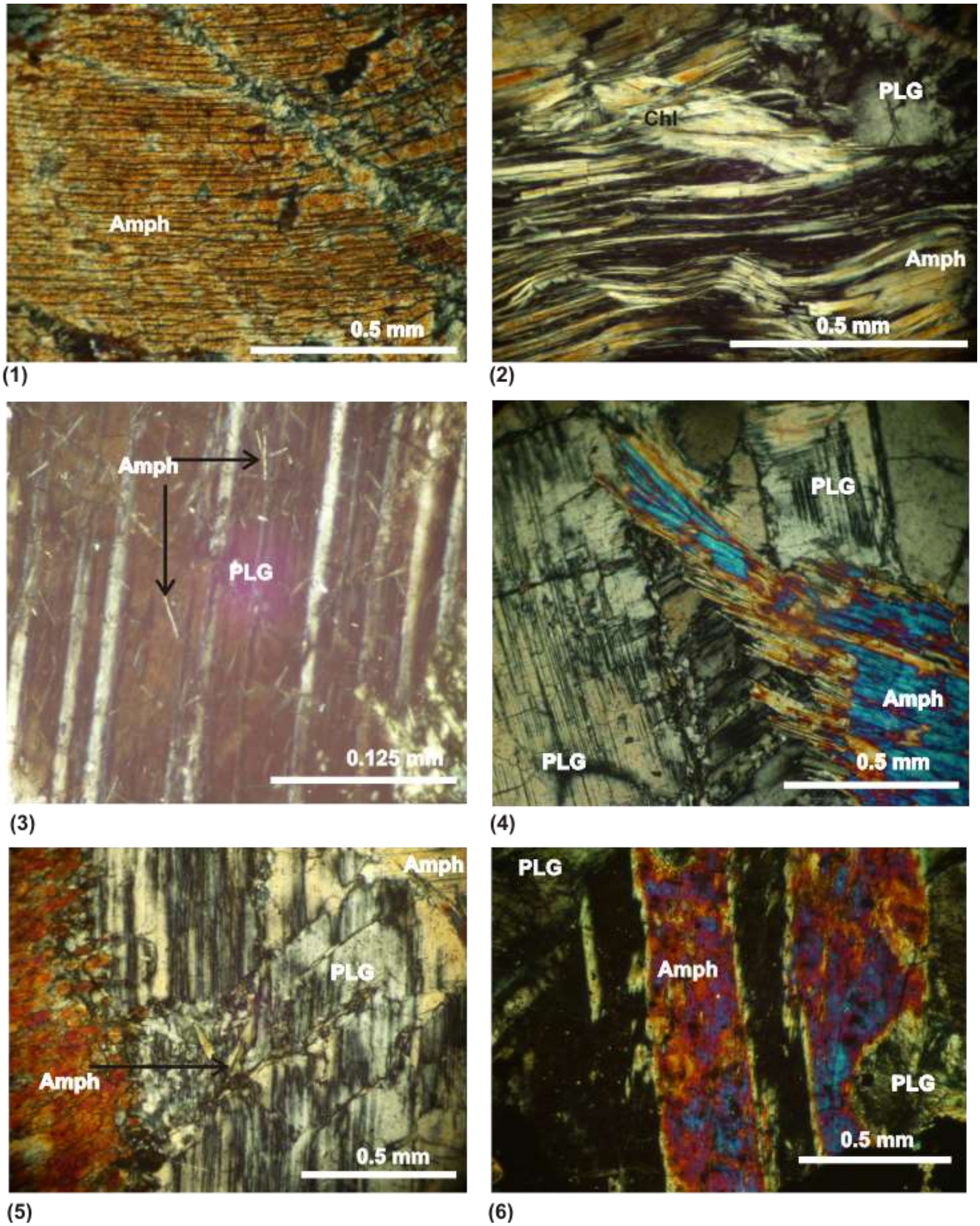
Amph
0.5 mm
(1)
Chl
PLG
Amph
0.5 mm
(2)
Amph
PLG
0.125 mm
(3)
PLG
Amph
PLG
0.5 mm
(4)
Amph
PLG
Amph
0.5 mm
(5)
PLG
Amph
PLG
0.5 mm
(6)

***Chlorite*** ranges from 1-12 percent of the total volume of the layered gabbros, with pale green colour and faint pleochroism. Chlorite occurs as patches and present in many thin sections subordinate to secondary amphibole. It occurs as an alteration product (chloritization) after the pyroxenes and secondary amphiboles minerals. Its occurrence in the deformed plagioclase grains is rather restricted to the cracks, fractures, and grain boundaries.

***Epidote*** commonly occurs in small amount (Table 2-1). It is rare and restricted in the layered gabbroic rocks. It is usually found as an alteration product of the plagioclase due to sassuritization (epidotization) within sheared rocks.

***Opaque minerals*** are mostly magnetite ranging in amount (0.2-10.4). They form disseminated aggregates of very fine grained, or in some cases, occur as single grains and is commonly associated with alteration of pyroxene to secondary amphiboles (Plate 2.5.1), there is generally a strong association between oxide-rich regions and highly deformed and altered regions.

### 2.2.2 Marginal Gabbro:

Modal analysis of the marginal gabbro samples is shown in Table (2.1b). It is composed of plagioclase, fibrous secondary amphibole, chlorite, epidote, and secondary oxides.

Distinctly fibrous secondary amphiboles are mainly (tremolite actinolite) depending on extinction angle (13-21),they range in colour from colourless-yellowish green to strongly pleochroic ranging from deep green to yellowish green probably due to the higher Fe-content, and have elongated shape.

***Plagioclase*** varies in grain size (0.2-1.0 mm) and shape due to granulation. It is (An 80) in composition depending on extinction angle (36).

***Acicular secondary amphibole*** is also common in the marginal gabbro samples. In many cases, the plagioclase crystals are invaded by acicular crystals of amphiboles which might indicate that deformation took place after solidification of the marginal gabbro rocks.

***Chlorite*** is flaky in shape and mainly found as alteration product, also the marginal gabbros show abundant magnetite (Plate 2.5.2).

***Epidote*** is in general, more abundant than in the layered gabbro and pegmatoid gabbro, it is found as single crystals and small grain aggregates (Plate 2.5.3).

Marginal gabbro samples show high alteration intensity than the layered gabbro and dyke of pegmatoid gabbro rocks and the nonpseudomorphic alteration type is the most common.

The marginal gabbro samples show orientation forming a weak foliation manifested by the alternating of plagioclase and ferromagnesian minerals (distinctly fibrous secondary amphibole and/or chlorite). In this case, a schistose texture is formed. This tectonic texture is the most common texture and is observed in all thin sections of the marginal gabbro samples.

### 2.2.3 Dyke of Pegmatoid Gabbro:

The primary minerals in pegmatoid gabbro include calcic plagioclase which is the most abundant mineral in the studied specimens of the pegmatoid gabbro, followed by clinopyroxene and magnetite .The secondary mineral assemblages include secondary amphiboles and chlorite. Modal analysis is shown in Table (2.1a).

The majority of plagioclases are fresh without any traces of alteration and they show limited granulation near boundaries of large plagioclase grains (Plate 2.5.4). In general, plagioclase grains of the pegmatoid gabbro display undulose extinction, subgrain formation and deformation twins.

Also noteworthy, the pegmatoid gabbro samples are slightly altered where the style and intensity of alteration in these rocks is different from that in layered gabbros and marginal gabbros which show partial to complete alteration. The pseudomorphic alteration is most common in the pegmatoid gabbro samples and strongly related to crystal-plastic deformation. In addition, the studied rocks of pegmatiod gabbro are slightly granulated (Table 2.2a).

***Pyroxene*** forms (4.1-13.1) percent of the modal, and it is relatively fresh without alteration, colorless with weak pleochroism, and it is augite in composition according to extinction angle ($44^0$).

In some cases, the secondary amphiboles occur as small blebs within the pyroxene grains, some of which are aligned along cleavage planes, as well as, vein fillings by secondary amphibole (Plate 2.5.5).

***Amphiboles*** are secondary, by replacement after pyroxene minerals. It is less fibrous and green in color and strongly pleochroic, varying from green to brownish green.

***Chlorite*** is pale green in color, flaky in shape.

***Opaque oxide*** occurs within secondary amphibole as alteration product of Fe-rich minerals.

The dyke of pegmatoid gabbro rocks have been found and described in many parts of ophiolite complex in the world; such as ,Apolygenetic ophiolite complex, Central Iran (Ghasemi et al.,2002), Mayari-Baracoa ophiolite belt, Eastern Cuba (Marchesi et al.,2006), Southern Albanian ophiolites (Koller et al., 2006), and in Trinity ophiolite (Stremmel and Suhr., 2007).

## Plate (2.5)

**Plate (2.5.1): Photomicrograph of sample W71 (P.P.L.), showing opaque minerals in the layered gabbro.**

**Plate (2.5.2): Photomicrograph of sample W78 (P.P.L.), showing opaque minerals in the marginal gabbro.**

**Plate (2.5.3): Photomicrograph of sample W78 (X.N.), showing a single crystals and small grain aggregates of epidote in marginal gabbro.**

**Plate (2.5.4): Photomicrograph of sample K3 (X.N.), showing limited granulation near boundaries of large plagioclase grains.**

**Plate (2.5.5): Photomicrograph of sample K3 (X.N.), showing the secondary amphiboles which occur along cleavage planes and veins**

# Plate (2.5)

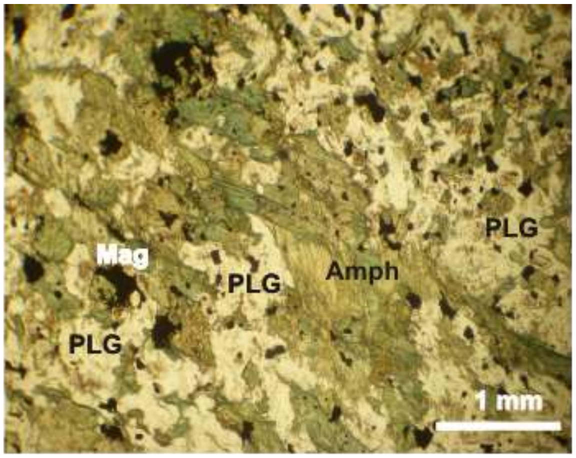


(1)

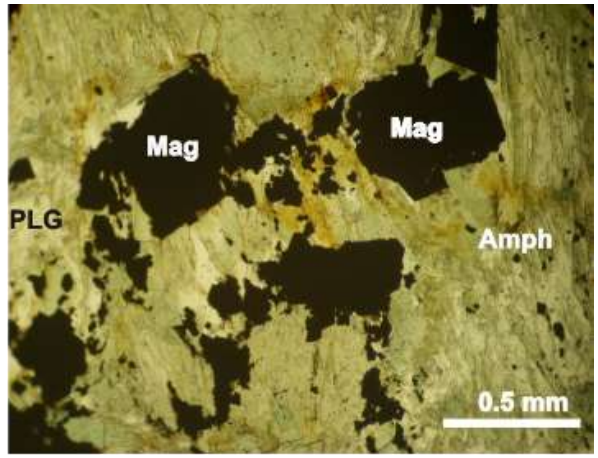


(2)

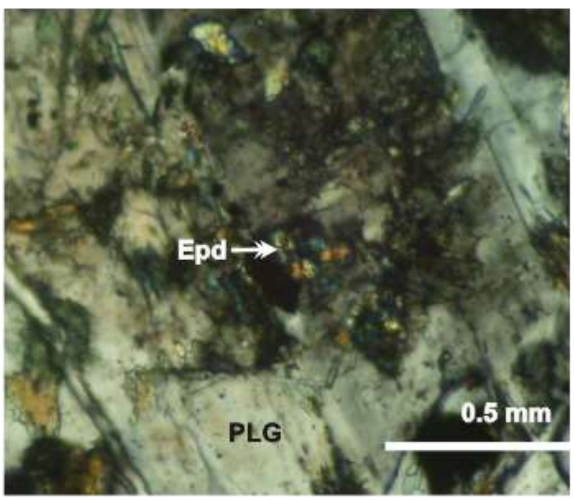


(3)

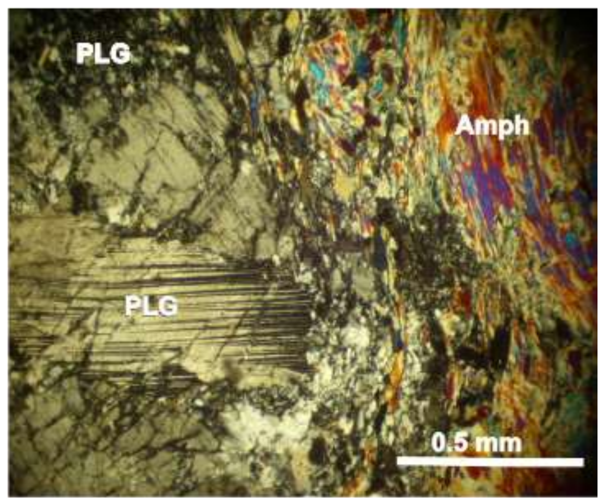


(4)

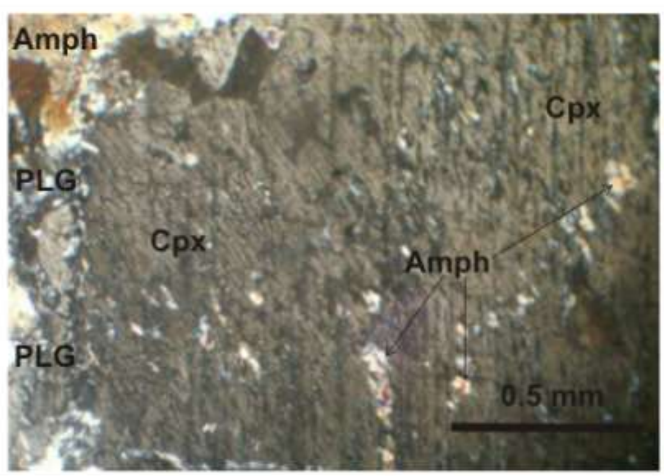


(5)

### 2.3 Discussion:

The gabbros in this study area experience deformation, alteration and/or metamorphism and hence they show complex manifestation. Studied samples are mainly composed of mineral assemblages including plagioclase, pyroxene (clinopyroxene and in rare cases orthopyroxene), secondary amphiboles, chlorite, epidote, sericite, and magnetite.

Based on field relationship, three groups of gabbroic rocks are recognized; the layered gabbro, which is found in the three sections; the marginal gabbro which appears in the lower part of W-sections, and dyke of pegmatoid gabbro which is found in the upper part of K-location.

The three groups show partial to complete alteration. The alteration is pervasive with conversion of pyroxene to secondary amphibole (tremolite-actinolite), in many cases, rough optical continuity with minor amount of chlorite. Coish and others (1986) assumed that the dominance of actinolite/chlorite suggests that clinopyroxene, are the principle original minerals. Plagioclase remains relatively fresh in appearance; it is unzoned with variable grain size and shape due to granulation.

The observations described concerning gabbros of the Mawat ophiolite complex result from the evolution of deformation conditions with time and range from magmatic textures to deformation textures. The former includes hypediomorphic granular, intergranular, poikilitic, ophitic, and sub-ophitic textures. The deformation textures are most common in studied samples, where cumulus fabrics may be obscured by deformation during obduction (Best.,1982). Deformational twining of plagioclase is common where the studied samples show bending, tapering, and crossing of different sets.

Augustithes, (1978) indicated that most polysynthetic deformation twins of plagioclase takes place by post solidification processes.

The layered gabbro samples show crystal-plastic deformation, where the transition from igneous textures to crystal-plastic deformation texture is marked by increasing abundance of deformation twins, subgrain boundaries in plagioclase. These types of deformation took place under high temperature were more likely deformed at temperature near solidus (Blackman et al., 2006). It is important to note that the gabbros of ophiolites are related to derivation from fast-spreading ridges, such as Oman ophiolite (Nicolas, 1989), do not have extensive crystal-plastic fabrics.

Some of plagioclase crystals are clouded by microscopic inclusions of iron oxide, sericite, epidote, and acicular amphibole. This is attributed to introduction of some component or to exsolution due to metamorphism (Whintney, 1972).

In a few samples, e.g. sample K33, K24, K30 and K33a; quartz is present as a fine grain aggregate and vein-filling, as also observed by Jassim (1972) in the western part of the banded gabbro of the Mawat ophiolite complex near Amadin area representing zones of minor acidic intrusions and he concluded that this mineral was introduced after the crystallization of gabbro due to the emplacement.

Urilitization and sussuritization are most common in gabbros of the studied samples. Jassim (1973) assumed that urilitization of the Mawat ophiolite complex took placed before the deformation.

The microscopic textural features of these rocks, the unzoned nature of minerals and their modal variation in abundance strongly suggest that they are cumulate in origin. The pseudomorphic habit of secondary minerals clarifies that this alteration is hydrothermal in origin. Such type of alteration have been described in many worldwide ophiolites; in gabbro of North Cape, New Zealand (Hopper and Smith,1996), in Troods massif, Cyprus(Gass and Swewing, 1973),and have been attributed to hydrothermal circulation of hot sea water.

All samples of the marginal gabbro,at ultramafic/gabbro contacts and in narrow shear zones within the layered gabbro had undergone shearing. In this case, schistose texture is well developed. Al-Hassan (1982) indicated that the schistose texture in Penjwin gabbros reflects the emplacement and thrusting movement. Williams et al. (1954) and Hatch et al. (1961) assumed that in sheared and schistose rocks, much of the feldspars may be granulated to smaller size and much or all the pyroxenes are replaced by fibrous amphiboles. Such types of processes are attributed to low-temperature/high stress i.e. upper green schist farcies conditions (Blackman et al., 2006).

In general these rocks have absence of annealing in these textures indicating a solid state deformation (Agar and Liod, 1997).This type of deformation has been recorded by many authors e.g. Terry and Heidelbach, (2006) and Ilnicki (2002).The pervasive of deformation in solid state and schistosity, and in some rocks overprint of metamorphism effects were recorded in the fabrics of Alpine ultramafic rocks (Best, 1982).

Sheared zones are commonly impregsted with iron oxide minerals, and are typically associated with alteration of ferromagnesian minerals which causes expulsion of iron. The alteration processes are facilitated by fluid penetrating along shear zones, as also recorded by Mevel and Cannat (1991) in the oceanic gabbros from slow-spreading ridges; in the gabbros from

Indian Ocean (Stakes el al., 1991) and in the gabbros from Hess Deep (Mevel and Stamodi, 1996).

The dyke of pegmatoid gabbro sits as schlieren within the ultramafic body (Ser Shiw area). These dykes also were recognized by Al-hassan (1982) in Penjwin complex and his conclusion was that they represent pockets of the anatectic basaltic melt which were not released to high levels. Cannat (1995) indicated that these dyke swarms gabbros were observed in Mid-Atlantic Ridge, and he suggests that the crust in these settings is a complicated mixture of gabbroic plutons and partially serpentinized peridotite and that these observations are related to slow-spreading ridges. It is important to note that the dykes of Mawat gabbros which are observed in the present study were not recorded before among the studies concerning the Mawat ophiolite complex.

## 3.1 Preface

The geochemical characteristics of the gabbroic rocks have been studied through the analysis of thirty-two samples comprising the layered, marginal and pegmatoid gabbros of the three locations for Mawat ophiolite. The results of the analysis of major oxides in weight percent and the trace elements in ppm are given in Table (3.1). Table (3.2) shows the averages of the analysis in the three locations. Rare earth elements concentrations are listed in table 3 (Appendix). Depending on thin section descriptions, it is very difficult to get complete fresh samples without any sign of alteration, where many major and some trace elements show mobility, hence, the emphasis in geochemical study will concentrate on some elements which are relatively less affected by alteration and metamorphism processes. These elements are employed to get more information about fractional crystallization of magma, magmatic affinity as well as tectonic setting.

Major elements analyses were carried out at the State Company for Geological Survey and Mining using wet chemical analyses methods. Trace elements including rare earth elements were analyzed by ICP-JY 170 ULTRALE at Office National DES Hydrocarbures ET DES Mines (ONHYM), Morocco, (Appendix)

Table (3.1): Bulk chemical analysis of major (wt%) and elemenate ratios in K, W and R-locations for the Mawat gabros. GG: World average of rocks (Lamaitre, 1976), and normative mineral persents

| Sample No. | $SiO_2$ | MgO | $Al_2O_3$ | $TiO_2$ | Cao | $Na_2O$ | $K_2O$ | FeO | $Fe_2O_3$ | $FeO^t$ | $H_2O^+$ | $H_2O^-$ | SUM | $FeO^t/MgO$ | Mg# | $Fe_2O_3/FeO+Fe_2O_3$ | Rock type |
|---|---|---|---|---|---|---|---|---|---|---|---|---|---|---|---|---|---|
| K3 | 43.36 | 10.27 | 21.35 | 0.04 | 17.15 | 0.57 | 0.06 | 3.31 | 0.49 | 3.75 | 1.84 | 0.32 | 98.71 | 0.365 | 71.26 | 0.129 | Peg.Gabb |
| K7 | 46.16 | 11.45 | 18.41 | 0.1 | 15.48 | 0.6 | 0.04 | 5.82 | 0.18 | 5.98 | 0.21 | 0.21 | 98.64 | 0.522 | 60.6 | 0.03 | Lay.Gabb |
| K11 | 47.1 | 9.8 | 16.99 | 0.13 | 14.94 | 0.63 | 0.07 | 8.62 | 0.38 | 8.96 | 1.39 | 0 | 100.01 | 0.914 | 47.2 | 0.042 | Lay.Gabb |
| K13 | 44.9 | 12 | 15.5 | 0.11 | 14.9 | 0.49 | 0.02 | 8.19 | 1.01 | 9.09 | 3.01 | 0 | 100.02 | 0.757 | 53.33 | 0.11 | Lay.Gabb |
| K15 | 47.52 | 9.8 | 18.41 | 0.1 | 13.83 | 0.54 | 0.07 | 8.31 | 0.09 | 8.39 | 1.06 | 0 | 99.72 | 0.856 | 47.96 | 0.011 | Lay.Gabb |
| K19 | 46.12 | 11.85 | 14.16 | 0.15 | 15.5 | 0.64 | 0.09 | 7.04 | 1.06 | 7.99 | 1.52 | 0 | 98.02 | 0.674 | 56.93 | 0.131 | Lay.Gabb |
| K20 | 46.56 | 11.3 | 16.52 | 0.11 | 13.7 | 0.42 | 0.07 | 8.62 | 0.53 | 9.09 | 2.17 | 0.01 | 99.95 | 0.804 | 50.74 | 0.058 | Lay.Gabb |
| K24 | 42.2 | 10.82 | 19.2 | 0.28 | 13.83 | 0.92 | 0.09 | 8.62 | 0.68 | 9.23 | 1.55 | 0 | 98.12 | 0.853 | 49.61 | 0.073 | Lay.Gabb |
| K43 | 50.04 | 8.2 | 17.7 | 0.14 | 12.73 | 0.82 | 0.13 | 7.04 | 1.21 | 8.12 | 1.93 | 0.04 | 99.85 | 0.99 | 47.77 | 0.147 | Lay.Gabb |
| K41 | 50.32 | 9.87 | 14.16 | 0.33 | 12.73 | 0.4 | 0.04 | 8.9 | 1.2 | 9.98 | 1.3 | 0 | 99.13 | 1.011 | 46.66 | 0.119 | Lay.Gabb |
| K36 | 47.9 | 9 | 15.81 | 0.4 | 13.73 | 0.84 | 0.04 | 8.04 | 1.66 | 9.53 | 0.82 | 0 | 98.07 | 1.058 | 46.92 | 0.171 | Lay.Gabb |
| K26 | 48.9 | 11.06 | 15 | 0.53 | 10.17 | 0.78 | 0.1 | 8.62 | 3.08 | 11.39 | 1.81 | 0.05 | 99.79 | 1.029 | 50.22 | 0.263 | Lay.Gabb |
| K29 | 47.16 | 10.27 | 14.63 | 0.3 | 13.83 | 1.02 | 0.14 | 8.47 | 2.68 | 10.88 | 0.99 | 0 | 99.22 | 1.059 | 48.77 | 0.24 | Lay.Gabb |
| K32 | 46.22 | 9 | 17.47 | 0.24 | 13.28 | 1.04 | 0.12 | 7.18 | 2.72 | 9.62 | 2.11 | 0.04 | 99.14 | 1.068 | 49.54 | 0.275 | Lay.Gabb |
| K33 | 40.96 | 9.3 | 17.1 | 0.8 | 15.48 | 0.45 | 0.03 | 10.2 | 2.9 | 12.81 | 1.08 | 0.11 | 98.12 | 1.377 | 41.79 | 0.221 | Lay.Gabb |
| W44 | 45.5 | 10.67 | 16.52 | 0.92 | 12.27 | 1.66 | 0.19 | 11.2 | 0.9 | 12.01 | 0.07 | 0.07 | 99.88 | 1.125 | 42.66 | 0.074 | Lay.Gabb |
| W45 | 46.9 | 9.48 | 19.4 | 0.06 | 17.15 | 0.48 | 0.04 | 5.31 | 0.09 | 5.39 | 1.01 | 0 | 99.91 | 0.568 | 45.23 | 0.017 | Lay.Gabb |
| W46 | 47.82 | 14.3 | 16.3 | 0.1 | 11.8 | 0.7 | 0.1 | 6.17 | 1.13 | 7.18 | 1.47 | 0 | 99.77 | 0.502 | 64.66 | 0.155 | Lay.Gabb |
| W51 | 45.7 | 11.46 | 18.41 | 0.11 | 15.49 | 0.73 | 0.06 | 5.17 | 1.33 | 6.36 | 1.37 | 0 | 99.69 | 0.554 | 63.88 | 0.205 | Lay.Gabb |
| W55 | 46.36 | 9.2 | 18.88 | 0.15 | 14.94 | 0.7 | 0.04 | 5.6 | 1.3 | 6.77 | 0.97 | 0.08 | 98.09 | 0.735 | 56.12 | 0.188 | Lay.Gabb |
| W57 | 49.32 | 11.5 | 13.8 | 0.16 | 12.27 | 0.63 | 0.04 | 9.91 | 0.94 | 10.75 | 1.34 | 0.02 | 99.83 | 0.934 | 47.58 | 0.087 | Lay.Gabb |
| W61 | 48.8 | 11.4 | 13.45 | 0.19 | 12.17 | 0.71 | 0.08 | 10.92 | 0.23 | 11.12 | 1.39 | 0.02 | 99.33 | 0.975 | 44.73 | 0.021 | Lay.Gabb |
| W60 | 50.96 | 10.07 | 15.2 | 0.18 | 13.6 | 0.67 | 0.04 | 7.75 | 0.3 | 8.02 | 1.48 | 0.01 | 100.23 | 0.796 | 50.83 | 0.037 | Lay.Gabb |
| W64 | 47.32 | 9.4 | 17.74 | 0.14 | 14.93 | 0.62 | 0.03 | 6.32 | 1.43 | 7.6 | 2.05 | 0.03 | 99.86 | 0.808 | 53.53 | 0.185 | Lay.Gabb |
| W67 | 56.54 | 7 | 12.87 | 0.16 | 13.08 | 0.43 | 0.05 | 7.05 | 0.7 | 7.68 | 2.02 | 0.03 | 99.86 | 1.097 | 43.75 | 0.09 | Lay.Gabb |
| W71 | 47.08 | 11 | 14.8 | 1.25 | 9.95 | 1.33 | 0.1 | 9.05 | 2.6 | 11.39 | 1.83 | 0 | 98.73 | 1.035 | 48.88 | 0.223 | Lay.Gabb |
| W78 | 51.24 | 7.9 | 16.52 | 0.43 | 8.85 | 2.8 | 0.11 | 6.17 | 4.03 | 9.79 | 1.19 | 0 | 98.83 | 1.239 | 50 | 0.395 | Mar.Gabb |
| R78 | 47.32 | 14.2 | 14.16 | 0.1 | 13.83 | 0.62 | 0.06 | 7.04 | 0.71 | 7.67 | 1.76 | 0 | 99.72 | 0.54 | 61.15 | 0.092 | Lay.Gabb |
| R81 | 48.02 | 12.1 | 15.08 | 0.08 | 14.3 | 0.7 | 0.07 | 8.03 | 0.12 | 8.13 | 1.5 | 0 | 99.98 | 0.671 | 54.07 | 0.015 | Lay.Gabb |
| R85 | 48.02 | 9.4 | 18.17 | 0.1 | 16 | 0.52 | 0.04 | 4.88 | 1.92 | 6.6 | 0.83 | 0 | 99.68 | 0.702 | 60.21 | 0.282 | Lay.Gabb |
| R88 | 49.02 | 9 | 17.1 | 0.28 | 12.73 | 0.8 | 0.1 | 10.21 | 0.24 | 10.42 | 0.43 | 0 | 99.88 | 1.157 | 40.9 | 0.023 | Lay.Gabb |
| R93 | 46.42 | 11.25 | 17.94 | 0.06 | 13.82 | 0.66 | 0.02 | 5.17 | 1.18 | 6.23 | 1.7 | 0.03 | 98.13 | 0.553 | 63.55 | 0.186 | Lay.Gabb |
| GG | 50.14 | 7.59 | 15.48 | 1.12 | 9.58 | 2.39 | 0.93 | 7.62 | 3.01 | 10.33 | 0.11 | 0.11 | 97.78 | 0.098 | 57.64 | 0.283 | Gabbro |

(Lay.Gabb,layered gabbro;Mar.marginal gabbro and Peg.Gabb.,pegmatoid gabbro)

Table (3.2): Bulk chemical analysis of trace elements (ppm) in K, W and R-locations for the Mawat gabbros

| samble no | Rock type | Co | Cr | Cu | Ni | Sr | V | Y | Zn | Mn | Zr | Zr/Y |
|---|---|---|---|---|---|---|---|---|---|---|---|---|
| K3 | Peg.Gabb | 84 | 119 | 52 | 142 | 65 | 180 | 7 | 25 | 320 | 21 | 3 |
| K7 | Lay.Gabb | 73 | 282 | 18 | 173 | 105 | 132 | <5 | 19 | 756 | 25 | nd |
| K11 | Lay.Gabb | 76 | 263 | 47 | 143 | 78 | 156 | 6 | 42 | 1094 | 27 | 4.5 |
| K13 | Lay.Gabb | 89 | 208 | 202 | 166 | 98 | 222 | <5 | 39 | 500 | 26 | nd |
| K15 | Lay.Gabb | 80 | 134 | 227 | 110 | 86 | 198 | <5 | 36 | 917 | 21 | nd |
| K19 | Lay.Gabb | 81 | 171 | 233 | 137 | 63 | 261 | 5 | 27 | 923 | 22 | 4.4 |
| K20 | Lay.Gabb | 84 | 185 | 1378 | 176 | 54 | 226 | <5 | 66 | 1108 | 39 | nd |
| K24 | Lay.Gabb | 83 | 99 | 56 | 137 | 109 | 192 | 7 | 44 | 926 | 33 | 4.7 |
| K43 | Lay.Gabb | 88 | 104 | 123 | 115 | 201 | 570 | 7 | 44 | 807 | 33 | 4.7 |
| K41 | Lay.Gabb | 76 | 363 | 9 | 149 | 122 | 240 | 10 | 67 | 1410 | 31 | 3.1 |
| K36 | Lay.Gabb | 75 | 250 | 217 | 146 | 92 | 305 | 9 | 48 | 985 | 35 | 3.8 |
| K26 | Lay.Gabb | 87 | 192 | 95 | 120 | 128 | 540 | 8 | 97 | 1182 | 31 | 3.87 |
| K29 | Lay.Gabb | 79 | 551 | 34 | 194 | 80 | 256 | 9 | 60 | 1138 | 35 | 3.88 |
| K32 | Lay.Gabb | 85 | 64 | 52 | 116 | 158 | 323 | 6 | 61 | 1380 | 22 | 3.66 |
| K33 | Lay.Gabb | 87 | 92 | 111 | 107 | 192 | 622 | 7 | 58 | 1179 | 27 | 3.85 |
| W44 | Lay.Gabb | 115 | 308 | 96 | 241 | 283 | 182 | 18 | 41 | 849 | 45 | 2.5 |
| W45a | Lay.Gabb | 68 | 236 | 68 | 140 | 85 | 117 | <5 | <5 | 650 | 32 | nd |
| W46 | Lay.Gabb | 79 | 216 | 145 | 154 | 75 | 154 | <5 | 25 | 878 | 29 | nd |
| W51 | Lay.Gabb | 75 | 134 | 27 | 147 | 101 | 150 | <5 | <5 | nd | 30 | nd |
| W55 | Lay.Gabb | 73 | 122 | 40 | 119 | 107 | 175 | <5 | <5 | 674 | 30 | nd |
| W57 | Lay.Gabb | 85 | 429 | 113 | 196 | 65 | 217 | 8 | 48 | 1237 | 28 | 3.5 |
| W61 | Lay.Gabb | 91 | 543 | 175 | 221 | 66 | 255 | 10 | 60 | 1273 | 36 | 3.6 |
| W60 | Lay.Gabb | 67 | 398 | 51 | 222 | 117 | 75 | <5 | <5 | 954 | 34 | nd |
| W64 | Lay.Gabb | 77 | 158 | 232 | 142 | 65 | 200 | <5 | 18 | 833 | 33 | nd |
| W67 | Lay.Gabb | 66 | 144 | 22 | 130 | 130 | 220 | <5 | 37 | 1179 | 27 | nd |
| W71 | Lay.Gabb | 88 | 355 | 118 | 181 | 190 | 178 | 17 | 82 | 1128 | 44 | 2.58 |
| W78 | Mar.Gabb | 70 | 128 | 50 | 113 | 106 | 263 | 12 | 73 | 1144 | 33 | 2.75 |
| R78 | Lay.Gabb | 84 | 684 | 155 | 250 | 63 | 164 | <5 | 52 | 903 | 27 | nd |
| R81 | Lay.Gabb | 82 | 135 | 134 | 146 | 69 | 168 | <5 | 36 | 922 | 36 | nd |
| R85 | Lay.Gabb | 71 | 163 | 126 | 143 | 66 | 140 | <5 | 11 | 767 | 30 | nd |
| R88 | Lay.Gabb | 77 | 133 | 26 | 121 | 81 | 123 | 8 | 38 | 1230 | 27 | 3.37 |
| R93 | Lay.Gabb | 74 | 161 | 17 | 133 | 87 | 129 | <5 | <5 | 726 | 18 | nd |

n.d.= Not determined

## 3.2 Comparison with World Average:

The major oxides have been compared with world averages of similar gabbroic rocks given by Lemaitre (1976) (Table 3.1). This shows that the rocks of the present study exhibit the following geochemical characteristics:

1-The MgO and CaO contents are higher than average.

2-Total alumina is about normal.

3-The $TiO_2$, $K_2O$ and $Na_2O$ contents are lower.

4- Total iron is about normal in K-location and slightly lower in W and R location.

These general geochemical characteristics show that the gobbros of the present study are more calcic and mafic than world average. They also reflect their high content of plagioclases and pyroxenes and may support the hypothesis of their origin from mantle materials.

### 3.3 Geochemistry of Major Elements:

The major elements concentration and their averages are illustrated in Tables (3.1 and 3.2). The variations of major oxides with topographic elevations are shown in Figure (3.1a, b and c) and the correlations between them are illustrated from the zigzag patterns. The variabilities in the major oxides contents with elevations could be attributed to layering nature as well as alteration processes.

Taking into account that silica is the dominant contributor to the chemical variance, Harker diagrams have been employed (Fig. 3.2) to show the variations of various oxides against silica, although silica has a variable range of variation (42-51%) and mobile under alteration /and or low grade metamorphism conditions (Hamphis and Thompson, 1978a and 1978b; Miyashiro et al, 1971., Pearce, 1975). FeO and $Fe_2O_3$ are calculated as total iron $FeO^t$ .The diagrams illustrate the following variations:

MgO, $Al_2O_3$ and CaO show very weak negative correlations with $SiO_2$ due to their scattering nature (Fig. 3.2 a, b and d).These relations could reflect the crystallization of pyroxenes and calcic plagioclase from the early stages. The relations between the other oxides; $Na_2O$, $K_2O$, FeOt and $TiO_2$ are not clear (Fig. 3.2 e, f, g and c), which might be related to the mobility of these oxides as well as the mobility of silica.

To clarify more the trends of various oxides and by taking into account that the rocks of the present study are all basic (gabbroic) and Mg-rich mafic minerals crystallize early from basaltic magmas and hence decrease with increasing fractionation processes, MgO relations with other oxides have been recommended on Harker diagrams (Fig. 3.3). $SiO_2$ shows more or less negative relation with MgO (Fig. 3.3 a). This trend may be associated with fractionation of pyroxene minerals which are the first phases to crystallize out of the melt.

Table (3.3): show the minimum, maximum and averages of the analysis in the three locations.

| | K-Location | | | W-Location | | | R-Location | | |
|---|---|---|---|---|---|---|---|---|---|
| **Major Oxides** | **Min** | **Max** | **Aver.** | **Min** | **Max** | **Aver.** | **Min** | **Max** | **Aver.** |
| **$SiO_2$** | 42.2 | 50.32 | 48.36 | 45.5 | 51.24 | 48.62 | 47.32 | 49.02 | 47.76 |
| **$Al_2O_3$** | 14.16 | 21.35 | 16.82 | 12.87 | 19.4 | 16.15 | 14.16 | 18.17 | 16.49 |
| **$TiO_2$** | 0.04 | 0.8 | 0.25 | 0.06 | 1.25 | 0.32 | 0.28 | 0.06 | 0.12 |
| **FeO** | 3.75 | 12.81 | 8.99 | 5.39 | 12.01 | 8.67 | 6.23 | 7.81 | 7.81 |
| **$Fe_2O_3$** | 0.09 | 3.08 | 1.32 | 0.09 | 4.03 | 0.25 | 0.12 | 1.92 | 0.83 |
| **MgO** | 8.2 | 12 | 10.26 | 7 | 14.3 | 10.28 | 9 | 14.2 | 11.19 |
| **CaO** | 10.17 | 17.15 | 14.1 | 8.85 | 17.15 | 13.04 | 12.73 | 16 | 14.13 |
| **$Na_2O$** | 0.4 | 1.04 | 0.68 | 0.43 | 2.8 | 0.95 | 0.52 | 0.8 | 0.66 |
| **$K_2O$** | 0.02 | 0.14 | 0.07 | 0.03 | 0.19 | 0.07 | 0.02 | 0.1 | 0.06 |
| **$H_2O^+$** | 0.21 | 3.01 | 1.52 | 0.07 | 2.05 | 1.35 | 0.43 | 1.76 | 1.24 |
| **Mg#** | 41.79 | 71.26 | 51.28 | 42.66 | 64.66 | 50.98 | 40.9 | 63.55 | 55.97 |
| **$Fe_2O_3/FeO^t+Fe_2O_3$** | 0.011 | 0.275 | 0.134 | 0.017 | 0.395 | 0.139 | 0.015 | 0.282 | 0.119 |
| **$FeO^t/MgO$** | 0.365 | 1.377 | 0.889 | 0.502 | 1.239 | 0.864 | 0.54 | 1.57 | 0.724 |
| **Ni** | 107 | 194 | 142 | 113 | 241 | 167.2 | 121 | 250 | 158 |
| **Cr** | 64 | 551 | 205.2 | 122 | 543 | 264.2 | 133 | 468 | 255.2 |
| **V** | 132 | 622 | 294.9 | 75 | 263 | 182.2 | 123 | 168 | 144.8 |
| **Co** | 73 | 89 | 81.8 | 66 | 115 | 79.5 | 71 | 84 | 77.6 |
| **Sr** | 54 | 201 | 108.7 | 65 | 283 | 115.8 | 63 | 87 | 73.2 |
| **Cu** | 9 | 1378 | 190.3 | 22 | 232 | 44.7 | 17 | 155 | 91.6 |
| **Zn** | 19 | 97 | 48.9 | nd | 82 | nd | nd | 52 | nd |
| **Mn** | 320 | 1410 | 975 | 650 | 1273 | 981.7 | 726 | 1230 | 909.6 |
| **Zr** | 21 | 39 | 28.5 | 18 | 36 | 33.4 | 18 | 36 | 27.6 |
| **Y** | nd | 10 | nd | nd | 18 | nd | nd | 8 | nd |

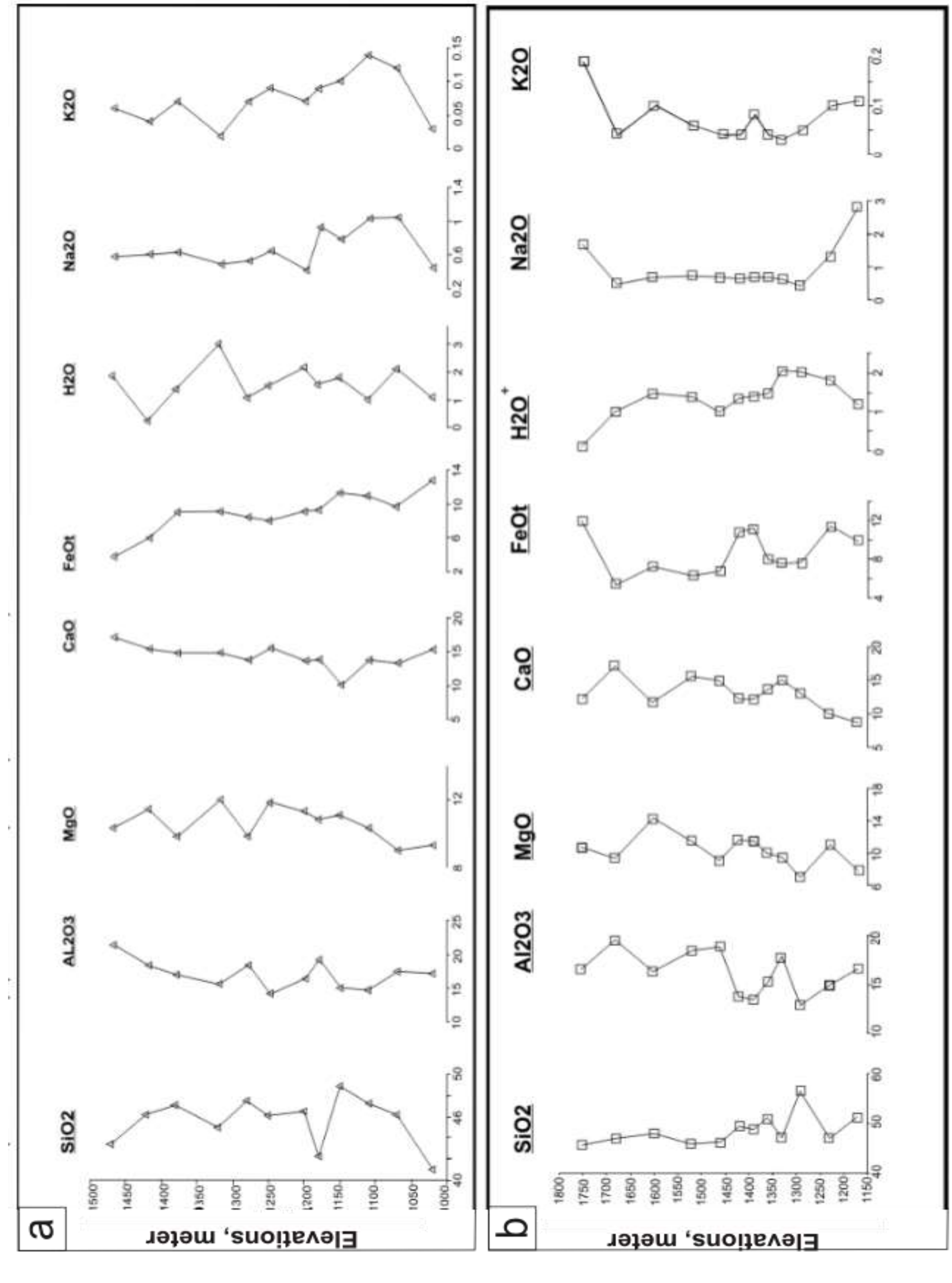


Figure(3.1 a, b and c): Selected major elements versus elevations (meter) for the Mawat gabbros. (a= K- location) and (b= W- location) ( c= R- location)

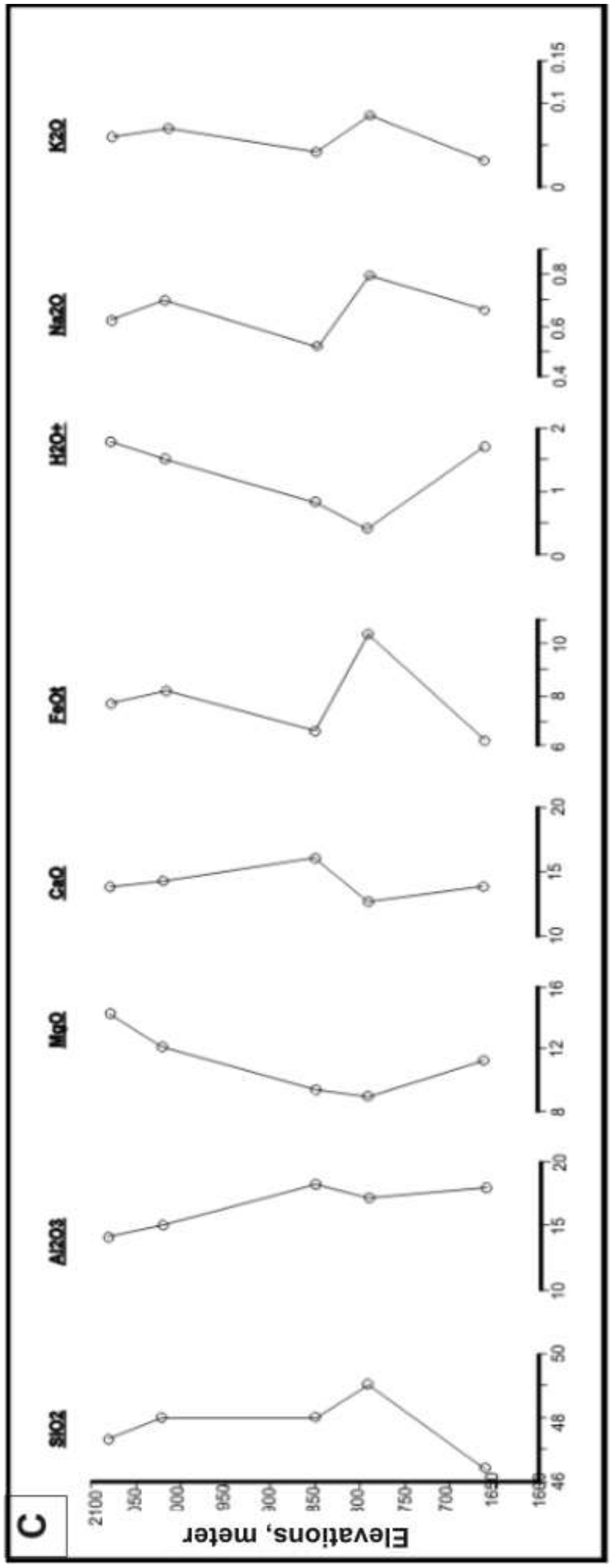


| LEGEND | |
|---|---|
| Sample No | Topographic higher |
| K3 | 1470 |
| K7 | 1420 |
| K11 | 1380 |
| K14 | 1320 |
| K15 | 1280 |
| K19 | 1250 |
| K20 | 1200 |
| K24 | 1180 |
| K26 | 1150 |
| K29 | 1110 |
| K32 | 1070 |
| K33 | 1020 |
| W44 | 1750 |
| W45 | 1680 |
| W46 | 1600 |
| W51 | 1520 |
| W55 | 1460 |
| W57 | 1420 |
| W61 | 1390 |
| W60 | 1360 |
| W64 | 1330 |
| W67 | 1290 |
| W71 | 1230 |
| W78 | 1170 |
| R78 | 2080 |
| R81 | 2020 |
| R85 | 1850 |
| R88 | 1790 |
| R93 | 1660 |

Figure (3.1 ): continued

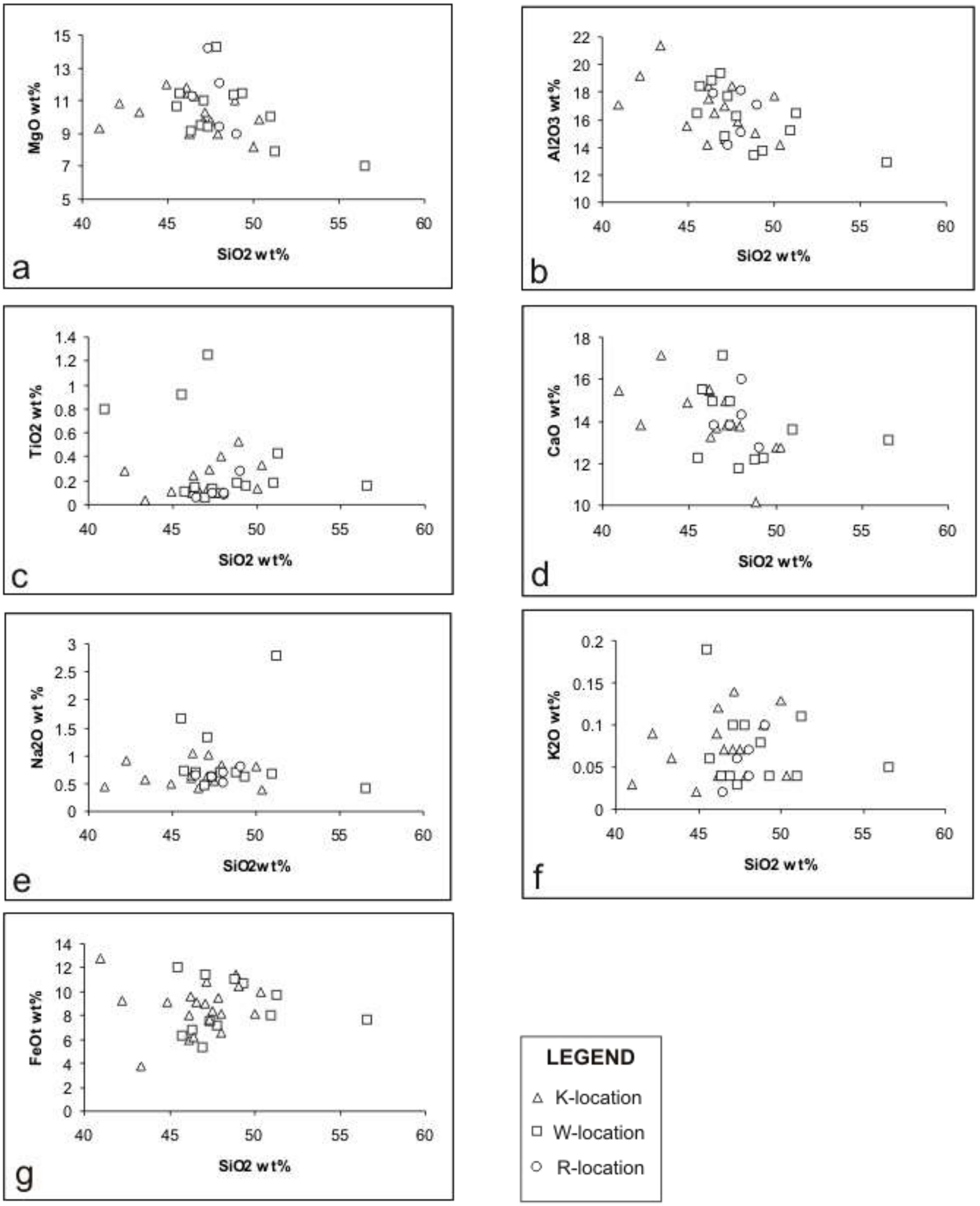


Figure (3.2): Variation diagrams of major oxides with SiO2 of the analyzed samples.

Alumina and CaO show poor positive correlations with MgO (Fig. 3.3 b and c). This is attributed to the crystallization and fractionation of the plagioclase and clinopyroxenes. The fractionation of plagioclase minerals is represented by positive correlation trend when plot $Al_20_3$ against CaO (Fig. 3.4). These elements are primarily correlated with the modal abundance of plagioclase. Cann, (1969); Coish, (1977) and Humphris and Thompson, (1978b), indicated that the $Al_2O_3$ is immobile under alteration conditions. Iyer and Ray( 2003) indicated that Al shows no conclusive exchange between seawater and ocean-floor basalt (OFB). While CaO and MgO are mobile under alteration conditions (Hajash, 1975., Bischoff and Dickson, 1975., Coish, 1977).

The lack of good correlation trends of MgO with $Na_2O$, $K_2O$ and $FeO^t$ (Fig. 3-3 d, e and f) is attributed to the mobilities of these oxides during alteration.

MgO relation with $TiO_2$ (Fig. 3.3 g) indicates contribution of $TiO_2$ in the later stage, the mineral phase crystallizing is titano-magnetite).This is supported by the positive relation between FeO and $TiO_2$ (Fig. 3.5).

$Fe_2O_3$ content considered a scale for various stages of alteration (Hart, 1970). In the present study, the pegmatoid gabbros have lower $Fe_2O_3$ content than the layered and marginal gabbros (Table 3.1). This indicates that the pegmatoid gabbros are less affected by alteration.

Oxidation ratio ($Fe_2O_3$/FeO+$Fe_2O_3$) also illustrates the effect of alteration (Iyer and Ray 2003).This ratio is 0.39% in marginal gabbros, 0.22% in layered gabbros and 0.13% in pegmatoid gabbro (Table 3.1). This ratio illustrates that pegmatoid gabbro is less affected by alteration and it corresponds with the petrographic observations which show that pegmatoid

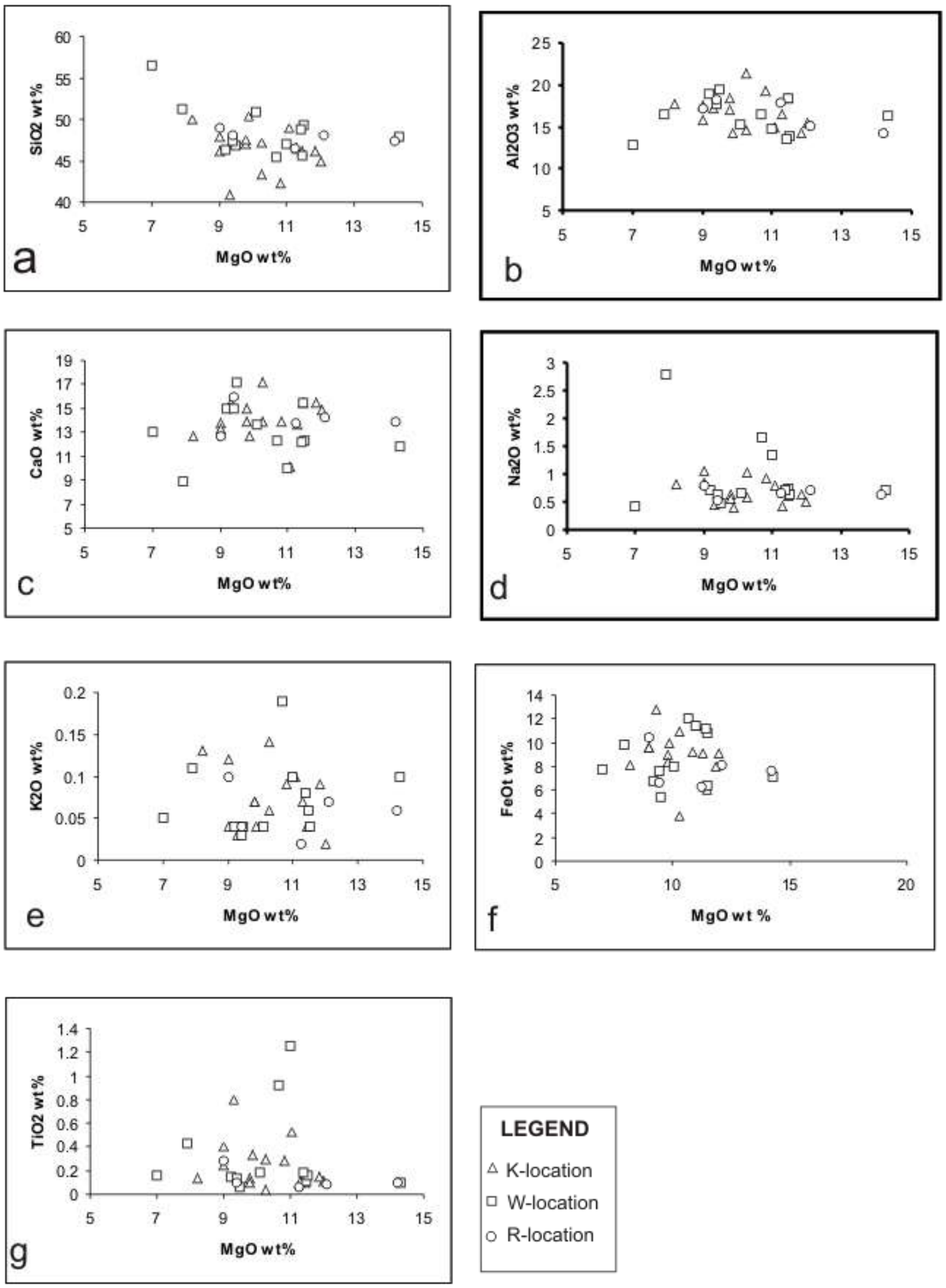


Figure (3.3): Variation diagrams of major oxides with MgO of the analyzed samples.

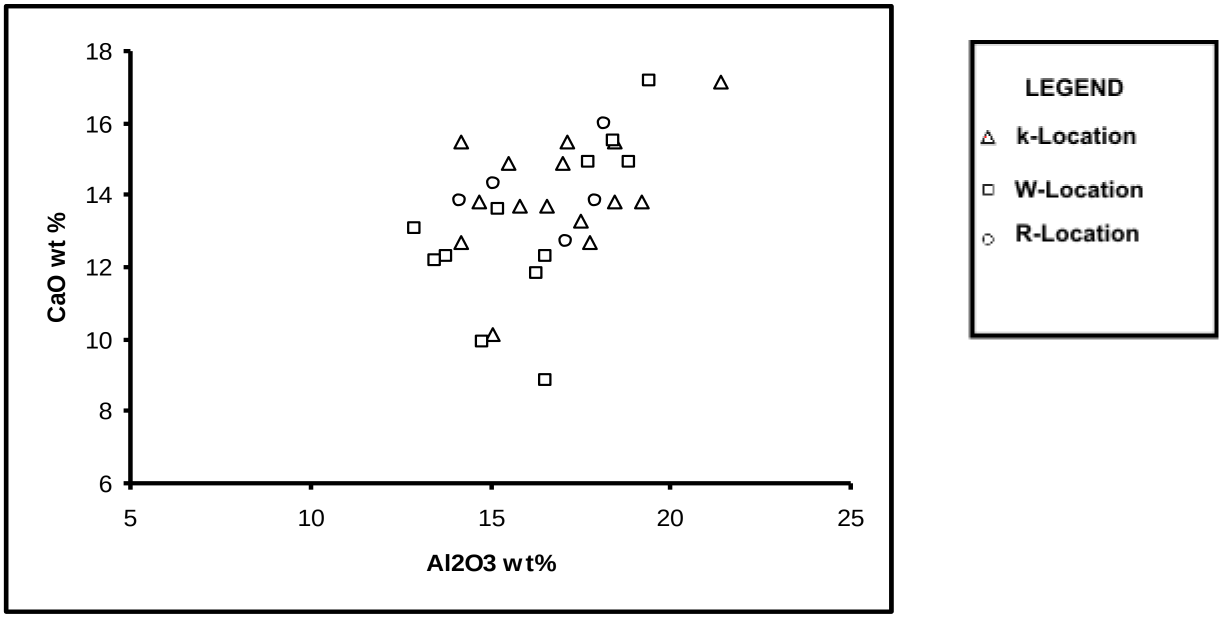


Figure (3.4): Relation of CaO with $Al_20_3$ in the analyzed samples.

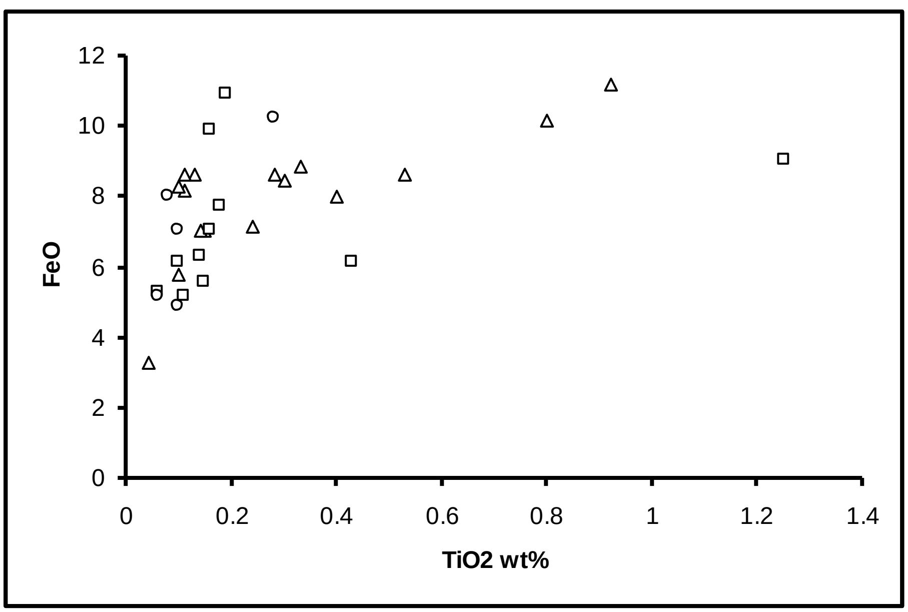


Figure (3.5): Relation of FeO with $TiO_2$ of the analyzed samples gabbros have lesser amounts of secondary minerals than both layered and marginal gabbros.

The $FeO^t$/ MgO ratio of Miyashiro (1975) can also illustrate the fractionation paths of major oxides (Fig. 3.6). Generally all oxides except $K_2O$ show very weak positive or negative relations with $FeO^t$/MgO ratio; $Al_2O_3$, CaO and MgO have negative correlations with $FeO^t$/MgO (Fig. 3-6 a, b and c). These related correspond with crystallization of calcic-plagioclase and clinopyroxene from early stages of fractionation, $FeO^t$ and $TiO_2$ however, show positive trends with $FeO^t$/MgO (Fig. 3.6 h and d) indicating crystallization of Fe-Ti oxides in the late stages of fractionation. $Na_2O$ and $K_2O$ show positive relations with $FeO^t$/MgO (Fig. 3.6 e and f) may be attributed to addition of these oxides by sea –water (Iyer and ray 2003).

The more or less linear relation between $SiO_2$ and $FeO^t$/MgO (Fig.3.6 g) can be attributed to the narrow range of $SiO_2$ content in the studied samples (Table 3 .1).

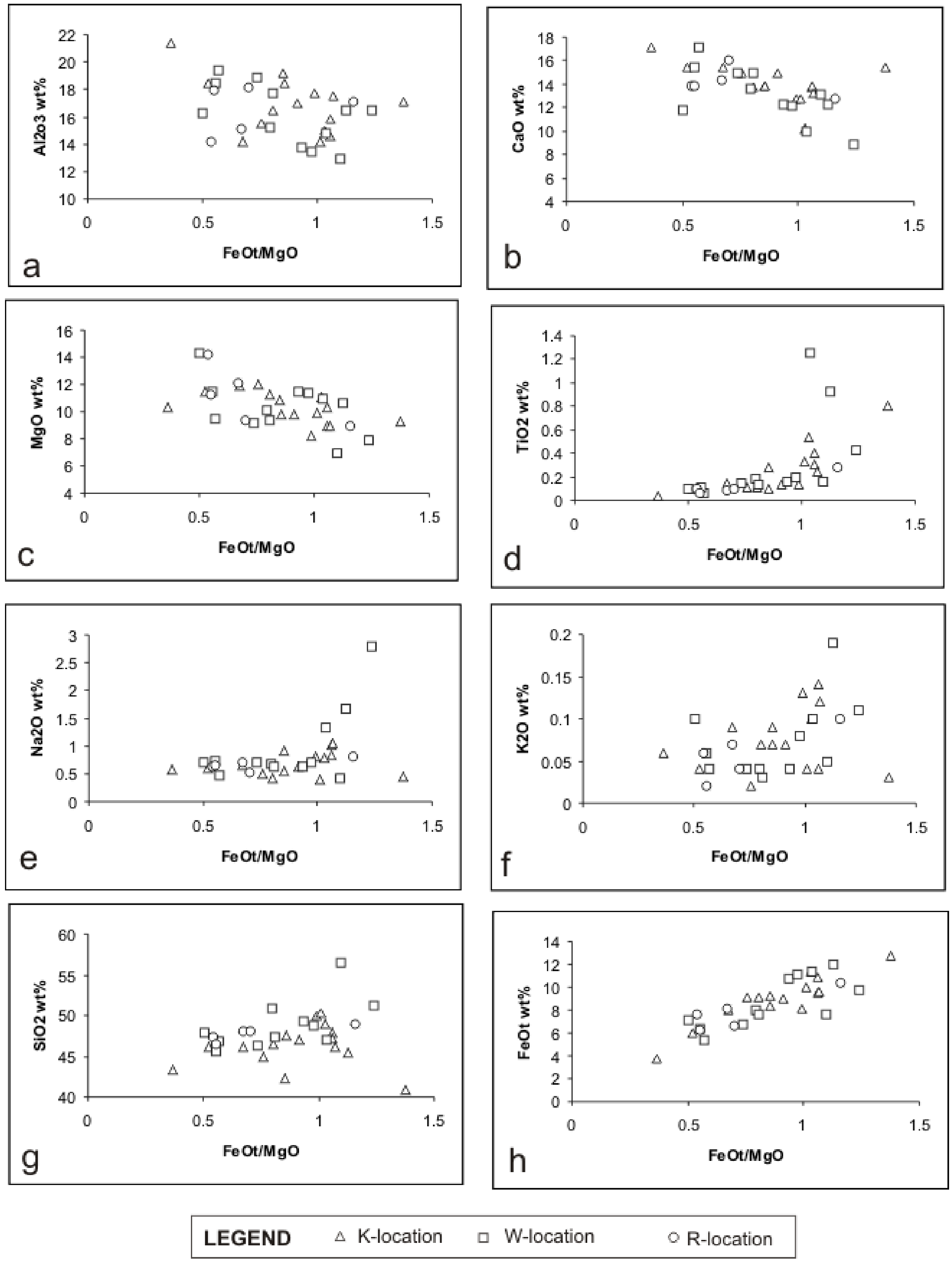


Figure (3.6): Variation diagrams of major oxides with respect to the FeOt/MgO as fractionation index of the analyzed samples.

### 3.4 Geochemistry of Trace Elements:

The behaviour of the trace elements relatively represent a good monitoring image of the evolution of the magma, where they mostly accommodate in the structures of the major phases. The content of some trace elements in the analyzed rocks are shown in Table (3.1), and the averages in Table (3.2).

Figure (3.7 a,b and c) show variation of the selected trace elements with the elevations for the analyzed samples which relatively illustrate the abundance and distribution of the trace element concentrations, The patterns also show the relationships of trace elements with each other.

Variation diagrams have been constructed for the trace elements Ni, Cr, Co, Sr, V, Zn, Y, and Zr versus MgO (Fig. 3.8) and versus $FeO^t/MgO$ ratio (Fig. 3.9). The diagrams illustrate that Ni and Cr and to lesser extent Co are positively correlated with MgO (Fig. 3.8 a, b and c), while their relations with FeOt/MgO is negative (Fig. 3.9 a, b and c). These elements are compatible with ferromagnesian minerals and are fractionated to the early phases such as clinopyroxene minerals (Pearce and Cann, 1973; Floyed and Winchester 1975; Coish, 1977 Pearce and Norry, 1979; Cox et al, 1979).

Vanadium shows negative trend with MgO (Fig. 3.8 d). It is easily partitioned into iron oxide minerals and it has high partition coefficient 27 in magnetite mineral (Cox et al, 1979). This is indicated from the high concentration of V in some of the analyzed samples which show a hight content of magnetite (Fig. 3.9 d).

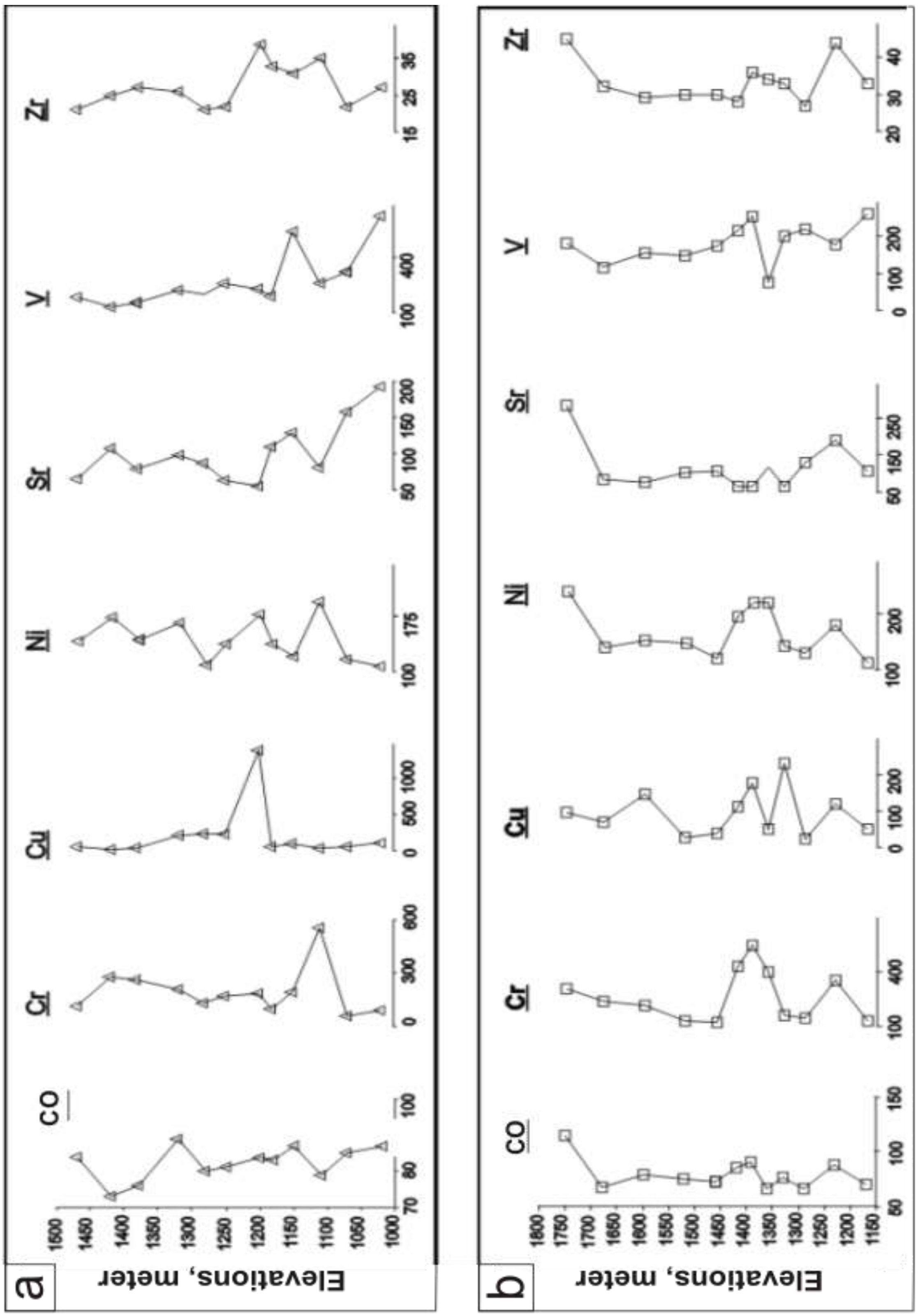


Figure(3.7 a, b and c): Selected trace elements versus elevations (meter) for the Mawat gabbros. (a= K- location) and (b= W- location) ( c= R- location)

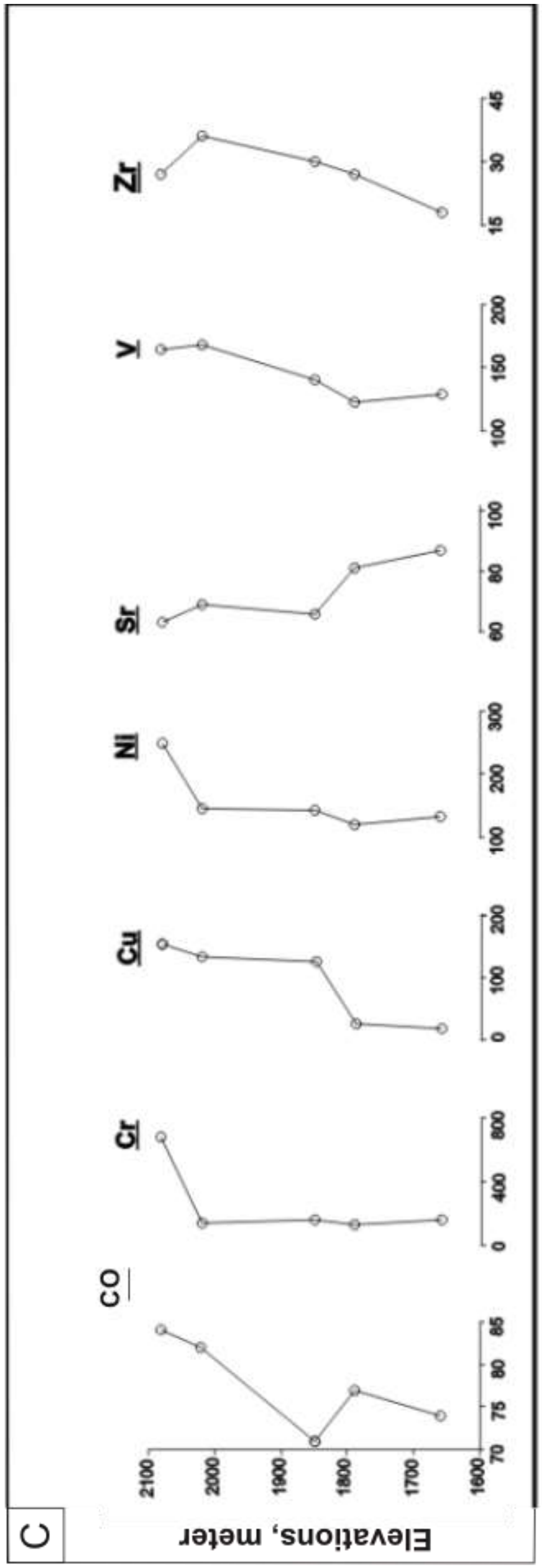


| LEGEND | |
|---|---|
| Sample No | Topographic higher |
| K3 | 1470 |
| K7 | 1420 |
| K11 | 1380 |
| K14 | 1320 |
| K15 | 1280 |
| K19 | 1250 |
| K20 | 1200 |
| K24 | 1180 |
| K26 | 1150 |
| K29 | 1110 |
| K32 | 1070 |
| K33 | 1020 |
| W44 | 1750 |
| W45 | 1680 |
| W46 | 1600 |
| W51 | 1520 |
| W55 | 1460 |
| W57 | 1420 |
| W61 | 1390 |
| W60 | 1360 |
| W64 | 1330 |
| W67 | 1290 |
| W71 | 1230 |
| W78 | 1170 |
| R78 | 2080 |
| R81 | 2020 |
| R85 | 1850 |
| R88 | 1790 |
| R93 | 1660 |

Figure (3.7 ): continued

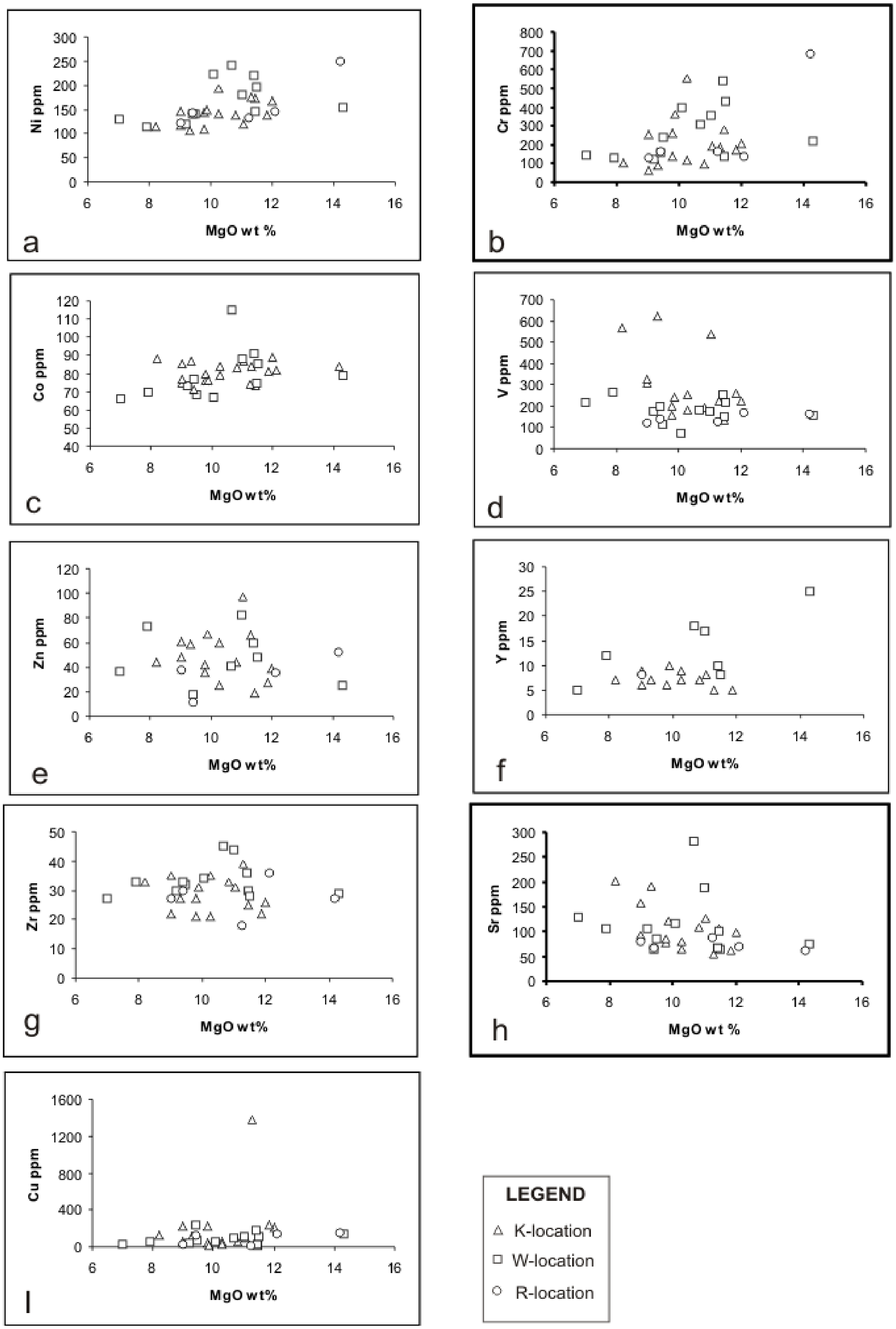


Figure (3.8): Variation diagrams of trace elements with MgO

Zn, Y, and Zr have no clear trend with MgO (Fig. 3.8 e, f, and g), while they are positively related to $FeO^t/MgO$ (Fig. 3.9 e, f, and g). These relations can be attributed to their accommodation in the late stage of mineral phases, due to the incompatibility of the elements. Y, and Zr are incompatible elements and preferentially partitioned into the liquid phases during melting and fractional crystallization processes (Mason, 1952; Pearce and Cann, 1973; Winchester and Floyed, 1975; Winchester and Floyd, 1977; Alabaster et al, 1982; White, 2005., Torres-Alvarado at al 2007). While Zn is moderately incompatible (White, 2005).

Sr relation with MgO (Fig. 3.8 h) shows negative correlation trend. This indicates that Sr is not consumed by the ferromagnesian minerals, but by plagioclase mineral (Mason, 1952., Mason and Moore, 1982., Goldschmidt, 1962). Sr has partition coefficient (1.3) with plagioclase mineral (Cox et al, 1979). Sr also increases with advancing fractional crystallization. This is supported by the relationships between Sr and $FeO^t/MgO$ ratio shown in (Fig. 3.9 h). Cu shows a linear relations with both MgO and $FeO^t/MgO$ (Fig. 3.8 i) and (Fig. 3-9 i). Copper have maximum abundance in mafic rocks compared with the other igneous rocks, and may separate early, either as immiscible sulfide or as sulfide crystals (Krauskopf, 1979). The Mn versus $FeO^t/MgO$ ratio (Fig. 3.9 j) shows an increase in manganese content with advancing fractional crystallization, indicating accommodation of the manganese in the ferromagnesian minerals (Mason, 1952., Mason and Moore, 1982).

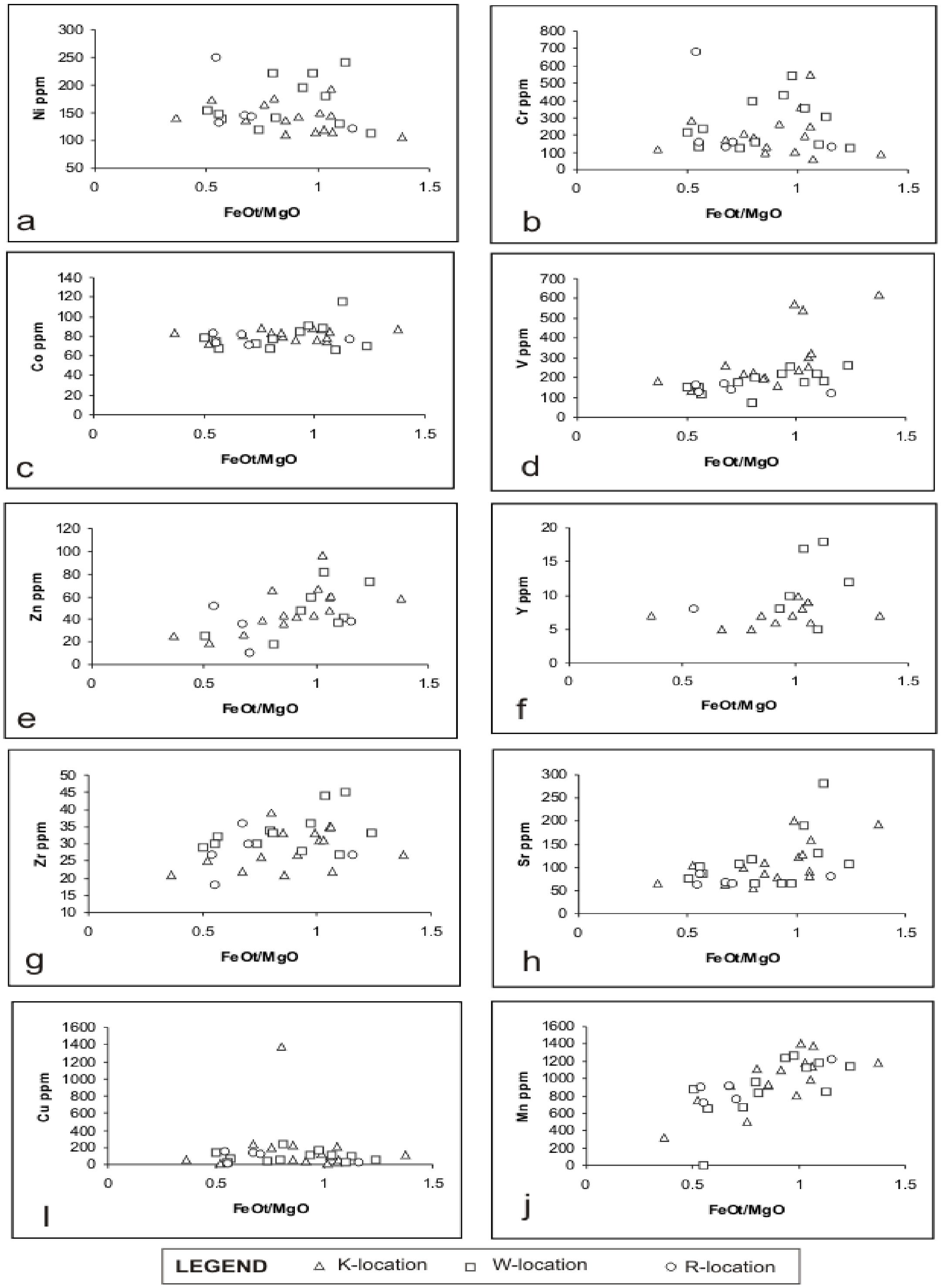


Figure (3.9): Variation diagrams of trace elements with respect to the $FeO^t/MgO$ as fractionation index.

### 3.5 Transition Element Patterns:

This is proposed by Allogere and others in (1968) using transition elements (Ti, V, Cr, Mn, Fe, Co, Ni, Cu, Zn). These elements are relatively immobile during alteration and metamorphism conditions (Pearce and Cann, 1973., Pearce, 1975); hence, the concentrations of these elements in the rocks reflect the composition of the original magma.

The transition elements of analyzed samples from the Mawat gabbros are normalized to the chondrite values (after Mason, 1971) and are plotted (Figure 3.10). Chromium, Ni and to lesser extent Co show depletion trends. These elements are compatible with early forming phases such as olivine and clinopyroxene. Decrease of Ni and Cr through the rocks indicates olivine fractionation, whereas Cr decrease indicates spinel or clinopyroxene fractionation (Wilson, 1989). It is noted, that Ni is more depleted than Cr which might indicate that pyroxene was fractionated rather than olivine minerals. This matches with all thin sections descriptions which show presence of pyroxene and absence of olivine minerals. This is consistent with the observation of Al-Hassan (1982) in the Penjwin gabbros. The Ti and V elements show enrichment. These elements are incompatible with the early forming minerals and hence they are concentrated and enriched in the residual melting with advancing fractionation process. These elements show the same behaviour in melting and crystallization processes (Wilson, 1989) and are both a good indicator of the fractionation of Fe-Ti oxides.

All samples of the layered gabbros in all three locations show very similar trends as well as the marginal gabbros and pegmatoid gabbros (Figure 3.10).

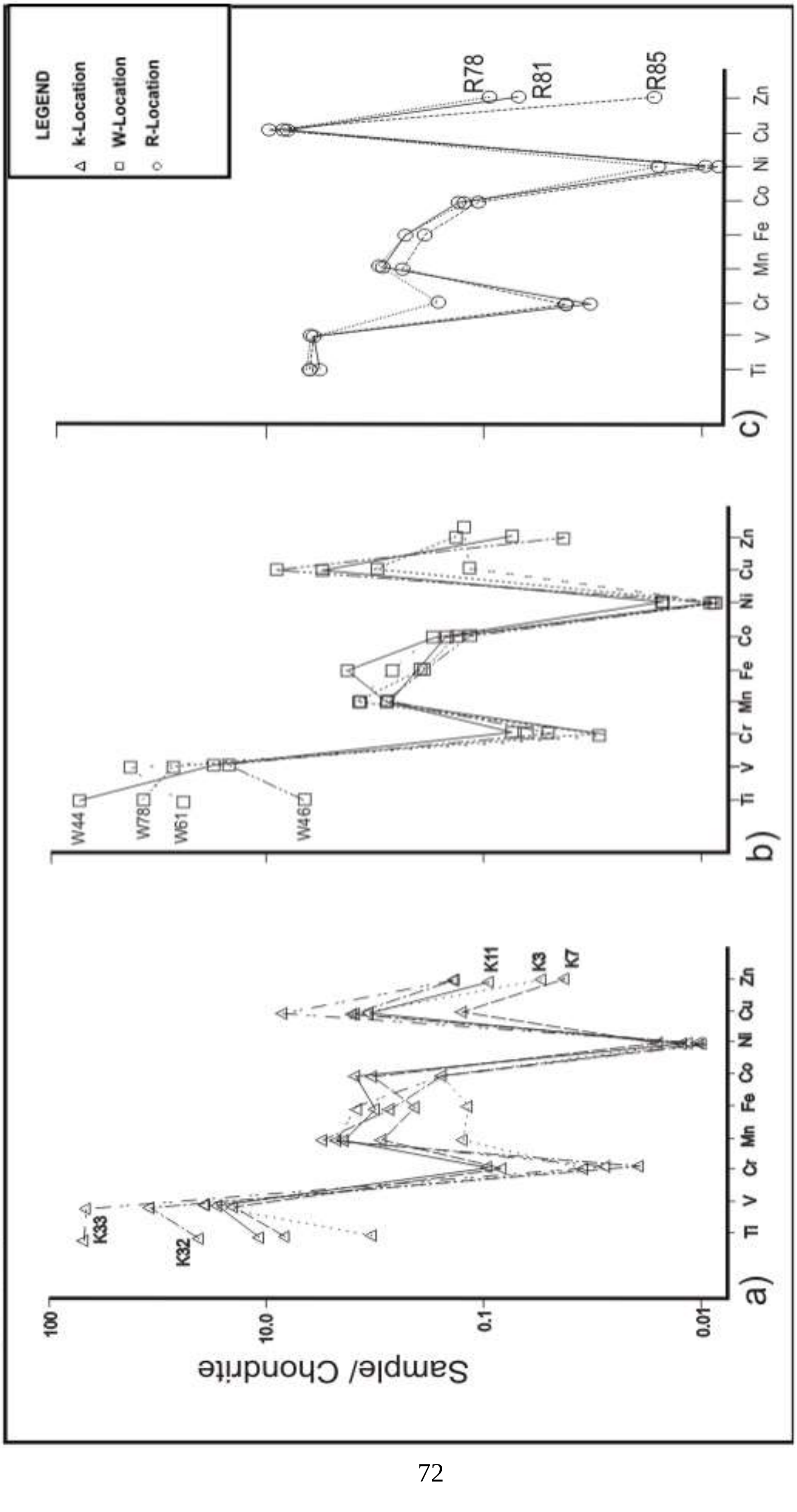


Figure (3.10 a, b and c ): The chondrite - normalized values for the transition elements of the Mawat gabbros against atomic number.

### 3.6 Magma Series:

***Magma series*** represent a group of rocks that are genetically related with each other and have common chemical and possibly mineralogical characteristics (comagmatic). Other terms are used which are synonymous to magma series are magma affinity, magma type and association. Different variation diagrams are used for the determination of magma series using major and trace elements.

The relationship between the differentiation index ***$FeO^t/MgO$*** and ***$FeO^t$, $SiO_2$ and $TiO_2$*** Figure (3.11 a, b and c) illustrated that these have relatively low range of $FeO^t/MgO$ and cannot follow a definite trend in $SiO_2$ versus $FeO^t/MgO$ ratio diagrams but show more or less a definite tholeiitic trend in $TiO_2$ versus $FeO^t/MgO$ diagram which may be attributed to the mobilities of $SiO_2$ and immobility of $TiO_2$ and $FeO^t$ .

Miyashiro (1975) proposed the uses of FeOt/MgO ratio to indicate the type of magmatic composition. This ratio in the analysed samples is less than two and ranging from 0.36 to 1.37 with an average of 0.85 (Table 3.1) this ratio correlates with tholeiitic composition.

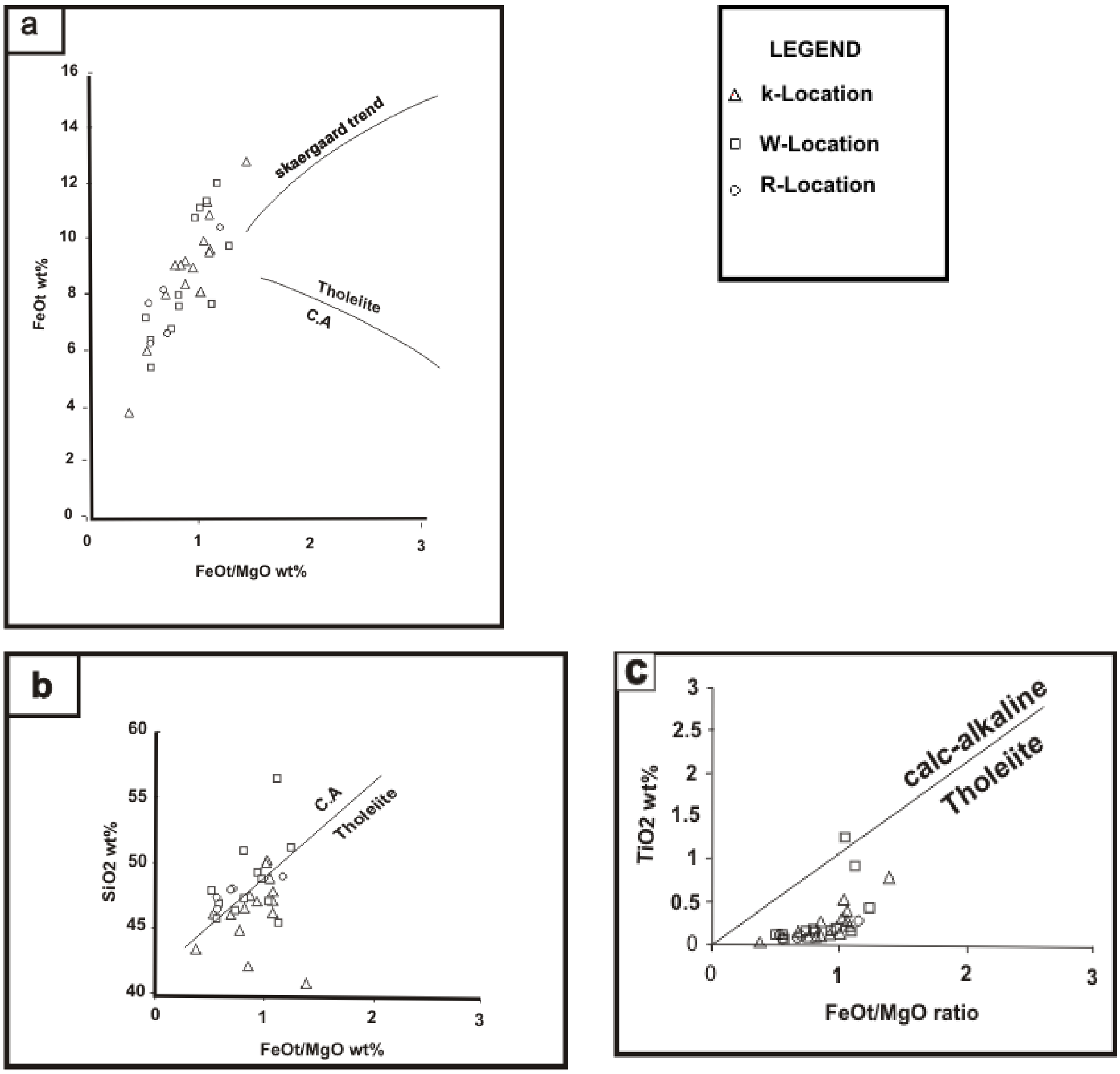


Figure (3.11): Plots of $FeO^t$, $SiO_2$ and $TiO_2$ versus $FeO^t/MgO$ ratio of the present study. The tholeiitic, calc-alkaline and Skaergaard trends are after Miyashiro (1975).

The ratio of the immobile elements ***Zr/Y*** is also employed to distinguish between tholeiitic and calc-alkaline affinities in both fresh and altered rocks (Lesher et al, 1986 and MacLean and Barrett, 1993).The tholeiitic magma have Zr/Y ratio that ranges between 3-5. The Mawat analysed samples from the present study show an average of 3.45 (Table 3.2) which emphasizes the tholeiitic nature of the rocks.

Figure (3.12) after Middlmost (1975) illustrates the relationships and the distinction between three magma series in terms of ***$K_2O$ and $SiO_2$*** contents. The rocks lie within low K-subalkalic series.

The contents of ***($Na_2O$+ $K_2O$),(FeO+ $Fe_2O_3$) as $FeO^t$ and MgO*** of the analyzed samples were recalculated to 100% and plotted on ***AFM diagram*** (Fig. 3.13) shows a comparable trend with the skaergaard complex of tholeiitic affinity. The total alkali-poor nature of the Mawat gabbros is clearly shown in this Figure. Also the Fe-enrichment trend with decreasing MgO can be correlated with tholeiitic trend.

The majority of the analysed samples are located within the tholeiitic field on ***MgO – $Al_2O_3$ -($FeO^t$ + $TiO_2$ )*** (Fig.3.14).

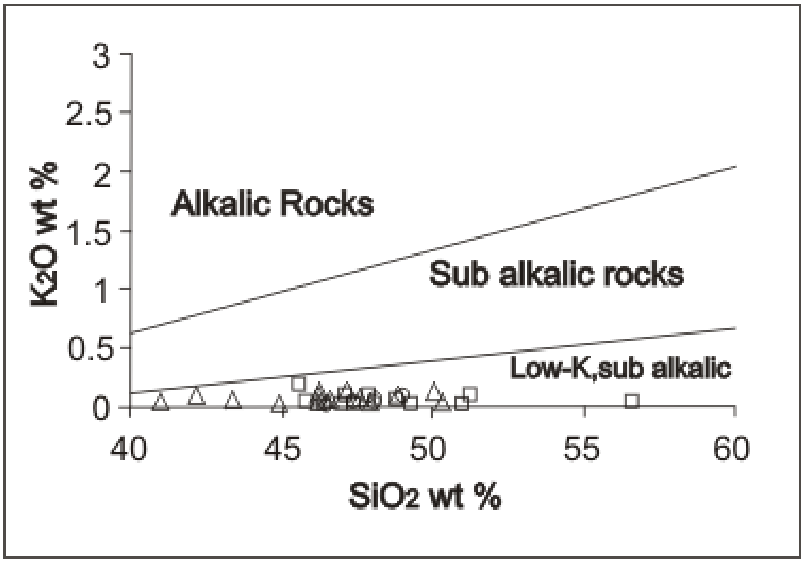


Figure (3.12): $SiO_2$- $K_2O$ diagram plots for Mawat gabbros (After Middlmost, 1975), discriminats low-k, sub alkalic.

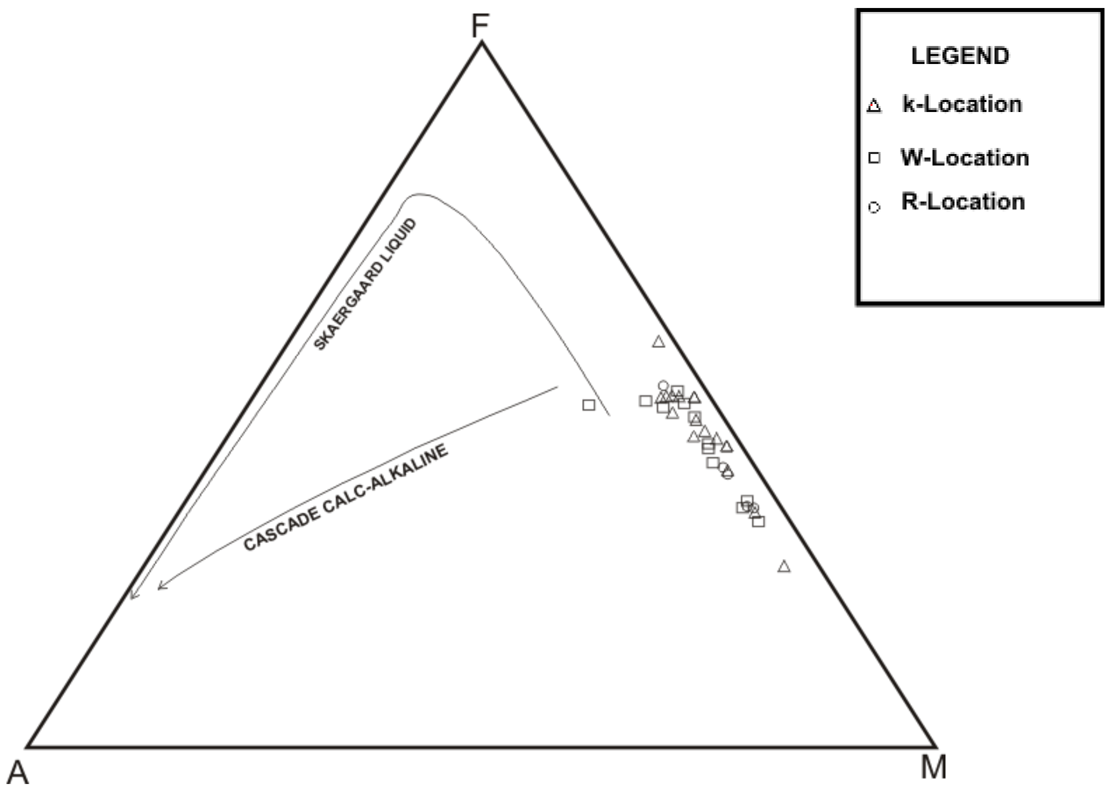


Figure (3.13): AFM diagram for the Mawat gabbros. The Tholeiitic and calc-alkaline trends are after Coleman (1977).

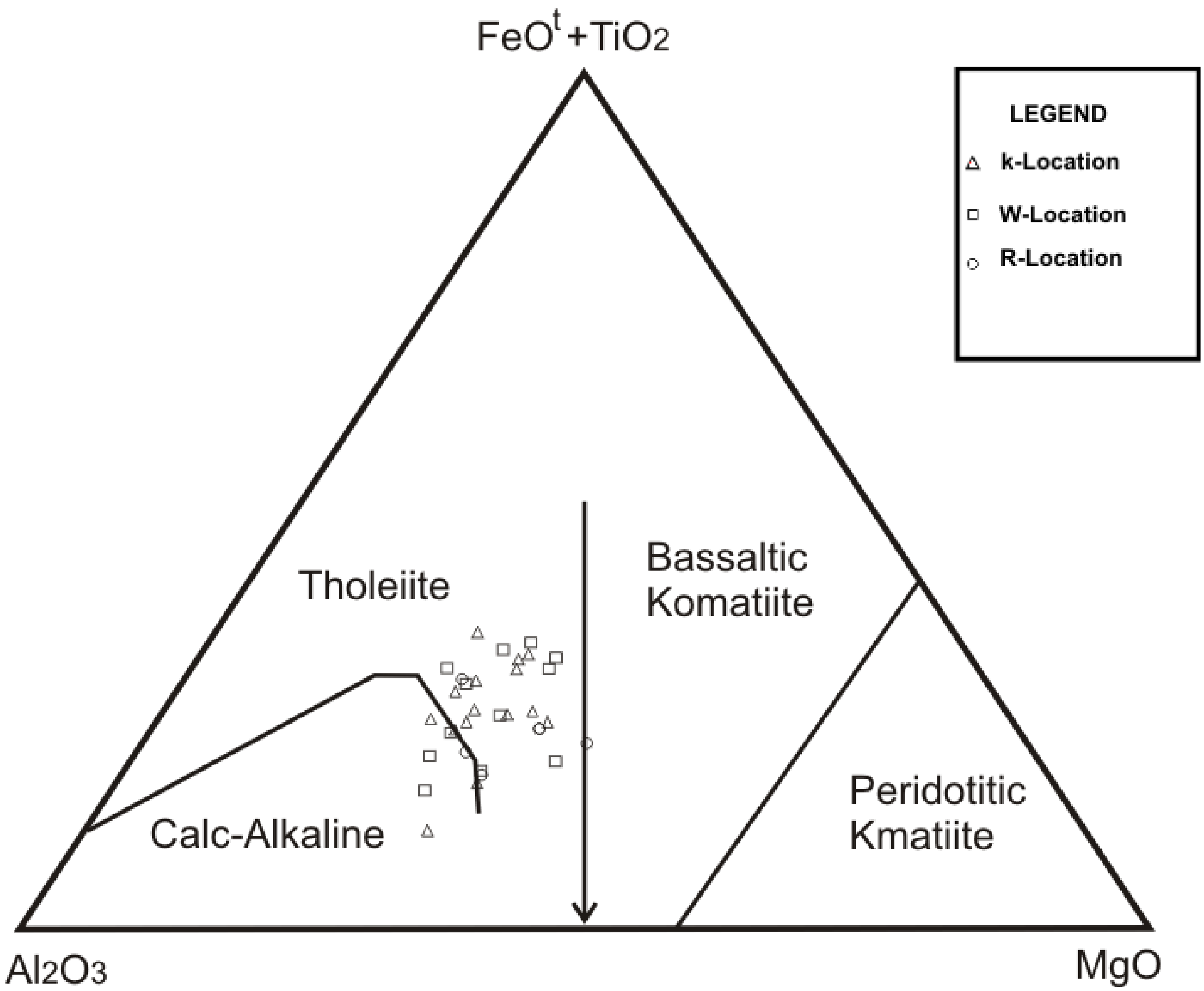


Figure (3.14): $Al_2O_3$- FeOt + $TiO_2$-MgO diagram (Jensen 1976) for the Mawat gabbros.

### 3.7 Geochemical Classification of the Rocks:

Geochemical classification of the present study, different diagrams have been employed using major elements. ***Total–alkali-silica (TAS)*** diagram ( Le Maitre et al.1989 and Le Maitre, 2002) is used for ultrabasic, basic, intermediate and acid rocks fields on the basis of their silica content (Fig. 3.15). Most analysed samples of Mawat gabbros are located in the field of gabbro of sub-alkaline character. The silica and total alkalis show enrichments in few plotted samples which may be attributed to the effect of alteration. However, some gabbroic samples show deviation from gabbro field, specially, marginal gabbros (sample, W78) fall in the diorite quartz, while pegmatoid gabbros (sample, K3) and some layered gabbros samples fall in the field of picro-basalt. This is attributed to the removal or addition of silica (Pearce, 1975).

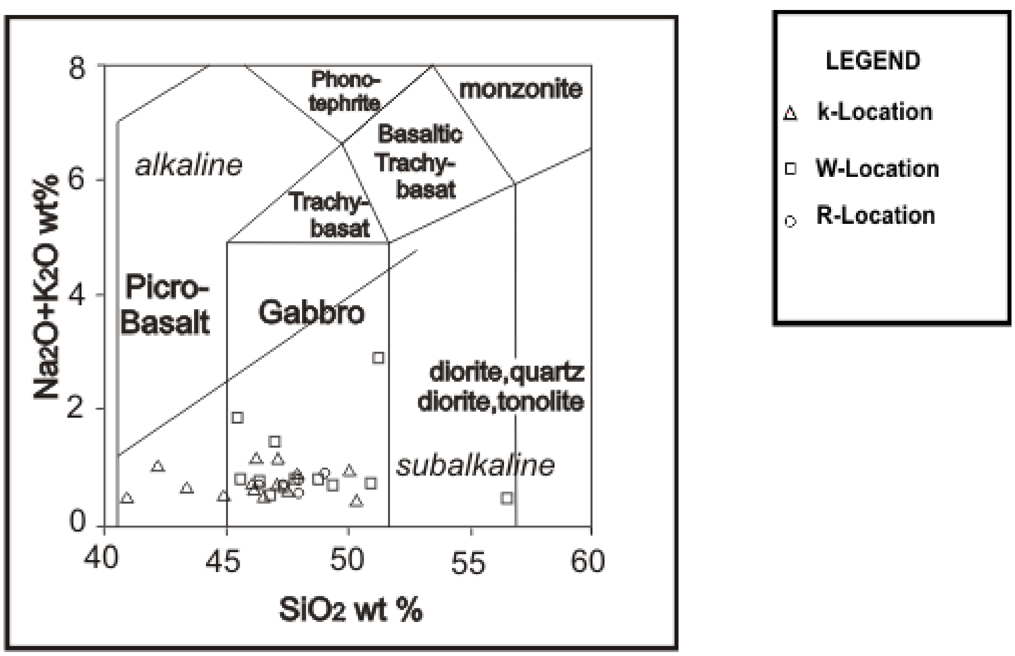


Figure (3.15): $SiO_2$ versus($Na_2O+K_2O$) diagram (After Le Maitre et al., 1989 and Le Maitre, 2002). For geochemical classification of the analyzed samples

The triangular diagram ( ***$MgO$-$CaO$-$Al_2O_3$*** ) Colleman , 1977 is used to distinguish between mafic and ultra mafic cumulate rocks; and accordingly the gabbros of Mawat ophiolite complex fall in the composition fields of mafic cumulate rocks (Figure 3.16).

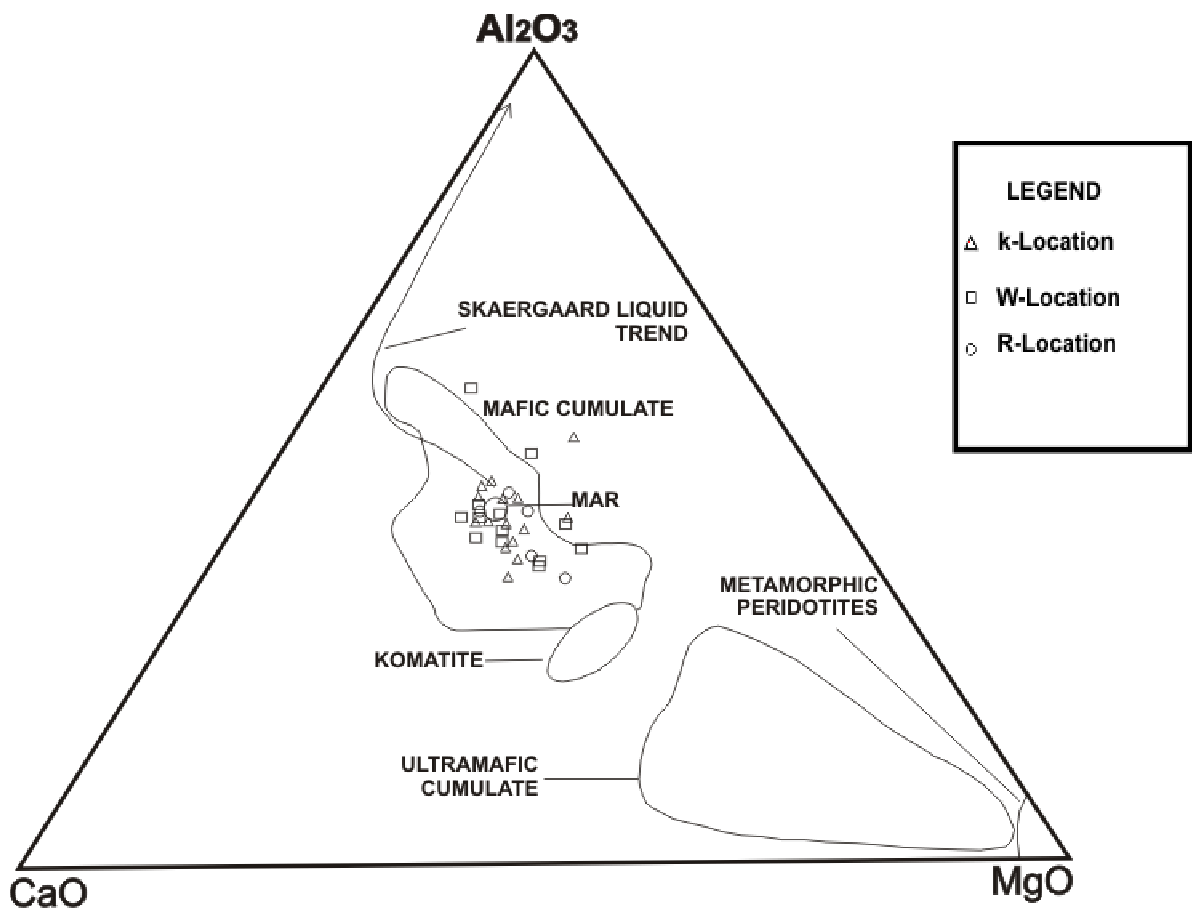


Figure (3.16): Triangular diagram of CaO- $Al_2O_3$ -MgO for the Mawat gabbros (After Colleman 1977). MAR: represent average composition of mid-Atlantic ridge.

### 3.8 Normative Minerology:

Table (3.1) shows normative mineral composition of the gabbros of Mawat based on the chemical analysis. Plotting the normative mineralogy on the tetrahedron diagram proposed by Yoder and Tilley (1962) and Thompson (1984) (Fig. 3.17) show that the majority of the samples cluster within the field of (ol-di-hy), as the major phases .The presence of normative olivine which is absent in thin section identification might be attributed to the relatively high MgO, and moderate $SiO_2$ contents (Al-Hassan., 1982). This diagram also shows the relationship of the Mawat gabbros to the fields of Galapagos Island basalts and MORB (after White et al, 1993).

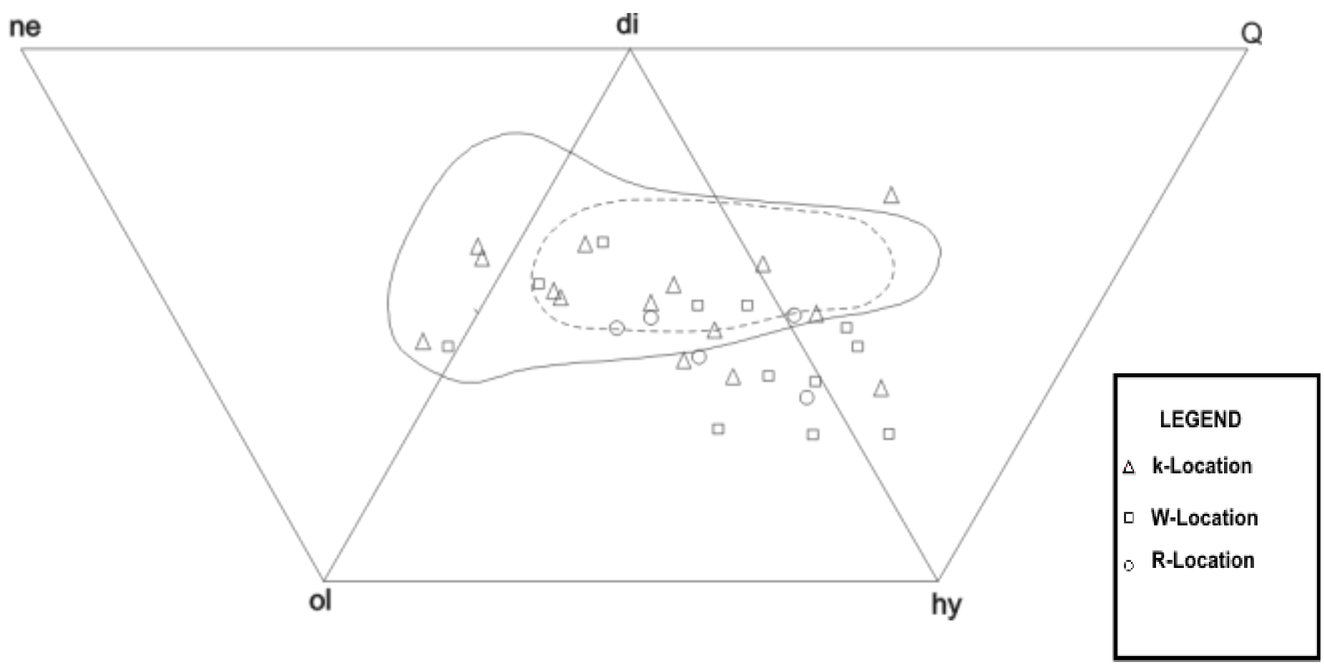


Figure (3.17) Tetrahedron normative mineralogy (nephelen- olivine-diopside-hypersthen-quartz) diagram of Yoder and Tilley (1962), and Thompson (1984). The solid line (Galapagos Island basalts) and the dotted line (MORB) (after White et al, 1993).

Table (3.4): Normative mineralogy percent in K, W and R- locations for the Mawat gabbros.

| samble no | Rock type | Quartz | Orthoclase | Albite | Anorthite | Nephelene | Diopside | Hypersthine | Olivine | Magnetite | Ilmenite | SUM |
|---|---|---|---|---|---|---|---|---|---|---|---|---|
| K3 | Peg.Gabb | — | — | — | 57.86 | 2.41 | 23.25 | — | 15.62 | 0.78 | 0.08 | 100 |
| K7 | Lay.Gabb | — | 0.24 | 5.07 | 48.72 | — | 23.93 | 5.69 | 15.9 | 0.26 | 0.19 | 100 |
| K11 | Lay.Gabb | — | 0.41 | 5.36 | 44.34 | — | 25.32 | 13.54 | 10.23 | 0.55 | 0.25 | 100 |
| K13 | Lay.Gabb | — | 0.12 | 4.14 | 41.55 | — | 28.02 | 5.6 | 18.9 | 1.46 | 0.21 | 100 |
| K15 | Lay.Gabb | — | 0.41 | 4.56 | 48.36 | — | 17.37 | 22.36 | 6.62 | 0.13 | 0.19 | 100 |
| K19 | Lay.Gabb | — | 0.53 | 5.41 | 37.51 | — | 34.11 | 6.29 | 14.32 | 1.54 | 0.29 | 100 |
| K20 | Lay.Gabb | — | 0.41 | 3.55 | 43.99 | — | 20.91 | 19.63 | 10.53 | 0.77 | 0.21 | 100 |
| K24 | Lay.Gabb | — | 0.53 | 2.62 | 49.2 | 2.79 | 17.65 | — | 25.69 | 0.99 | 0.53 | 100 |
| K43 | Lay.Gabb | 4 | 0.77 | 6.93 | 45.32 | — | 15.78 | 25.18 | — | 1.75 | 0.27 | 100 |
| K41 | Lay.Gabb | 4.76 | 0.24 | 3.38 | 37.58 | — | 22.56 | 29.11 | — | 1.74 | 0.63 | 100 |
| K36 | Lay.Gabb | 0.42 | 0.24 | 7.1 | 40.71 | — | 24.01 | 24.35 | — | 2.41 | 0.76 | 100 |
| K26 | Lay.Gabb | 2.87 | 0.59 | 6.59 | 38.46 | — | 10.99 | 35.02 | — | 4.47 | 1.01 | 100 |
| K29 | Lay.Gabb | — | 0.83 | 8.74 | 35.54 | — | 27.89 | 14.98 | 7.56 | 3.89 | 0.57 | 100 |
| K32 | Lay.Gabb | — | 0.71 | 8.85 | 44.28 | — | 19.65 | 16.91 | 5.2 | 3.94 | 0.46 | 100 |
| K33 | Lay.Gabb | — | — | — | 46.89 | 0.14 | 27.66 | — | 19.58 | 4.21 | 1.52 | 100 |
| W44 | Lay.Gabb | — | 1.12 | 12.45 | 37.12 | 0.86 | 19.5 | — | 25.83 | 1.31 | 1.81 | 100 |
| W45a | Lay.Gabb | — | 0.24 | 4.06 | 51.02 | — | 27.99 | 5.92 | 10.53 | 0.13 | 0.11 | 100 |
| W46 | Lay.Gabb | — | 5.92 | 41.88 | — | — | 14.58 | 24.98 | 10.81 | 1.64 | 0.19 | 100 |
| W51 | Lay.Gabb | — | 0.35 | 6.17 | 47.42 | — | 24.61 | 2.95 | 16.36 | 1.93 | 0.21 | 100 |
| W55 | Lay.Gabb | — | 0.24 | 5.92 | 49.39 | — | 21.99 | 14.78 | 5.5 | 1.89 | 0.29 | 100 |
| W57 | Lay.Gabb | — | 0.24 | 5.32 | 35.77 | — | 21.45 | 35.14 | 0.42 | 1.36 | 0.3 | 100 |
| W61 | Lay.Gabb | — | 0.47 | 6 | 34.59 | — | 22.45 | 30.91 | 4.89 | 0.33 | 0.36 | 100 |
| W60 | Lay.Gabb | 2.87 | 0.24 | 5.66 | 38.02 | — | 24.63 | 27.8 | — | 0.44 | 0.34 | 100 |
| W64 | Lay.Gabb | — | 0.18 | 5.24 | 46.47 | — | 23.78 | 19.57 | 2.42 | 2.07 | 0.27 | 100 |
| W67 | Lay.Gabb | 16.82 | 0.3 | 3.63 | 34.29 | — | 26.65 | 16.99 | — | 1.02 | 0.3 | 100 |
| W71 | Lay.Gabb | — | 0.59 | 11.33 | 35.8 | — | 12.54 | 30.54 | 3.05 | 3.77 | 2.38 | 100 |
| W78 | Mar.Gabb | 2.98 | 0.65 | 23.66 | 33.51 | — | 9.56 | 22.98 | — | 5.84 | 0.82 | 100 |
| R78 | Lay.Gabb | — | 0.35 | 5.49 | 36.54 | — | 26.98 | 13.87 | 15.55 | 1.03 | 0.19 | 100 |
| R81 | Lay.Gabb | — | 0.41 | 5.92 | 38.86 | — | 26.95 | 15.65 | 11.89 | 0.17 | 0.15 | 100 |
| R85 | Lay.Gabb | 0.17 | 0.24 | 4.39 | 47.74 | — | 25.98 | 18.51 | — | 2.78 | 0.19 | 100 |
| R88 | Lay.Gabb | — | 0.59 | 6.76 | 42.92 | — | 16.83 | 30.44 | 1.58 | 0.35 | 0.53 | 100 |
| R93 | Lay.Gabb | — | 0.12 | 5.58 | 47.33 | — | 19.09 | 18.55 | 7.51 | 1.71 | 0.11 | 100 |

(Lay. Gabb. layered gabbro: Mar. Gabb. marginal gabbro and Peg. Gabb. pegmatoid gabbro)

### 3.9 Discussion:

The gabbros of Mawat have low concentrations of the $TiO_2$, $K_2O$, $Na_2O$, HFSE, REE, and high concentrations of the $Al_2O_3$, CaO and MgO. Silica shows a wide range. REE of Mawat gabbros below the detection limit (Appendix). As it is observed from field, and petrographic studies, there are three types of gabbros, which are in general different in their major and trace element contents. The marginal gabbros have high $Na_2O$, $K_2O$ and $Fe_2O_3$ and lower CaO, MgO compared with the layered and pegmatoid gabbros samples. The latter have relatively lower $SiO_2$ and higher CaO concentration than the other types. This is considered a common feature among the mafic dykes which are formed within the ultramafic ophiolite complexes; Horoman complex, Japan (Takazawa et al, 1999); gabbros of North Cape, New Zealand (Hopper and Smith, 1996). The enrichments of $Na_2O$ within marginal gabbro samples are attributed to alteration processes and the addition of these components by sea water (Iyer and Ray, 2003). On the other hand Oliver et. al., 2007 concluded that the alkali enrichment is due to seritization of plagioclase and not to magmatic processes.

The studied rocks are relatively depleted in Y. The behavior of yttrium resemble the HREE elements (Wilson, 1989., White, 2005), where it readily concentrates in accessory phases such as sphene , apatite and less in pyroxene (Wilson, 1989), hence, these rocks show low abundance of yttrium concentration.

The Mawat gabbroic rocks comprise abundant source of calcic-plagioclase and clinopyroxene and various amount of oxide minerals as a primary minerals, major and trace elements content mainly reflect the mode of these phases in the rocks. Despite alteration /and or metamorphism processes, the correlation trends between most elements such as the correlation between MgO versus $TiO_2$, Ni and Zr versus Ti suggest that the gabbros of Mawat have retained original igneous signatures. However, the cliopyroxene and magnetite fractionation is strongly evidenced in the relations of the major elements such as MgO, $TiO_2$, and $FeO^t$, which are supported by trace elements such as Ni, Cr, and Mn.

The fractional crystallization of the plagioclase minerals is strongly related to the variation of major elements such as CaO, $Al_2O_3$, and trace elements such as Sr. However, the relationship between sodium and calcium shows an increase in $Na_2O$ content with decrease in CaO concentration reflecting the presence of calcic plagioclase. This probably reflect the primary composition of magma. The low $K_2O$-concentrations was also recorded in the gabbros of Sabzevar ophiolite, North Central Iran (Shojaat et al., 2003), in gabbros of Kermanshah ophiolite, Zagros Suture Zone, Wetsern Iran (Ghazi and Hassanipak, 1998), in the ophiolitic gabbros of Aksaray and Kayseri, central Anatolian,Yurkey (Kocak et al., 2005), in gabbros of Hole 735 (Sonw, 2002) and in the gabbros of Middle America Trench (Dreyer, 2003).

The broad negative and positive correlations are observed between MgO and some major and trace elements and the rare systematic relationships between each other, obviously attributed to the layering nature which may cause some scatter in the chemical concentrations (pyroxene-rich layers and plagioclase- rich layers). Moreover, some of the chemical variations may be consequence of varying amount of felsic and mafic minerals due to fractional crystallization, and the effects of alteration. However, the most advanced stages of alteration where samples appear to have undergone variation in the $Na_2O$, $K_2O$, $SiO_2$ and $Fe_2O_3$, furthermore, these rocks show more abundance of secondary mineral assemblages, such as, tremoliteactinolitic, chlorite, secondary oxide, and epidote minerals. It is remarkable that the values of $Fe_2O_3/FeO$ ratios in the marginal gabbros are well above layered gabbros and pegmatoid gabbros, which is another indication of the effect of alteration processes represented by release of iron from the silicate minerals and results in the formation of secondary magnetite (Neal and Stanger, 1984).

Mawat gabbros show tholeiitic nature. This is supported by many lines of evidences: The $FeO^t/MgO$ ratio which is less than two reflects oceanic tholeiites (Miyashiro, 1973a). He supposed that this ratio is considered to be a measure of the degree of differentiation and accordingly, depending on this ratio, the rocks of the present study show relatively small degree of differentiation. Lesher et al, (1986), assumed that the ***Zr/Y*** ratio ranging between (3-5) for tholeiities, The Zr/Y ratios of gabbroic samples of Mawat ophiolite complex is (3.45) as an average, reflecting tholeiitic nature. The tholeiitic nature is also obvious by showing Fe-enrichment trend with decreasing MgO (***AFM diagram***).

## 4.1 Petrogenesis:

Depending on geochemical characteristics, gabbros of Mawat ophiolite are island arc tholeiite which represent the site of subduction of one oceanic lithosphric plate beneath another (Miyashiro et al, 1982., Best 1982).

Many researchers over the past decades have indicated that specific major and trace elements can be used to correlate with the characteristic magma source (Pearce and Flower, 1977., Pearce and Norry 1979., Pearce, 1982**.,** Langmuir et al, 1992).Therefore, the behaviour of major and trace elements are and their ratios useful to determine the type of magma.

Two major processes are included in the formation and evolution of the magma source; partial melting of the upper mantle peridotite and fractional crystallization.

### 4.1.1 Partial Melting:

Most magmas are generated in the upper asthinosphere of the earth (Blatt and Trancy, 1996). Under such conditions of depth, pressure changes and the presence of volatiles that associated with the rise of the magma near to the play an important role in partial melting. The trace elements concentrations of a melts may vary considerably during partial melting, and may provide valuable information about the actual mechanisms of magma generation in the mantle (Wilson 1989).

The Zr versus Zr/Y ratio diagram of Pearce and Norry (1979) is useful in the interpretation of magmatic processes. The variation in Zr concentration might be attributed to the fractional crystallization processes, whereas Zr/Y ratio variation is related to partial melting (Pearce and Norry, 1979). Plotting the analyzed samples of the present study on this diagram (Fig. 4.1 ) shows a small range in the Zr following the trend of depleted mantle source with average partial melting of 20%.

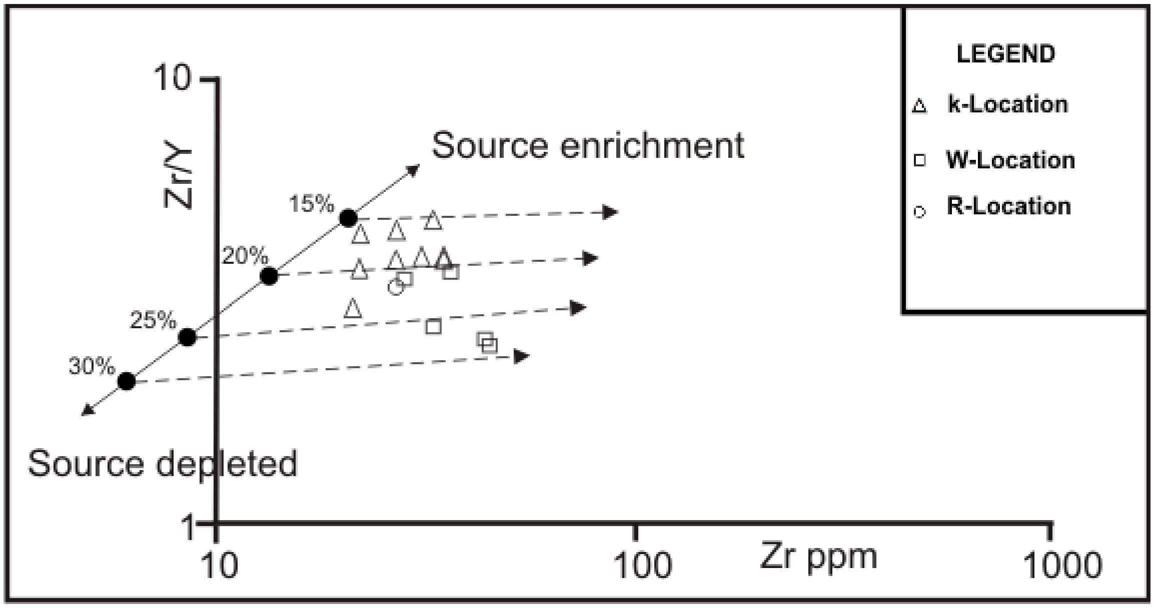


Figure (4.1): Mawat gabbro on diagram of Zr versus Zr/Y ratio of, (Pearce and Norry, 1979).

### 4.1.2 Fractional Crystallization:

The evolution of magma is often marked by fractional crystallization, the process of early forming minerals separated from the original magma which causing a change in the remaining composition of the melt.

Generally, all analyzed gabbros of the Mawat ophiolite in the three locations are geochemically related and are tholeiitic nature, the trends of the major and trace element contents reflect the fractional crystallization of calcic plagioclase and clinopyroxene. The relationships between MgO - $SiO_2$, CaO, Ni and Cr (Fig. 3.3 a and c ., Fig. 3.8 a and b), respectively clarify fractionation and accumulation of clinopyroxene minerals. The fractionation of the calcic plagioclase is related to the low $K_2O$ and $Na_2O$ and higher CaO and $Al_2O_3$ contents, supported by the negative correlations trends of $Al_2O_3$ and MgO, Ni contents. It is important to note that the clinopyroxenes are mostly replaced by secondary amphiboles and this is related to the CaO content of the whole rocks; the pegmatite gabbros and some samples of layered gabbros of the study area which are largely pseudomorphic in nature and the original textures had been preserved, show relatively higher CaO content compared to marginal gabbros which are most commonly non pseudomorphic in nature and the original textures have been deformed.

Leeman (1976) proposed that the relation between Ni and Cr is important in the determination of the fractionation of ferromagnesian minerals; where if there is a good more or less positive linear trend, a fractionation of only one major phase is indicated, whereas no good trend indicates fractionation of two major phases. Figure (4.2) shows the trend of the plotted samples of the present study and shows a relatively a positive relation. The good positive trend and the absence of olivine in all thin sections indicate that clinopyroxene is the major ferromagnesian phase present in Mawat gabbros. This suggests derivation either from previously fractionated source or from a melt which had been extensively fractionated by the removal of olivine (Wilson, 2001., Kocak et al, 2005). The partition coefficient of Cr and Ni are 4.7 and 2.6 respectively in clinopyroxene minerals (Cox et al, 1979).

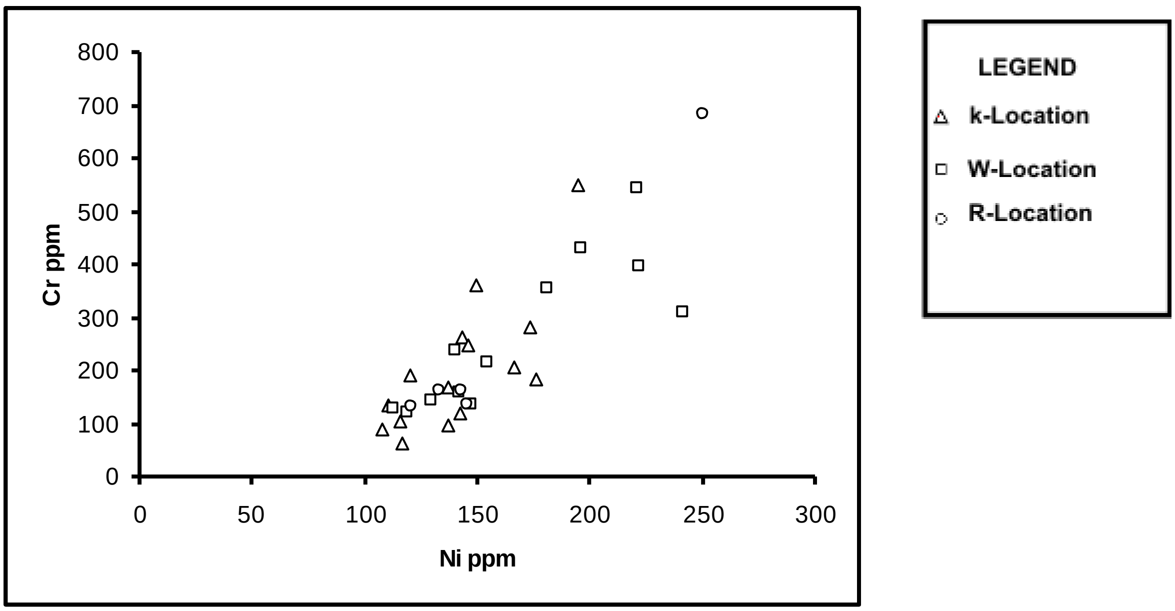


Figure (4.2): Plotes of gabbro samples on Ni-Cr Variation diagram.

The Mg# is considered as solidification index ***(100 Mg/(Mg+Fe)***. All Mawat gabbros have Mg# ranging from (40.9-64.66) with an average of (51.28). This ratio is slightly lower than those in primitive basalts (Mg# = ~70) (Roeder and Emslie, 1970.

The plot of Mg# versus $SiO_2/Al_2O_3$ (Fig. 4.3 a) shows a negative correlation trend which indicates fractionation and accumulation of the plagioclase minerals (Al- rich phases). This is supported by the positive relations between Mg# and CaO (Fig.4.3 b) and $Al_2O_3$ (Fig. 4.3 c). The relations between Mg# and MgO and CaO (Fig. 4.3 d and b) indicates fractionation of clinopyroxenes. The negative correlation between Mg# and $TiO_2$, $FeO^t$ and V (Fig. 4.3 e, f and g) indicates that these elements are not involved considerably in the early forming phases(plagioclase and clinopyroxene) and are contributed in late-stage mineral phases (Fe-Ti oxides).

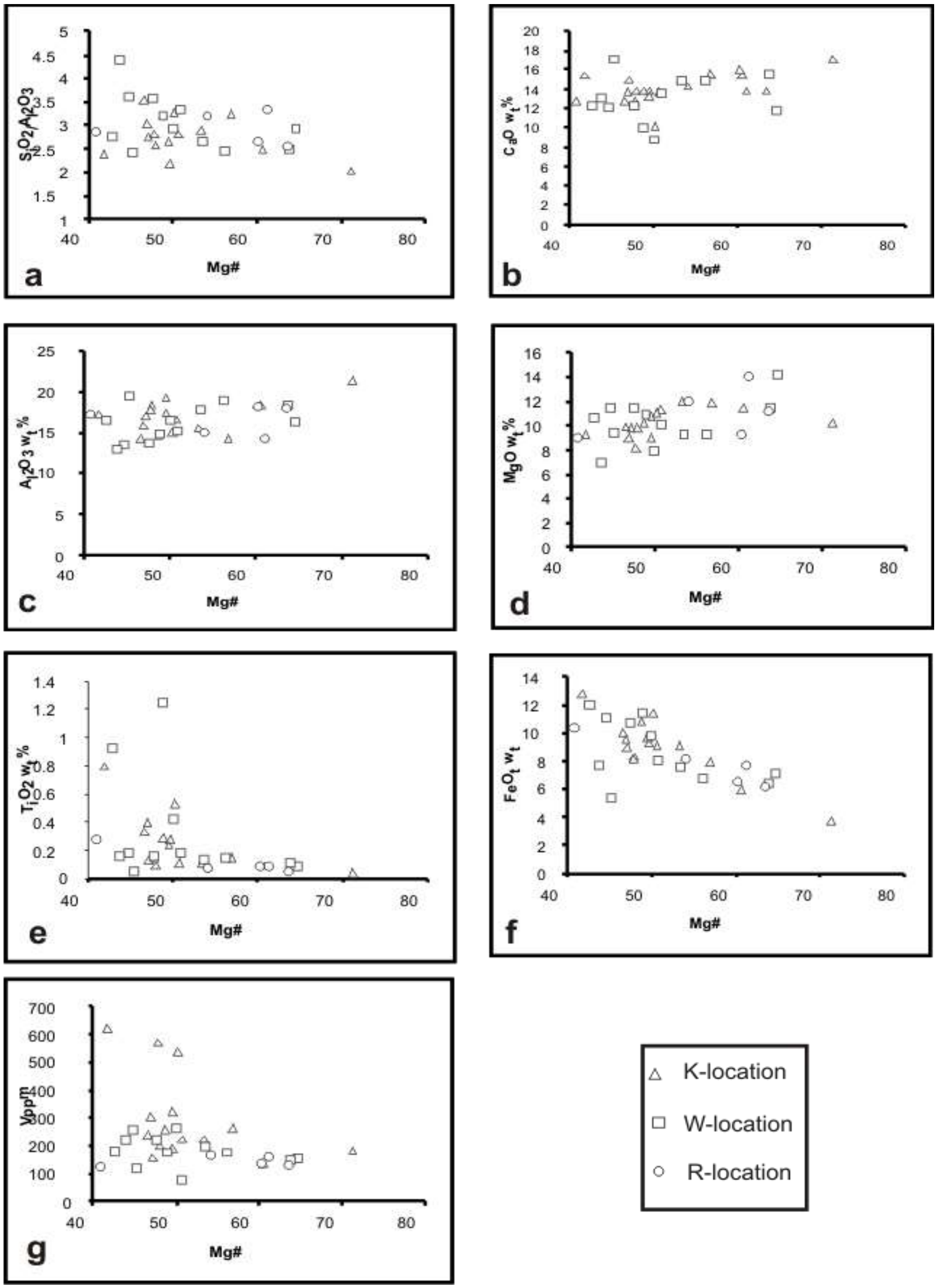


Figure (4.3): Relationships between Mg# and selected major and trace elements with of Mawat gabbros.

On ***Ti versus $Al_2O_3/TiO_2$*** (Fig. 4.4) and ***Ti versus Ti/Cr*** (Fig. 4.5), the trends of crystallization of major phases follow more or less the trends of both clinopyroxene and plagioclase.

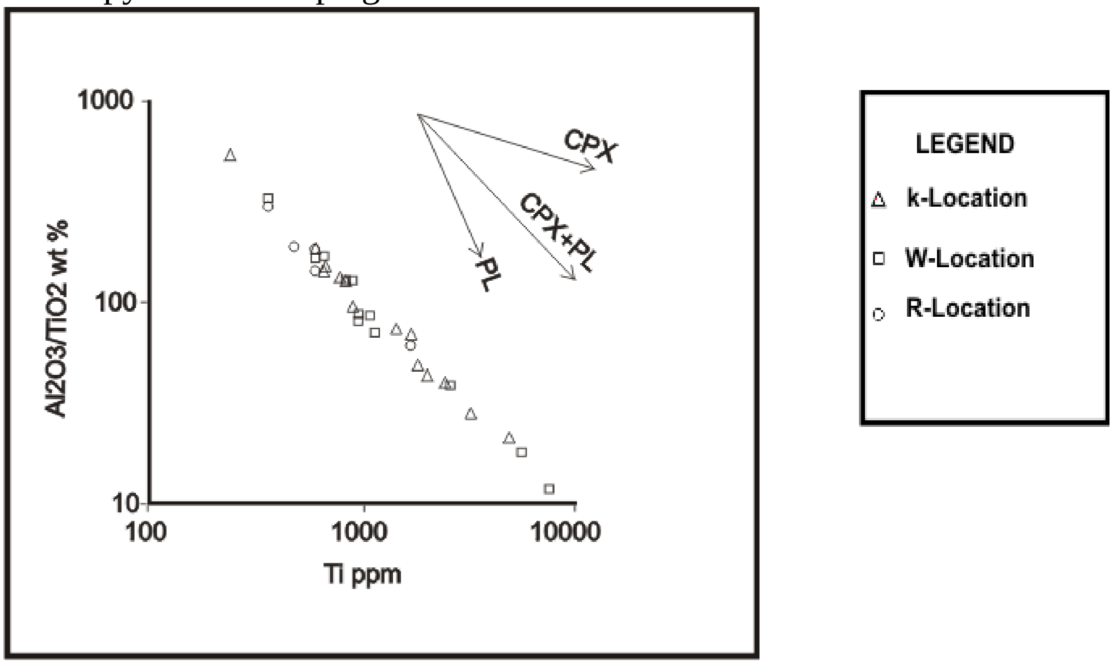


Figure (4.4): Ti versus Al2O3/TiO2 diagram (Pearce and Flower, 1977) for the Mawat gabbros.

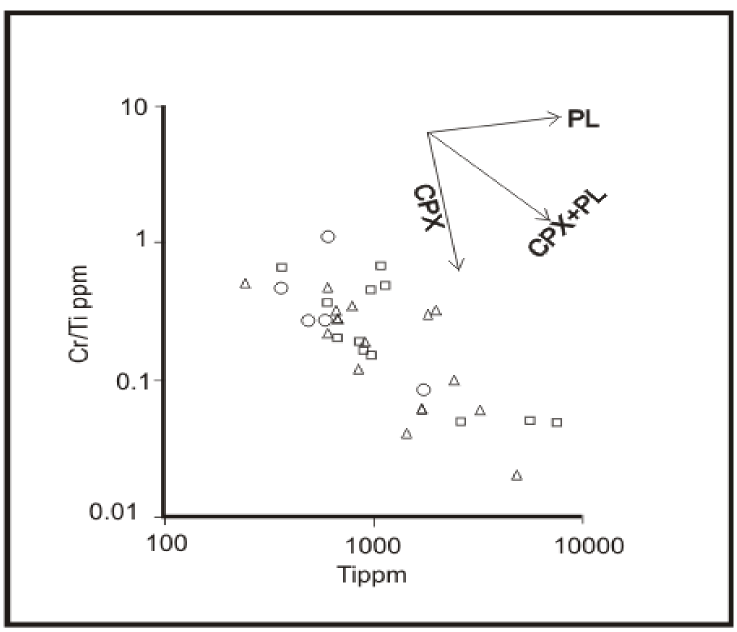


Figure (4.5): Ti versus Cr/Ti diagram for the Mawat gabbros. (Pearce and Flower, 1977).

## 4.2 Tectonic Classification:

Ophiolite assemblage represents remnants of oceanic crust and upper mantle. There are varied possible settings for the generation of oceanic lithosphere. Most of the crust of oceanic basins is believed to have formed at spreading mid-ocean ridges where fractional melts of the mantle are injected into the divergent margins of oceanic plates, (Coleman, 1977). However, oceanic crust is also generated at other sites such as island arc, back-arc basins and intra-plate volcanic centers. Depending on certain geochemical parameters, it is possible to interpret the origin of the magmas in different tectonic settings. As it is obvious petrology and geochemy analyses, show the rocks of the present study are affected by alteration and metamorphism. Hence, the discrimination of the tectonomagmatic environment will depend on geochemistry of immobile elements:

Muller and Groves (1997) (Figure 4.6), discriminates between arc-related magma and within-plate related magma using ***$Al_2O_3$-$TiO_2$***. diagram . Plots of samples of the present study fall within arc-related magma setting.

Arculus et al. (1995) shows the tectomagmatic characters of fore-arc, island arc, back-arc, and mid-oceanic ridge on the ***$TiO_2$-$Al_2O_3$*** diagram Figure (4.7) shows that the plotted samples are located within the fore-arc settings; few samples, however are located within back arc and MORB. In general, the fore-arc ophiolites constitute most of the ophiolite occurrences in the world because of the higher possibility for on-land preservation of ophiolite along fore-arc margins during collision and obduction (Kato and Saka, 2006 in Faustino et al., 2006).

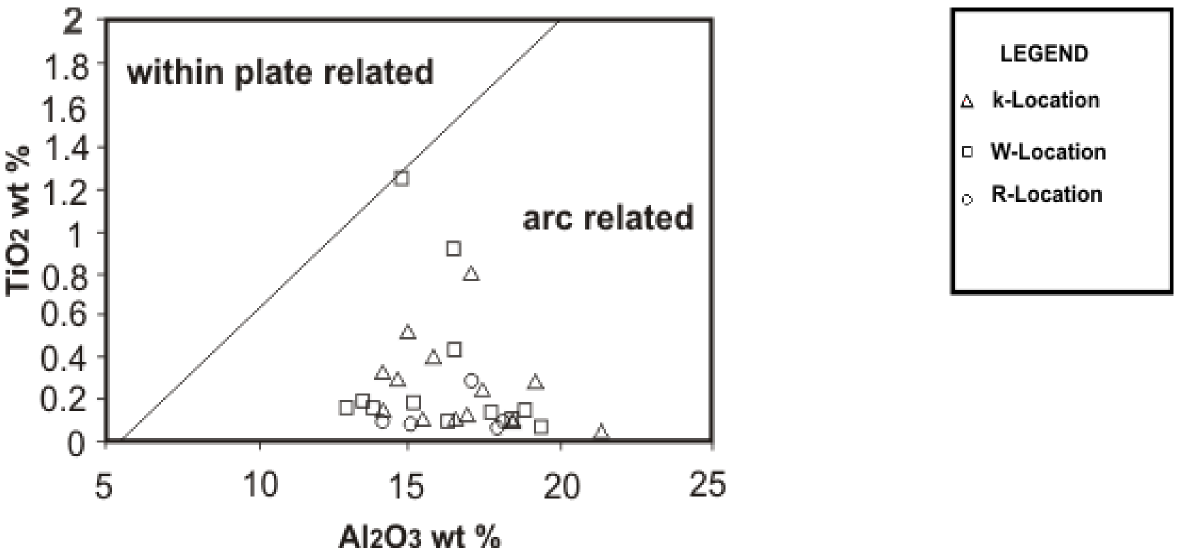


Figure (4.6): $Al_2O_3$-$TiO_2$ diagram in Mawat gabbros (After Muller and Groves., 1997).

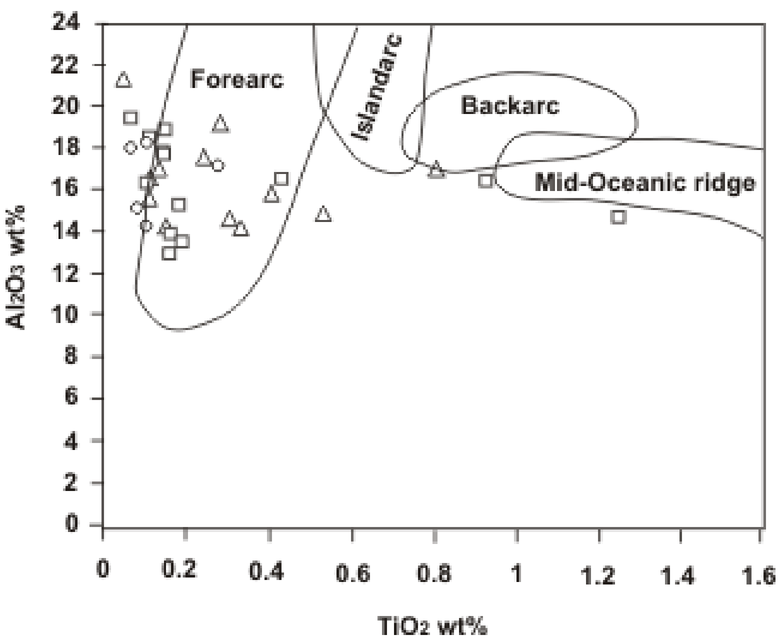


Figure (4.7): $TiO_2$-$Al_2O_3$ diagram (Arculus et al., 1995) in Mawat gabbros, discriminating fore-arc, island arc, back-arc and mid-oceanic ridge.

Pearce (1980) used immobile-incompatible elements ***Ti and Zr*** to discriminate the characteristics of ophiolites within plate lavas, arc lavas and mid-oceanic ridge basalt (MORB)) (Fig. 4.8 ). This diagram shows that most samples of the present study fall within or near the arc lava with some overlaping with the MORB field. The low content of both Ti and Zr is considered characteristic of arc lavas (After Pearce and Cann, 1973) (Fig.4.9).

***Ni-Ti/Cr diagram*** of Beccaluva et al. (1983), have proposed the relation between compatible elements Ni, Cr and incompatible element Ti to discriminate between island arc tholeiites (IAT), mid-oceanic ridge basalt (MORB), and the very low-Ti basalt. Mawat gabbroic samples fall in the very low-Ti basalt region with deviation of some samples into the MORB-field (Fig. 4.10).

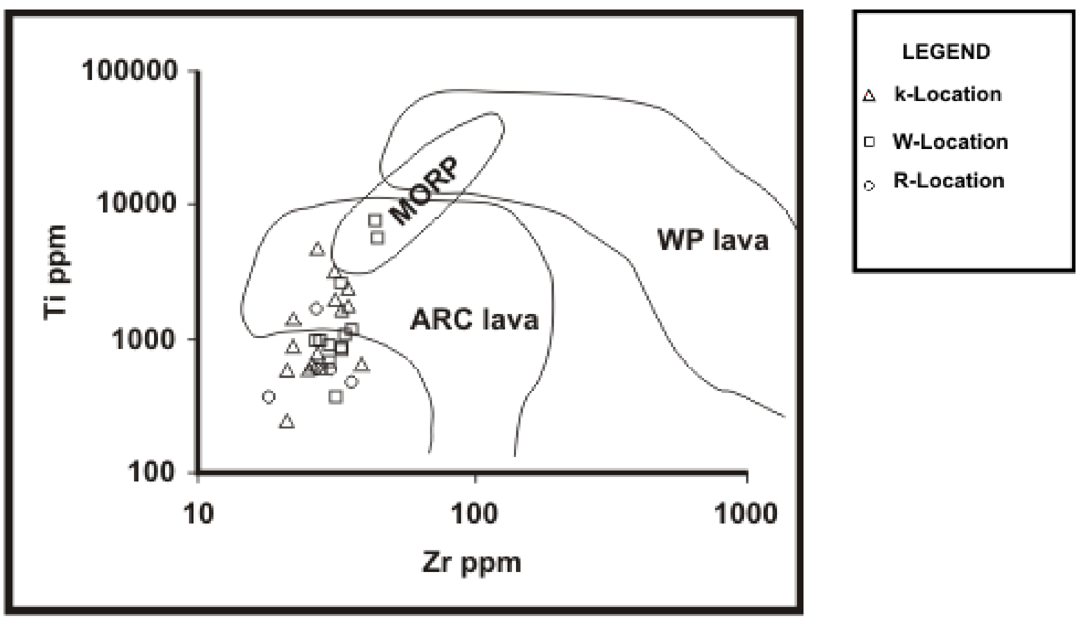


Figure (4.8): The Mawat gabbros plotted on the Zr vs Ti diagram, discriminating within plate lavas, arc lavas and mid-oceanic ridge basalt. (After Pearce, 1980).

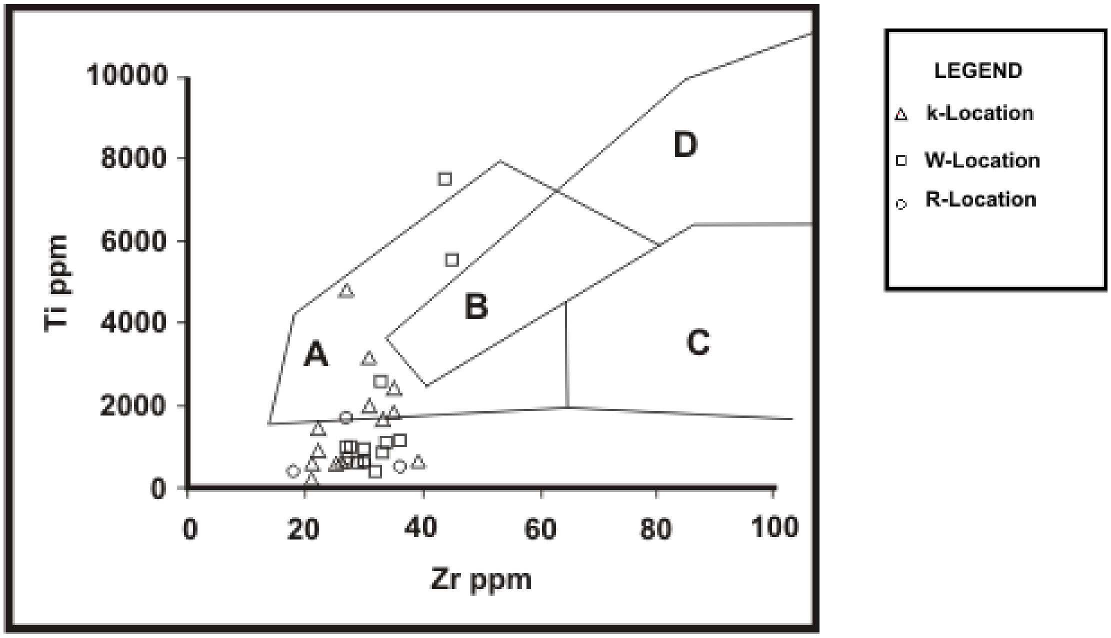


Figure (4.9): Zr-Ti diagram showing fields; A = Island Arc Tholeiite (IAT), C = Calc – alkaline Basalt (CAB), D = Mid Oceanic Ridge Basalt (MORB) and B = All the Three Types. (After Pearce and Cann, 1973).

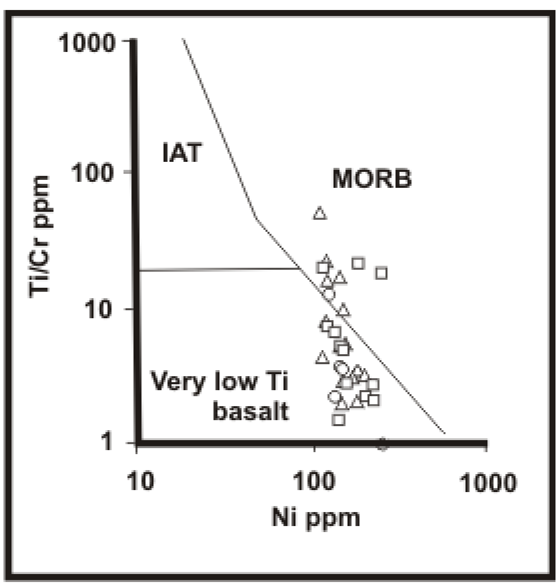


Figure (4.10): Ni-Ti/Cr diagram for the Mawat gabbros, discriminating island arc tholeiites (IAT), mid-oceanic ridge basalt (MORB) and the very low-Ti basalt. (After Beccaluva et al., 1983).

The ***$TiO_2$-MgO diagram*** of Laurent and Hebert, 1989. Shows the distinction between $TiO_2$-rich alkaline basalts, low-MgO low $TiO_2$ basalts, and very low $TiO_2$ boninite. Most gabbros of Mawat ophiolite fall in the field of very low $TiO_2$ boninite (Fig. 4.11).

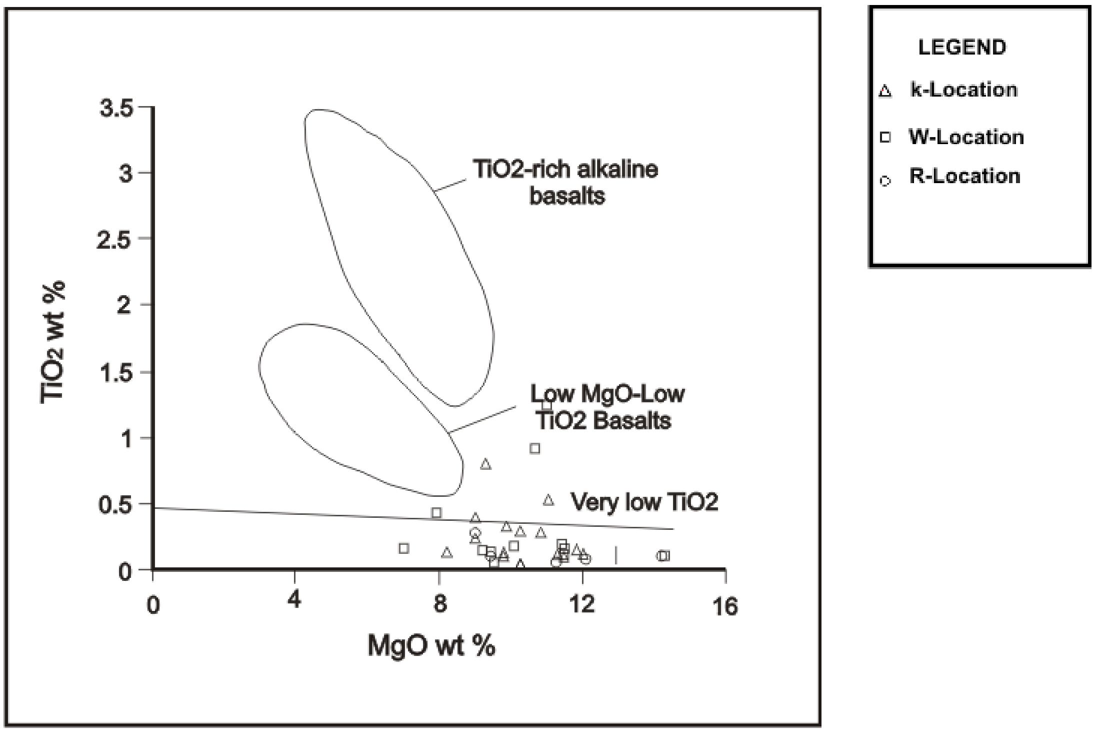


Figure (4.11): Plots of Mawat gabbro samples on MgO- TiO2 diagram showing fields of TiO2-rich alkaline basalts, low-MgO low TiO2 basalts, and very low Tio2 boninite. (After Laurent and Hebert., 1989).

Pearce (1982) proposed the ***Y-Cr diagram*** to illustrate the relationship between chromium as a compatible immobile element and yttrium as an incompatible immobile element. Figure (4.12) shows the positions of the gabbroic samples of Mawat which are within and to the left of the field of (VAB). Generally, all Mawat gabbroic samples show the character of the arc-basalts which characterized by low Cr and Y concentrations.

The ***Ti-V diagram*** is useful to distinguishes between island arc tholeiites (IAT), mid oceanic ridge basalts (MORB), back arc basin basalt (BABB) and ocean island basalt (OIB) (Fig. 4.13). Diagram is divided into different fields according to Ti/V ratio (Shervais, 1982). Ti/V ratio of less than 10 represents boninite, between 10 and 20 represents island arc tholeiite; between 20-50 is for mid-oceanic ridge and back arc basin basalt whereas the ratio more than 50 is for ocean island basalts. Most gabbro samples fall within the field of V/Ti ratio less than 10 with deviation of some samples. Low Ti and low V/Ti ratio is characteristics of supra-subduction zone setting (Shervais and Kimbrough, 1985., Shervias, 1990., Celik, 2007., Pearce, 2003., Celik and Chiaradia, 2007), and according to the geochemical characters of the gabbros of the present study we can conclude that Mawat ophiolite most like the environment of supra-subduction zone setting.

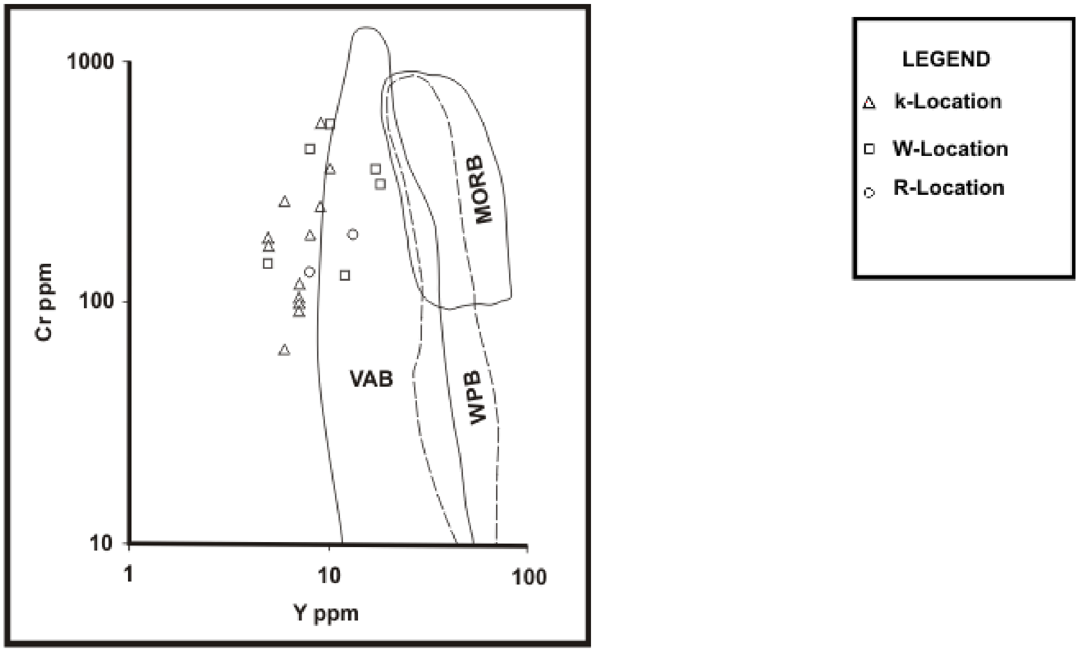


Figure (4.12): Y-Cr diagram showing the positions of the plotted gabbro samples, fields of volcanic arc basalt (VAB), mid-oceanic ridge basalt (MORB), and within-plate basalt (WPB). (After Pearce, 1980., 1982)

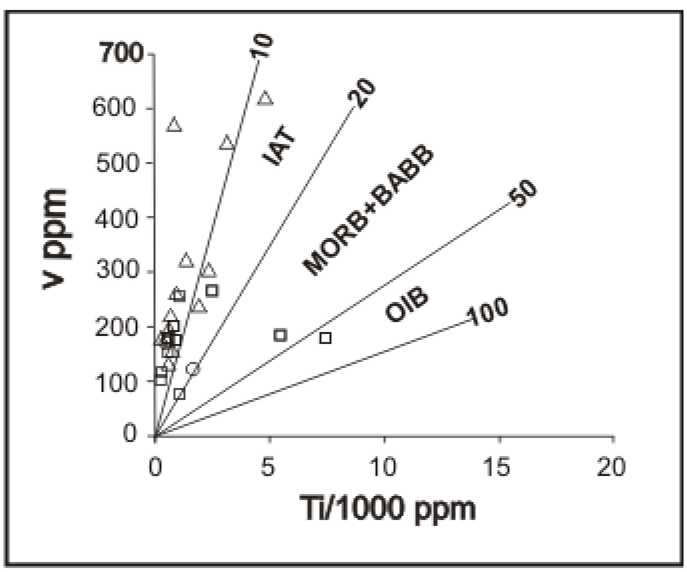


Figure (4.13): Ti-V diagram discriminating of island arc tholeiites (IAT) , mid oceanic ridge basalts (MORB)+ back arc basin basalt (BABB) and ocean island basalt (OIB).The plotted sample. (After Shervais, 1982)

**4.3 Discussion:**

Ophiolitic complex is generated in different tectomagmatic environments (Miyashiro, 1973., Colleman, 1977., Wilson, 1989). Most of the ophiolite complexes are either oceanic or island arc origin (Church and Coish, 1976). The tectomagmatic environment of gabbroic rocks of Mawat ophiolite complex is compared with different tectonic settings. Mawat gabbros are most likely formed in an island arc tholeiites environment (IAT), as indicated by the tight cluster of analyzed samples into (IAT) field, where arc represented the site of subduction of one oceanic lithosphric plate beneath another (Miyashiro et al ,1982 ., Best 1982., Wilson, 1982). This is similar to Tethyan ophiolite along the Zagros suture zone of other localities such as Kermanshah ophiolite in the western Iran (Ghazi and Hassanipak, 1998); Sabzevar ophiolite, north central Iran (Shojaat et al., 2003); and the Aksaray and Kayseri ophiolite, Turkey (Kocak et al., 2005).

According to petrographical and geochemical data presented above, gabbros of the Mawat ophiolite complex in the three locations are probably derived from similar parental magma.

Although geochemical features which are important for the interpretation of the partial melting and fractional crystallization are likely to be obliterated during alteration or metamorphism; special attention will be drawn to elements supposed to be relatively inert in alteration or metamorphism. The petrogenetic study shows partial melting is not more 30% according the Zr versus Zr/Y diagram of Pearce and Norry, (1979). The crystallization and accumulation of major mineral phases in the Mawat gabbros were controlled by clinopyroxene and plagioclase. This conclusion is supported by the relation between Ti versus $Al_2O_3/TiO_2$ and Ti versus Ti/Cr. Fractionation and accumulation of the plagioclase minerals (Al- rich phases) is supported by several evidences; the negative correlation trend between Mg# and $SiO_2/Al_2O_3$ and the positive trends between Mg# versus CaO, and $Al_2O_3$ . The relation between Mg# and MgO and CaO indicates fractionation of clinopyroxenes. The absence of olivine in the mineral assemblages of Mawat gabbros suggests that olivine more likely had crystallized and early separated for the melt during the ascent of magma up word (Wilson, 2001). This conclusion is supported by the good positive trend between Ni and Cr. The typical crystallization sequence of tholeiites is olivine +clinopyroxene + plagioclase and iron titanium oxides (Batt and Tracy, 1996).

## 5.1 Conclusions:

This study has come to following conclusions:-

1- Depending on field relations, three groups of gabbroic rocks were recognized; **layered gabbro** which covers the major part in all rocks of the three locations. Two main types of igneous layering are recognized in the layered gabbros. The first is the grain size layering; and the second one is the compositional layering. Both types of layering are commonly associated with each other. The **marginal gabbro** is restricted in the southern part of the study area, it is found in the lower part of W-location near Waraz village, and these rocks are intensely deformed .The third group is the **dyke of pegmatoid gabbro**, which occurs within the ultrabasic body (Ser Shiw area). The Megascopic features in the layered gabbros such as graded bedding, dimensions, and thicknesses of layering indicate gravitational crystal settling mechanism.

2-Petrogrphically, the Mawat gabbros, in general, are mainly composed of mineral assemblages including Ca-rich plagioclase (labradorite to bytownite), pyroxene (clinopyroxene (augite) and in rare cases orthopyroxene). Olivine is absent. Secondary minerals include amphiboles (tremolite, actinolite), chlorite, epidote, sericite, and magnetite. The Mawat gabbros experience deformation and alteration and/ or metamorphism with conversion of pyroxenes to secondary amphibole (tremolite-actinolite). Plagioclase remains relatively fresh in appearance.

3-Three types of deformation were recorded in these rocks including crystal-plastic deformation, semibrittle deformation and brittle deformation. Crystal-plastic deformation occurs in the layered gabbro, while brittle deformation is most common in the marginal gabbro.

4- Based on the petrographical observations, urilitization is the most common. Urilitization has taken place during the deformation at is showed petrographically.

5- Both magmatic and deformational textures are observed. The magmatic textures include hypediomorphic granular, intergranular, poikilitic ophitic and sub-ophitic textures. The deformation textures are the most common in the studied samples, and the cumulus fabrics may be obscured by deformation probably during emplacement and thrusting. All samples of the marginal gabbros, at ultramafic gabbro contacts and in narrow shear zones within the layered gabbro have undergone shearing. In such cases, a schistose texture develops which is attributed to low-temperatures/high stress. The transition from igneous texture to crystal-plastic deformation texture is marked by the increasing abundance of deformation twins, subgrain boundaries in plagioclase. These types of deformation took place under high temperature almost at temperature near solidus.

6- Sheared gabbros are commonly impregeted with iron oxide minerals, and they are typically associated with alteration of ferromagnesian minerals which causes explosion of iron during alteration.

7- Deformation twins of plagioclase took place by post solidification of primary twins due to dynamic deformation. Studied samples show bending, tapering, and crossing of different sets.

8- The microscopic textural features of these rocks, the unzoned nature of minerals and their model variation in abundance strongly suggest that they are cumulate in origin.

9- The pseudomorphic habit of secondary minerals suggests that this alteration is hydrothermal in origin.

10- The geochemical analyses of Mawat gabbtros have low concentrations of the $TiO_2$, $K_2O$, $Na_2O$, HFSE, REE, and high concentrations of the $Al_2O_3$, CaO and MgO. The marginal gabbros have high $Na_2O$, and $Fe_2O_3$ and lower CaO, MgO compared to the layered and pegmatoid gabbros. The latter have relatively lower $SiO_2$ and higher CaO concentration than the other types. Fractionation index ($FeO^t/MgO$) has restricted ratio ranging between (0.36-1.37) in all Mawat gabbros reflecting oceanic tholeiites nature. This ratio also shows that Mawat gabbros have experienced relatively a small degree of differentiation. The $Fe_2O_3$ and $H_2O$ content of Mawat gabbros indicates that they have been subjected to alteration and metamorphism processes.

11- On the basis of chemical classification, the Mawat gabbros are classified into gabbroic of cumulate nature.

12- Discrimination diagrams for the tectomagmatic setting of Mawat gabbroic shows that they are island-arc tholeiite (IAT) with very low Ti and low V/Ti which is the characteristics of island –arc setting of.

13- The evolution and differentiation of the parental magmas are controlled by two mechanisms: (a) partial melting with an average not exceeds 30% of a depleted upper mantle source, and (b): fractional crystallization which is dominated by the presence of two major phases; the calcic-plagioclase and clinopyroxene. Olivine is absent as determined by the relation between Ni and Cr which leads to conclude that the magma source has fractionated by the removed of olivine.

**5-2 Recommendations:**

1- Dating for the different types of gabbros (layered, marginal and dike swarms pegmatoid gabbros).

2- Prob micro-analyses for certain minerals such as pyroxenes amphiboles to determine the chemical compositions of these minerals and to use them in the determinations of the temperature and pressure of the magma.

3- Detailed structural field study for determining the magma chamber location .

***DETERMINATION OF MAJOR ELEMENTS:***

1- 0.5g of oven dray (100-110° C) sample is taken in a Pt- crucible (W1).

2- Add fussion mixture (about six times of the samples weight and mix thoroughly using glass rod.

3- Melt the mixture on a gas burner then cool.

4- Heat at 1000° C for 10 minute in a muffle furnace, and then allow to cool at air.

5- Cover the mixture with warm distilled water until the content is disintegrated.

6- Pour the content into 400 ml beaker, add at least 25 ml of concentrated HCL by dropper and cover the beaker.

7- Warm on sand batch until the evolution of carbon dioxide is ceased.

8- Rinse and remove the cover and heat the sample to dryness.

9- Consequently crush any lump with glass rod.

10- Heat the powder formed for 1hr. at 100-1000° C (to dehydrate the silica) and cool.

11- Moisten the powder with 5 ml of concentrated HCL, then heat to dryness on sand bath with continuous disintegration of any lump.

12- Heat for 1 hour at temperature of (100-110° C).

13- Allow to cool, moisten the powder with 5 ml of concentrated HCL.

14- Add 70ml of warm distilled water rinse down the sides of sides of the beaker cover and heat to boiling for 1 minute.

15- Filter on filter paper No. 42 and receive the filterate by 250 ml volumetric flask.

A- Determination of $Fe_2O_3$, $Al_2O_3$, and $TiO_2$ (Colorimetric analysis).

B- Determination of CaO, MgO (using A.A.S).

16- Wash filter cake with hot distilled water until free form chloride, receive the wash in the same flask above.

17- Remove up the moist filter and place in a weighed (W2) porcelain crucible.

18 Dry in an oven at 100° C, char the paper by means of charing machine the ignite in a muffle furnace for an hour at 1000° C.

19-Allow to cool in a desiccators and weigh (W3).

20- The solution obtained in the volumetric flask is then completed to the mark and shasked thoroughly.

21- The solution is now ready for analyzing any soluble element.

22- $SiO_2$ %= ((W3-W1)/W2) *100

***DETERMINATION OF FeO:***

1- Weigh 0.5gm of oven dey (100° C) sample in Pt-crucible.

2- Wet thoroughly with distilled water.

3- Add 10ml of 1:1 $H_2SO_4$, cover and heat nearly to boiling over a hot plate.

4- Add 5ml of concentrated HF without covering for (10-15) minutes.

5-400ml beaker is prepared for adding (100-120) ml $H_2O$ +15ml of 1:2 $H_2SO_4$+ 5ML of 85% $H_2SO_4$ + 25ml of saturated solution of boric acid.

6-Pour the crucible contents to the beaker and titrate against 0.05 N $KMnO_4$ quickly.

7- FeO%=Number of $KMnO_4$ mls * 0.719

***DETERMINATION OF (H2O$^+$):***

1- Weigh 1gm of oven der (100° C) samples in known weight porcelain crucible (weight of crucible+ 1gm samples = W1).

2-Transfer to a muffle furnace and gradually increase the temperature to 1000° C, leave at this temperature for 2 hours.

3- Remove the crucible from the furnace, let to cooling a desecrator, than weigh (W2).

4- L.O.I. %=( W2-W1)*100

***DETERMINATION OF K2O AND Na2O:***

1- Weigh 0.1gm of oven dry (110° C) in Pt- crucible.

2- Add 2ml of concentrated HNO3 +2ML of concentrated $HCLO_4$+ 10ML of concentrated HF.

2- Leave it on sand bath until dryness.

3- Add 5ml of 1:1 HCL and warm.

5- Filter or transfer to 100ml volumetric flask.

6- Send to A.A.S. Laboratory to determine the concentration of $K_2O$ and $Na_2O$.

***DETERMINATION OF TRACE ELEMENTS USING ICP TECHNIQUE:***

1- Weigh 0.5 gm of samples to the volumetric flask; add 10ml HF concentrated with 15ml HCL.

2- Heat at 70 C to dryness.

3- Add 15ml HCL concentrated with 15ml $HNO_3$ concentrated and heat again to dryness.

4- Add 25ml HCL.

5- Heat, filter and transfer to 50ml volumetric flask and complete to the mark.

6- Send to ICP laboratory to read the concentration (Ni, Cr, Cu, Co, Y, Zn, Zr, Mn).

***PRECISION:***

It is an estimation of the reproducibility of the results in replicate analysis of an element (s) in the same samples. Select two samples and divided into three portions .Each portion should have a different number. The results should be statistically treated in the following manner to estimate the precision.

$$\sqrt{[(X1-X)2+(X2-X)2\ldots\ldots\ldots(Xn-X)2]/n} \quad S=$$

P%= [2S/ $\bar{X}$]* 100 (at 95% confidence level) (Maxwell, 1968)

$X_1$, X2, …….. $X_n$ = are the actual readings of the different portions of the same samples.

n= is the number of readings,i.e. number of sample (s) portions analysed.

$\bar{X}$ = is the mean of readings for each element in the replicate analysis.

Table 1.show the precision of two selected samples

| Sample no. | contents | $SiO_2$ | MgO | $Al_2O_3$ | $TiO_2$ | CaO | $Fe_2O_3$ | FeO | $K_2O$ | $Na_2O$ |
|---|---|---|---|---|---|---|---|---|---|---|
| **K19** | average | 45.85 | 11.87 | 14.07 | 0.14 | 15.47 | 1.08 | 7.05 | 0.083 | 0.64 |
| | S.D | 0.29 | 0.095 | 0.069 | 0.014 | 0.026 | 0.016 | 0.041 | 0.0047 | 0.016 |
| | P%. | 19.33 | 6.33 | 4.6 | 0.93 | 1.73 | 1.06 | 2.73 | 0.3 | 1.06 |
| **W36** | average | 47.6 | 14.09 | 16.13 | 0.1 | 11.9 | 1.12 | 6.12 | 0.1 | 0.73 |
| | S.D | 0.2 | 0.14 | 0.123 | 0.005 | 0.08 | 0.012 | 0.09 | 0.008 | 0.045 |
| | P%. | 13.33 | 9.33 | 8.2 | 0.33 | 5.33 | 0.8 | 6 | 0.53 | 3 |

**ACCURACY:**

It is the closeness of the results to reality, by using international standards. These standard materials are to be used for estimating the accuracy of the analysis of the various elements. In this study were used two international standards (JGb = gabbro) (JB-1a =basalt) to estimating the accuracy shown table 2.

Table (2): compilation between published (-) and determined (*) international standard.

| Oxides | JGb-1(gabbro) | JB 1a(basalt) |
|---|---|---|
| $SiO_2$ (-) | 43.44 | 52.17 |
| (*) | 42.21 | 50.24 |
| MgO (-) | 7.83 | 7.75 |
| (*) | 8.2 | 6.8 |
| $Al_2O_3$ (-) | 17.66 | 14.51 |
| (*) | 18.03 | 15.76 |
| $TiO_2$ (-) | 1.62 | 1.3 |
| (*) | 1.58 | 1.3 |
| CaO (-) | 11.98 | 9.23 |
| (*) | 12.16 | 10.07 |
| $Fe_2O_3$ (-) | 4.89 | 2.52 |
| (*) | 3.06 | 2.30 |
| FeO (-) | 9.24 | 5.92 |
| (*) | 10.06 | 6.35 |
| $K_2O$ (-) | 0.62 | 1.46 |
| (*) | 0.50 | 1.64 |
| $Na_2O$ (-) | 1.23 | 2.74 |
| (*) | 0.96 | 1.98 |

Table 3. Chemical analysis of REE for the Mawat gabbros.

| Sample no. | Dy ppm | Er ppm | Gd ppm | Ho ppm | Lu ppm | Ce ppm | Eu ppm | La ppm | Nd ppm | Pr ppm | Sm ppm |
|---|---|---|---|---|---|---|---|---|---|---|---|
| K7 | <5 | <5 | 6 | <5 | <5 | <5 | <5 | <5 | <5 | <5 | <5 |
| W78 | <5 | <5 | 12 | <5 | <5 | <5 | <5 | <5 | 6 | <5 | <5 |
| W44 | <5 | <5 | <5 | <5 | <5 | 9 | <5 | <5 | 14 | <5 | <5 |
| W51 | <5 | <5 | <5 | <5 | <5 | <5 | <5 | <5 | <5 | <5 | <5 |
| W61 | <5 | <5 | <5 | <5 | <5 | <5 | <5 | <5 | <5 | <5 | <5 |
| R85 | <5 | <5 | <5 | <5 | <5 | 9 | <5 | <5 | 14 | <5 | <5 |
| R88 | <5 | <5 | <5 | <5 | <5 | <5 | <5 | <5 | <5 | <5 | <5 |

## List of Contents

## List of Figures

## List of Tables

## List of plates

- Agar, S. M., Casey, J. F., and Kempton, P. D. (1997): Textural, geochemical, and isotopic variations in gabbroic shear zones from the MARK area. In Karson, J. A., Cannat, M., Miller, D. J., and Elthon, D. (Eds.), Proc. ODP, Sci.Results, 153: College Station,TX (Ocean Drilling Program), pp.99-121.

- Akif, A., Al-Kaabi, A. and Saltran, V. (1972): Preliminary report on geology and mineralization of the Ser-shiw ultrabasic body. Unpubl. Report, NIMCO, Baghdad, Iraq.

- Alabaster, T., Pearce, J.A. and Malpas, J. (1982): The volcanic stratigraphy and petrogenesis of the Oman Ophiolite complex. Contrib. Min. Petrol.vol.81, pp 168-183.

- Alavi, M. (2004): Regional stratigraphy of the Zagros fold-thrust Belt of Iran and its proforerland evolution. Am. Jour. of Sci.vol.304, pp.1-20.

- Al-Hassan, M.E. (1975): Comparative petrology study between Mawat and Pejwin igneous complexes, NE Iraq. Unpubl. M. Sc. Thesis, Baghdad University, 114p.

- Al-Hassan, M.E. (1982): Petrography, Minerology and Geochemistry of Penjwin igneous complex, Northeast. Unpubl. Ph. D. Thesis, University of Dundee.

- Al-Hashimi, A.R. and Al-Mehaidi, H.M. (1975): Cu-Ni-Cr dispersion in Mawat ophiolite complex, NE Iraq. Jour. Geol. Soc. Iraq, Spec. Issue, pp.37-44.

- Al-Mehaidi, H.M. (1974): Report on geological investigation of Mawat- Chowarta area, Northeastern Iraq. Site Inv. Co. Unpubl. Report G.S.M. Lib, Baghdad, Iraq, 54p.

- Allegre, C. J., Javoy, M., Michard, G. (1968): Etudede la distribution et l abundance des elements de transitions dons l ecorce terrestre, compare a celles des Terrres Rares. In: Ahrens, L.H. (ed.), origin and Distribution of the Elements, 914-928. Pergaman press.

- Aqrawi, A. M. A. (1990): Petrochemistry and petrogenesis of ultramafic and gabbroic rocks around Root mountain Mawat ophiolite complexes, N. E. Iraq. Unpubl. M. Sc. Thesis, Mosul University, 155p (in Arabic).

- Arculus, R.J., Gill, J.B., Cambary, H., Chen, W.and Stern, R.J. (1995): Geochemical evolution of arc systems in the Western Pacific: The ash turbidite record recovered by drilling. In: Taylor, B. and Natland, J. (eds.), Active margins and marginal basins of the Western Pacific. American Geophysical Union, Geophysical Monograph, Vol.88, pp.45-65.

- Aswad, K. J. (1999): Arc-continental collision in Northern Iraq as evidence by the Mawat and Penjwin ophiolite complexes. Raf. Jour. Sci. vol.10, no.1, pp. 55-61.

- Augustithis, S.S. (1979): Atlas of the textural patterns of basic and ultrabasic rocks and their genetic significance. Walter de Gruyter.393p.

- Aziz,R ., Al-Hafdh, N. and Al-Ghadanfary, E. (1993): Geochemistry and petrogenesis of the Walash volcanic in Darband, NE Iraq.Abhath Al-Yarmouk, Pure Science and Engineering series,Vol.2 pp.135-155.

- Beccaluva, L., Digirolamo, P., Macciotta, G. and Morra, V. (1983): Magma affinities and fractionation trends in ophiolites. Ofioliti, vol. 8, pp 307-323.

- Bellen, R.C., Wetzel, R. and Morton, D. (1959): lexique stratigraphique international Asie.Fasc.10, Iraq.Central National deal Recherches Scientifique, Paris, 333 p.

- Best, M.N. (1982): Igneous and Metamorphic Petrology. W. H. Freeman and Company, San Francisco, 630p.

- Bischoff, J. L., and Dickson, F. W. (1975), Seawater basalt interaction at 200_C and 500 bars: Implications for the origin of seafloor heavy metal deposits and regulation of seawater chemistry, Earth Planet. Sci. Lett., vol.25, pp 385–397,

- Blackman, D. K., B. Ildefonse, B. E. John, Y. Ohara, D. J.Miller, C. J. MacLeod, and the Expedition 304/305 Scientists (2006), Proceedings of the Integrated Ocean Drilling Program, Vol. 304/305, Integrated Ocean Drill. Program, College Station, Tex., doi: 10.2204/iodp. proc.304305.101.

- Blatt, H., and Tracy, R.J. (1996): Petrology, Igneous, Sedimentary and Metamorphic: W.H.Freeman, New York, 529p.

- Bolton, C.M.G. (1957): Explanation of the geological map-Kurdistan series, scale 1:100000 sheet K5 Chowarta .Site Inv. Co., Unpubl. Report, NIMCO, Baghdad, Iraq.

- Bolton, C.M.G. (1958): Geological map-Kurdistan, Sheet 4, Rania.Site Inv.Co., NIMCO, No.276.

- Boztug, D. Yagmur, M.Otlu, N. Tatar, S. Yessiltas, A. (1998): Petrology of the Post-Collisional, Within-Plate Yildizdag Gabbroic Pluton, Yildizeli-Sivas Region, Central Anatolia, Turkey. Jour. Earth Sciences vol.7, P37-51.

- Buda, G. and Al-Hashimi, W.S. (1977): Petrology of Mawat ophiolite complex, Northeasat Iraq.Jour.Geol. Soc.Iraq, vol. X, pp.69-98.

- Buday, T.and Jassim, S.Z. (1987): The Regional Geology of Iraq Vol.2, Tectonism, Magmatism, and Metamorphism.Geol.Surv.Min, Inv.Baghdad, 352p.

- Campbell, I. H. (1978): Some problems with the Cumulus theory. Lithos, vol.11, pp311-323.

- Cannat,M.,Karson,J.A., Miller, D. J(1995): Proc.ODP,Init.Repts.,153: College Station, TX (Ocean Drilling Program).

- Cann, J. R. (1969): Spilites from the Carlsberge Ridges, Indian Ocean. Jour. Petrol. vol.10, pp 1-19.

- Celik, O.F. (2007): Metamorphic sole rocks and their mafic dykes in the eastern Tauride belt ophiolite (southern Turkey): implications for

OIB-type magma generation following slab break--off.Geol. Mag., vol.144, no.5, p849-866.

- Celik, O.F., and Chiaradia, M. (2007): Geochemical and petrological of dike intrusions in the Lycian ophiolite (SW Turkey): a case study for the dike emplacement along the Tauride Belt Ophiolites.Int.Jour.Earth Sci. vol 144, no.5, pp 849-866.

- Church, B.N. (1975): Quantitative classification and chemical comparison of common volcanic rocks. Geologic Society of America Bulletin, vol. 86, p. 257-263.

- Church, W.R. and Coish, R.A. 1976. Oceanic versus Island Arc origin of ophiolites. EPSL 31, p. 8-14. Sub Dec 15 1975

- Coish, R.A. (1977): Ocean floor metamorphism in the Betts Cove ophiolite, Newfoundland.Contrib.Mineral.Petrol. Vol.60pp.255-270.

- Collemam, R. J., 1981. Tectonic setting for ophiolite obduction in Oman. *Journal of Geophysical Research*. (Special Issue), vol 86, pp2497-2508.

- Colleman, R.G. (1977): Ophiolites: ancient oceanic Lithosphere: New York, Springer-Verlag, 229p.

- Coish,R.A.,Perry,C.D., Anderson and Bailey (1986): Metavolcanic rocks from the Stowe formation .Vermont: Remnants of Ridge and interpolate volcanism in the Iapetus ocean . Am. Jour. of Sci. vol. 286. pp1-28.

- Cox, K.G., Bell, J.D., and Pankhurst, R.J. (1979): The interpretation of igneous rocks. George Allen and Unwin, Boston, 450p.

- Dreyer, B (2003): Pertrologic and trace element geochemical constraints on the petrogenesis of igneous units cored during ODP Legs 170 and 205, Middle America Trench offshore Costa Rica pp 1-39.

- Etabi, W. (1972): Petrography of Mawat igneous complex. Unpubl. Report, NIMCO, Baghdad, Iraq.

- Faustino, D. V., Yumul, Jr, G. P., Dimalanta, C. B., De Jesus, J.V., Zhou, M.F., Aitchison, J. C.,Tamayo, Jr, R. A.(2006): Volcanic-hypabyssal rock geochemistry of a subduction-related marginal basin ophiolite:Southeast Bohol Ophiolite-Cansiwang Melange Complex, Central Philippines. Geosciences Jour. vol.10, no.3, pp291-303.

- Farjo, S. F. Y., 2006, Geochemistry and petrogenesis of the volcanic rocks of Mawat ophiolite complex, NE-Iraq. Unpubl, M. Sc. Thesis, Mosul University.

- Floyd, P.A., and Winchester, J.A. (1975): Magma type and tectonic setting discrimination using immobile element. Earth Planet. Sci. vol. 27, pp 211-218.

- Gass, I. G. and Smewing, J. D. (1973): Intrusion, extrusion and metamorphism at constructive margins: evidence from the troodos Massif, Cyprus. Nature vol.242, pp26-29.

- Gass, I.G., Lippard S.J. and Shelton A.W. (1986): The ophiolite of Northern Oman. Geological Society, Oxford London, 177p.

- Ghazi, A.M.., Hassanipak, A.A. (1998): Geochemistry of sub alkaline and alkaline extrusive from the Kermanshah ophiolite, Zagros Suture Zone, Western Iran: implications for Tethen plate tectonics. Journal of Asian Earth Sciences, vol.17, pp319-332

- Ghasemi, H., Juteau, T., Bellon, H., Sabzehei, M., Whitechurch, H., and Ricou L. (2002): The mafic-ultramafic complex of Sikhoran (Central Iran): a polygenetic ophiolite compex. C. R. Geoscience, vol. 334, pp 431-438.

- Goldschmidt, V.M, (1962): Geochemistry. Oxford university press. 730p.

- Hart, R. A. (1970), Chemical exchange between seawater and Deep Ocean Basalts. Earth Planet. Sci. Lett. vol. 9, pp. 269–279.

- Hatch, F. H., Wells, A. K., Wells, M. K. (1961): Petrology of the Igneous Rocks .12 Th edition .Thomas Murby, London.515 p.

- Hajash, H. (1975): Hydrothermal processes along mid-ocean ridges: An experimental investigation, Contr. Min. Petr. vol 53, pp 205-226.

- Hopper, D.J., Smith, I. E. (1996): Petrology of the gabbro and sheeted basaltic intrusives at North Cape, New Zealand. New Zealand Journal of Geology and Geophysics, vol.39, pp389-402.

- Heron, A. M., and Less, G.M. (1943): The zone of nappes in Iraq Kurdistan .Unpubl. Report, G. S. M. Lip. Baghdad Iraq.

- Humphris, S.E. and Thompson. (1978a): Hydrothermal alteration of oceanic basalts by seawater.Geochim.Cosmochim.Acta, vol.42, pp.107-125.

- Humphris, S.E. and Thompson. (1978b): Trace element mobility during hydrothermal alteration of oceanic basalts, Geochim.Cosmochim.Acta, vol.42, pp.127-136.

- Ilnicki, S. (2002): Amphibolites and metabasaltes from the Izera block, West Sudetes.

- Iyer, S. D. (1999): Alteration of basaltic glasses from the Central Indian Ocean. J. Geol. Soc. India, vol 280A, pp 1-58.

- Irvine, T.N. (1980b): Magmatic density currents and cumulus processes. American Journal of Science, vol, pp 280-58.

- Iyer, S. D. and Ray, D. (2003): Structure, tectonic and petrology of mid-oceanic ridges and the Indian scenario. Current Sci., vol. 85, no3. pp 277-289.

- Janousek, V., Braithwaite C. J. R., Bowes, D.R. and Gerdes, A. (2004): Magma- mixing in the genesis of Hercynian calc-alkaline granitoids: an integrated petrographic and geochemical study of the Sazava intrusion, Central Bohemian Pluton, Czech Republic. Lithos, vol.78, pp 67-99.

- Jassim, S.Z. (1972): Geology of the Central sector of Mawat complex. Jour. Geol. Soc. Iraq, vol.6 pp.82-92.

- Jassim, S. Z. (1973) Geology of Central Sector of Mawat igneous complex, northeastern Iraq, J. Geol. Soc. Iraq, vol 6,pp 83-92.

- Jassim, S.Z. and Al-Hassan, M.I.S. (1977): Petrography and origin of the Mawat and Penjwin igneous complexes: A coimparison. Jour.Geol. Soc. Iraq, Spec Issure, pp169-210.

- Jassim, S. Z. and Goff J. C. (2006): Geology of Iraq. Parague and Moravian Museum Brno. 341 P.

- Jensen, L. S. (1976): Anew Cation plot for classifying subalkalic volcanic rocks .Ontario Div.Mines.Misc.p.66.

- Kato, K. and Saka, Y. (2006): New modal for the Early cretaceous developmentof SW Japan based on basic rocks of the Chichibu composite Terrane. This volume

- Kocak, K., Isik F., Arsalan M., Zedef V. (2005): Petrological and source region characteristics of ophiolitic hornblende gabbros from the Aksaray and Kayseri regions, central Anatolian crystalline complex, Turkey. Journal of Asian Earth Sciences, Vol.25, p883-891.

- Koller, F., Hoeck, V., Mesiel, T., Ionescu,C., Onuzi, K., and Ghega, D. (2006): Cumulates and gabbros in southern Albanian ophiolites their bearing on regional tectonic setting. Geological society, London, Special Publications, vol.206, pp 267-299.

- Krauskopf, K.G. (1979): Introduction to geochemistry (2nd), Mc Graw-Hill, New Yourk, 617p.

- Kimbrough, D. L., Moore, T. E. (2003): Ophiolite and volcanic are assemblages on the Vizcaino peninsula and Cedros Island, Baja California Sur, Mexico: forearc lithosphere of the Cordilleran magmatic arc. Geological, Sci. of Am. special paper, vol.374, pp.1-29.

- Langmuir. C. H., Klein E.M. and Plank, T. (1992): Petrological Systematics of Mid Ocean ridge basalts: Constraints on melt generation beneath Oceanic ridges in Morgan J.P., Blackman. D. K. and Sinton. J. M. (eds). Mantle flow and melt Generation at Mid-Ocean Ridges. Geophysical of Monography.vol.71 pp183-280.

- Laurent, R. and Heberi, R. (1989). The volcanic and intrusive rocks of the Quebec Appalachian ophiolites (Canada) and their island arc setting. Chemical Geology, vol. 77, pp 287-302.

- Lehner, H. P. (1954): Report on a geological survey of the north of Chwarta. GEOSURV, int. rep. No. 264.

- Lemaitre, R.W (1976): The chemical variability of some common igneous rocks: Jour. of petrology, vol.17/4, pp.589-637.

- Leeman, W.P. (1976): Petrogenesis of Mckinney (Snake River) olivine tholeiite in the light of rare earth elements and Cr/Ni distributions. Geol.Soc. Bull, vol.87, pp1582-1586.

- Lesher, C. M., Goodwin, A. M., Campblell, I. H. and Gorton, M. P. (1986): Trace element geochemistry of ore-associated and barren, felsic metavolcanic rocks in the superior province, Canada. Can. j. Earth Sci.vol.23, pp 222-237.

- Le Maitre, R.W., Bateman, P., Dudek, A., Keller, J., Lameyre, J., Le Bas, M.J., Sabine, P.A., Schmid, R., Sorensen, H., Streckeisen, A., Woolley, A.R. and Zanettin, B., 1989, A Classification of Igneous Rocks and Glosarry of Terms. Recommendations of the International Union of Geological Sciences, Subcommission on the Systematics of Igneous Rocks. Blackwell, Oxford, 193p.

- Le Maitre R W 2002 Igneous Rocks: A classification and glossary of terms (Cambridge: Cambridge University Press) 236 p.

- Mason, B (1952): Principles of Geochemistry (third edition), New York, London Sydney.

- Mason. B. (1971): Hanbook of elemental abundances in Meteorites, Gordon and Breach, New York, 555p.

- Marchesi, C., Garrido, C. J., Godard, M., Joaquin, A., Gervilla, P. F., and Moreno, J.B.(2006): Petrogenesis of highly depleted peridotites and gabbroic rocks from the Mayari-Baracoa Ophiolitic Belt (eastern Cuba). Contrib Mineral Petrol., vol.151, pp 717-736.

- MacLean, W.H and Barrett, T.J. (1993): Lithogeochemical techniques using immobile elements. Jour. Of Geochemical Exploration, vol.48, pp109-133.

- Mashek, J. and Etabi, W. (1973): Petrology of the Mawat igneous-metamorphism complex, NE Iraq. Unpubl Report, NIMCO, Baghdad, Iraq.

- Mason, B. and Moore, C. B. (1982): Principles of Geochemistry (4th Ed), John Wiley and sons, 344p.

- Maxwell, J. A., 1968. Rock and minerals analysis. John Wiley and Sons, New York, 584p.

- Mevel, C, Stamoudi, C. (1996): Hydrothermal alteration of the upper-mantel section at Hess Deep. Mevel, C., Gillis, K.M., Allan, J.F and Mevel, C., and Cannat, M. (1991): Lithspheric stretching and hydrothermal processes in oceanic gabbros from slow-spreading rides. In Peters,T., Nicolas, A., and Coleman, R.J.(Eds.), Ophiolite Genesis and Evolution of the Oceanic Lithosphere: Dordrecht (Kluwer),293-312.

- Middlmost, E.A.K. (1975): The basalt clan .Earth Sci. Rev. vol.11, pp.337-364.

- Middlmost, E.A. K. (1975): The basalt clan. Earth Sci. Rev. vol.11, pp337-364.

- Miller,C.,Thoni,M.,Frank,W.,Schuster,R.,Melcher,F.,Meisel,T.,Zanetti,A.(2003): Geochemistry and tectonomagmatic affinity of the Yungbwa ophiolite,SW Tibet. Lithos, vol. 66, pp155-172.

- Mirza, T. A. (2008): Petrogenesis of the Mawat ophiolite complex and associated chromitite, Kurdistan region, NE Iraq Unpubl. Ph. D. Thesis, University of Sulaimanya, 189p.

- Miyashiro, A. (1973a): The Troodos ophiolitic complex was probably formed in an island arc.Earth Plant. Sci.Lett. vol.19, pp 218-224.

- Miyashiro, A., Shido., Ewing, M. (1971): Metamorphism in the Mid-Atlantic Ridge near 24 and 30 N.Roy. Soc. London Phiolos. Trans .vol, pp589-603.

- Miyashiro, (1975): Classification characteristics, and origin of ophiolite. Jour. Geol. Vol 275, pp249-281.

- Miyashiro, A., Aki K., Celal Sengor, A.M., (1982): orogeny. Chichester. New York. Brisbane.Toronto.Singapore. 242p.

- Muller, D. and Groves, D. (1997): Potassic igneous rocks and associated gold-copper mineralization. Lecture Notes in Earth Sci., no. 56, 238 P.

- Musa, E. O. (2007): Petrography, Geochemistry and Genesis of copper –Iron Mineralization and Associated Rocks in Waraz Area , Sulaimanya, NE Iraq. Unpubl. M. Sc. Thesis. University of Baghdad.155p

- Naldrett, A. J. and Cabri, L. J. (1976): Ultramafic and related mafic rocks: Their classification and genesis with special reference to the concentration of nickel sulfides and platinum-group elements: Econ.Geol. vol.71, pp.1131-1158.

- Neal, C. and Stanger, g. (1984): Calcium and magnesium hydroxide precipitation fron alkali ground water in Oman, and their significance to the process of serpentinization. Min. Mag vol. 48, pp237-241.

- Nicolas, A. (1989): Structures in ophiolites and dynamics oceanic lithosphere (Kluwer, Dordrecht).

- Numan, N. M. S. (1997): A plate tectonic scenario for the Phanerozoic succession in Iraq. Jour. Geol. Soc. Iraq, vol. 30 (no.2), pp. 50-78.

- Oliveros, V., Morata, D., Aguirre, L., Feraud, G., Fornari, M. (2007): Jurassic to early cretaceous subduction-related magmatism in the Coastal Cordillera of northern Chile (18 30 – 24 S): geochemistry and petrogenesis. Revista Geologic de Chile, vol.34 no.2, pp 209-232.

- Parlak, O. (2000): Geochemistry and Significance of Mafic Dyke Swarms in the Pozanti-Karsanti Ophiolite (Southern Turkey).Turkish Jour. Earth Sci, vol.9.pp29-38.

- Peltonen, P., Kontinen, A., and Huhma, H. (1998): Petrogenesis of the Mantle Sequences of the Jormua Ophiolite (Finland): Melt Migration in the Upper Mantle during Palaeoproterozoic Continental Break-up.Jour. Of petrology, vol.39, no.2, pp297-329.

- Pearce, J.A. (1975): Basalt geochemistry used to investigate post-tectonic environment of Cyprus.Tectonophysics, vol.25, pp 41-67.

- Pearce, J.A. (1980): Geochemical evidence for the genesis and eruptive setting of lavas from Tethyan ophiolites.In Panayiotou, A. (ed), Ophiolite .Geol. Survey dept., Cyprus, pp261-272.

- Pearce, J.A. (1982): Trace elements characteristics of lavas from destructive plate boundaries In: Thorpe, R.S. (ed), Orogenic Andesites and Related Rocks, John Wiley and Sons, New York, pp.525-548.

- Pearce, J.A. (2003): Supra-subduction zone Ophiolites: The search for modern analogues, In: Delik, Y. and Newcomb, S. (eds.), Ophiolites concept and the evolution of geological thought: Boulder, Colorado, Geological Sci. of Am., Spec.Paper, vol.373, pp.269-593.

- Pearce, J.A. and Cann, J.R. (1971): Ophiolite origin investigated by discriminant analyses using Ti, Zr, Y. Earth Plan.Sci.Lett., vol.12, pp339-349.

- Pearce, J. A. and Cann, J. R. (1973): Tectonic setting of basic volcanic rocks determined using trace element analyses. Earth Planet.Sci.Lett., vol.19, pp290-300.

- Pearce, J.A., and Flower, M.F.J. (1977): The relative importance of petrogenetic variables in magma genesis at accreting plate margins: a preliminary investigatrion. Jour. Geol. Soc. London, vol.134, pp 103-127.

- Pearce, J.A. and Norry M.J. (1979): Petrogenesis implications of Ti, Zr, Y and Nb variations in volcanic rocks.Contrib.Min. Petro. vol.69, pp33-47.

- Ricou, L.E. (1971): Le Croissant ophiolitique Peri-Arab: Une ceinture de nappes mises en place an Cretace superieur.Rev. Geogr. Phys. Geol. Dyn. vol.13, pp.327-349

- Roeder, P.L.and Emslie, R.F. (1970): Olivine-liquid equilibrium: Contributions to Mineralogy and Petrology, vol.29, pp.275-289.

- Sapountzis, E. S. (1979): The Thessaloniki Gabbros. Jour. Of petrol.vol 20 part 1, pp. 37-70.

- Shastry, A., Srivastava , K. R., Chandra, R. and Jenner, G.A. (2001): Fe-Ti-enriched mafic rocks from south Andaman ophiolite suite: Implication of late stage liquid immiscibility. Curreut Sci., vol.80, no.3.

- Shervais, W.J. (1982): Ti-V plots and the petrogenesis of modern and ophiolitic lavas. Earth plant.Sci.Lett. vol.59, pp.101-118.

- Shervais, J.W. and Kimbrough, D. L. (1985): Geochemical evidence for the tectonic setting of the Coast Range ophiolite, A composite island arc - oceanic crust terrace in western California. Geology, vol.13, pp. 35–38.

- Shervais, J.W. (1990): Island arc and ocean crust ophiolites: contrasts in the petrology, geochemistry, and tectonic style of ophiolite assemblages in the California Coast Ranges. In; Malpas, J., Moores, E.M., Panayiotou, A. & Xenophontos, C. (eds) ophiolites: Oceanic crustal analogues, proceedings of the symposium Troodos 1987, Nicosia: Geological Survey Department, pp507-520.

- Shojaat, A., Hassanpiak, A. A., Mobasher, K., Ghazi, A. M. (2003): Petrology, geochemistry and tectonic of the Sabzevar ophiolite,North Central Iran. Journal of Asian Earth Sciences, Vol.xx, p1-15.

- Smirov, V. A. and Nelidov, V. (1962): Report on 1:200000 prospecting correlation of Sulaimaniya, Chwarta, Penjwin area, Carried out in (1962). GEOSURV, int. rep. no. 290.

- Snow, J. E. (2002): Major and trace element evolution of Hole 735B gabbros.Natland,J.H.,Dick,H.J.B.,Miller,D.J.,andVon Herzen, R. P. (Eds) Proceedings of the Oceanic Drilling Program, Scientific Results vol.176. p1-18.

- Stakes, D., Mével, C., Cannat, M., and Chaput, T. (1991): Metamorphic stratigraphy of Hole 735B. In Von Herzen, R.P., Robinson, P.T., et al., Proc. ODP, Sci. Results, 118: College Station, TX (Ocean Drilling Program), 153–180.

- Streisckein, A. (1976): To each plutonic rocks its proper name. Earth sci.Rev.vol.12, no.1.pp 1-23.

- Stremmel, K. and Suhr G. (2007): Gabbroic bodies in the Trinity Ophiolite. Goldschmidt Conference Abstracts.

- Tadesse, G., Allen, A. (2005): Geology and geochemistry of the Neoproterozoic Tuludimtu Ophiolite suite, western Ethiopia. Journal of African Earth Sciences.vol41, pp 192-211.

- Takazawa E., Erey, F.A., Shrimizn, N., Saal, A., and Obata, M. (1999): Polbaric Petrogenesis of Mafic Layered in the Horoman Peridotite Complex, Japan. Jour. of petrology, vol. 40, no.12, pp1827-1851.

- Takazawa, F. A., Frey, N., Shrimizn, A. S., and obata, M. (1999): Polybaric petrogenesis of Mafic layered in the Horoman peridotite complex,Japan,Jour. of petrol. vol. 40, no.12, pp 1827-1851.

- Terry, M.P. and Heidelbach, F. (2006): Deformation-enhanced metamorphic ractions and the rheolory of high-pressure shear zone, Western Gneiss Region Norway.Jour.metamorphic Geology.vol.24, pp 3-18.

- Thompsom, R.N. (1984): Dispatches from the basalt front; I, Experiment: Proceedings of the Geologists Association, vol.95 pp249-262.

- Torres-Alvarado1, I. S., Pandarinath1, K., Verma1, S. P., and Dulski2 P. (2007): Mineralogical and geochemical effects due to hydrothermal alteration in the Los Azufres geothermal field, Mexico. Revista Mexicana de Ciencias Geológicas vol. 24 , no. 1, pp. 15-24

- Yoder, H.S., Tilley, C.E. (1962): Origin of basalt magmas: an experimental study of natural and synthetic rocks systems.Jour.Petrol.vol.3, pp 342-532.

- Whinteney, P. R. (1972): Spinel inclusion in plagioclase of metagabbros from the Adirondack Highlands .Am. Min.vol.57, pp1429-1436.

- Williams, H.,Turner, F. J.,and Gillbert, C. M.(1954): Petrography:An Introduction to the study of Rocks in thin sections. Freeman and Company, INC.406 p.

- White, W.M., McBriney, A.R., and Duncan, R.A. (1993): Petrology and geochemistry of the Galapagos Islands; portrait of a pathological plume: our. Of Geophysical Research, B, Solid Earth and Planets, vol.98, pp.533-563.

- White, W.M. (2005): Geochemistry: an on-line textbook, http://www.geo.cornell.edu/geologyclasses/geoo455/chapters. HTML.

- Wilson, M. (1989): Igneous Petrogenesis-a Global Approach.Unwin Hyman, London.466p.

- Wilson, S. A. (2001): The geochemical analysis of Siluro-Devonian mafic dikes in the 15' Woodsville quadrangle, east-central Vermont: Unpublished senior thesis, Middlebury College, Middlebury, Vermont, 106 p.

- Winchester, J.A. and Floyed, P.A. (1976): Geochemical magma type discrimination: Application to altered and metamorphosed basic igneous rocks. Earth Planet.Sci. Lett. Vol.28, pp 459-469.

- Winchester, J. A. and Floyed, P. A. (1977): Geochemical discrimination of different magma series and their differentiation products using immobile elements.Chemical.Geo. Vol. 20, pp 325-343.

- Yoder, H. S. , Tilley, C.E.(1962): Origin of basalt magmas: An experimental study of natural and synthetic rocks systems. Jou. Petrol. Vol.3 pp 342-523.

- Zakaria, M. B. M. (1992): Petrology and geochemistry of the southern part of Mawat ophiolite complex, northeastern .Iraq Unpubl. M. Sc. Thesis, Mosul University (in Arabic).

## *Abstract*

*The gabbroic members of the igneous rocks from the Mawat ophiolite complex are located in the Zagros Suture Zone at the boundary between the Arabian and Iranian plates. They are related to post collision event with emplacement into the continental crust after collision between the Arabian and Iranian plates during Tertiary.*

*Three types of gabbroic rocks were recognized and studied: the layered gabbros which is the dominant type; the marginal gabbros which show higher deformation; and the dyke pegmatoid gabbros.*

*The layered gabbros exhibit two types of layering; compositional layering and grain size layering. Mechanical crystal setting is considered as the main process of layering.*

*In this study, the petrographic study of 100 thin sections showed that these rocks consist of calcic plagioclase (Bytownite in composition An 85, clinopyroxene (augite) and rarely orthopyroxene as the major mineral phases. Iron oxides, mainly magnetite is found as an accessory primary phase and as secondary after the Fe- Mg bearing mineral phases. The rocks in general experienced alteration with the formation of different secondary minerals. Amphibole (tremolite- actinolite) is abundant as alteration product of the pyroxenes associated with chlorite, epidote, sericite and secondary magnetite. Plagioclase attained relatively variable degrees of alteration the layered and pegmatoid gabbros.*

*Primary magmatic textures include hypediomorphic granular, intergranular, poikilitic, ophitic and sub ophitic textures whereas deformation textures are evident by granulation, secondary twinning, and schistose textures.*

*Three types of deformation were recognized; crystal-plastic, semi-brittle and brittle deformations. Pseudomorphic and non-pseudomorphic* *alterations were distinguished. The marginal gabbros are most affected by deformation and alteration.*

*Chemical study of 32 samples show that these rocks have low* $TiO_2$*,* $K_2O$*,* $Na_2O$*, HFSE, and REE, and high CaO, MgO and* $Al_2O_3$ *with restricted* $SiO_2$ *content. The marginal gabbros have higher* $K_2O$*,* $Na_2O$ *and* $Fe_2O_3$ *and lower MgO, CaO and* $Al_2O_3$ *as compared with pegmatoid and layered gabbros.*

*Mawat gabbros exhibit tholeiitic nature and experience small degree of differentiation (*$FeO^t/MgO$ *less than 2) with Mg# ranging from 40.9-64.6 with an average of 51.28 which is lower than that of primitive mantle. The very low- Ti and Zr and the low V/Ti (less than 10) in these rocks classify them as arc tholeiite. Comparison of the studied rocks with different magmas and rocks association lead to the conclusion that the basaltic composition and mafic cumulate are the characteristics of Mawat gabbros. The petrogenetic study indicated that these rocks were derived from depleted mantle source with average 30% partial melting. The fractionation process is controlled by crystallization and accumulation of two major phases; the plagioclase and clinopyroxene.*